DEVELOPMENT OF **ALBUMIN-BASED LYOPHILISOMES** AS **DRUG DELIVERY CAPSULE** FOR CANCER THERAPY

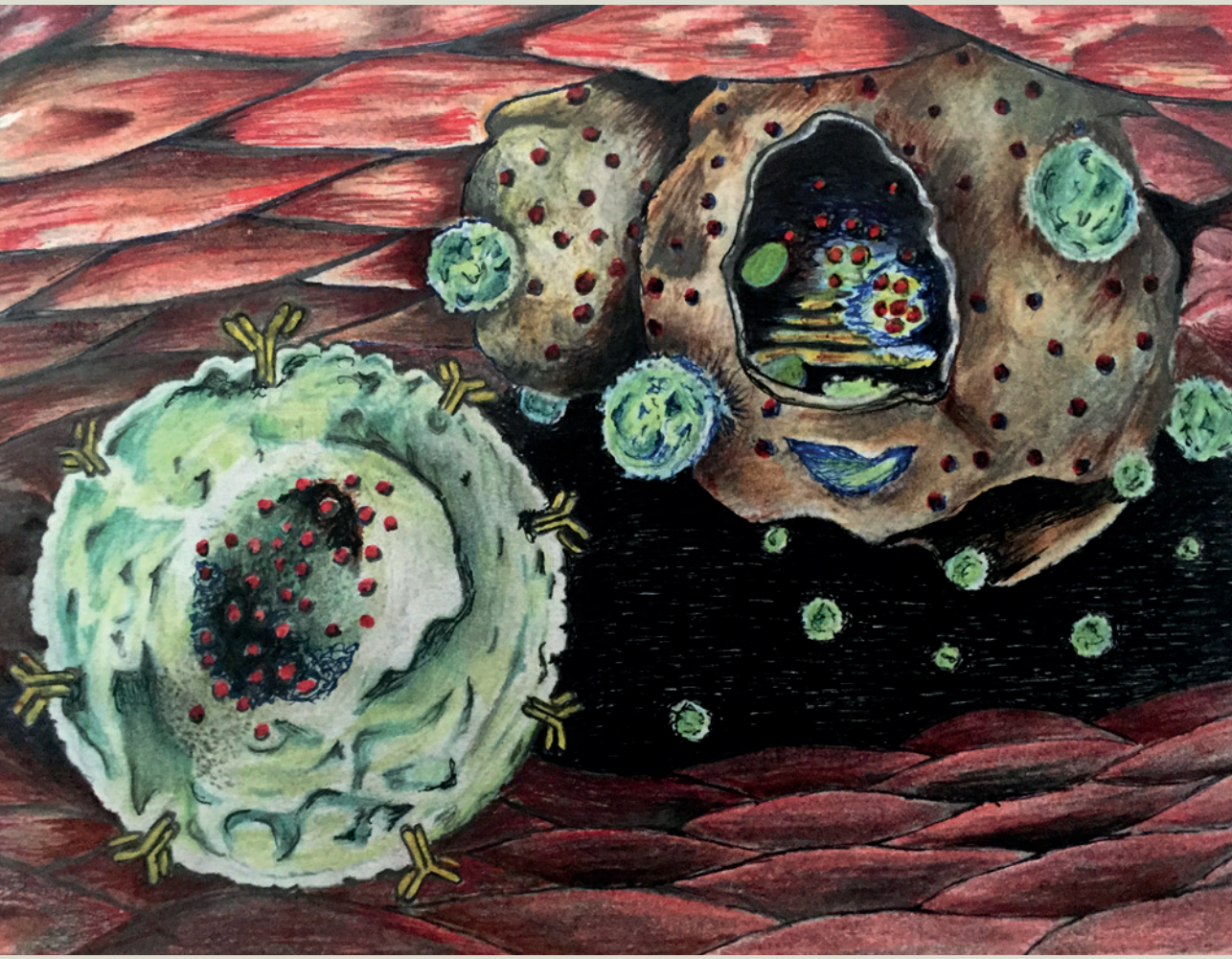

Etienne van Bracht

ISBN
978-94-6259-676-4

Cover Art
Ad and Brigitte Groenen

Cover and Lay-out
Promotie In Zicht, Arnhem

Print
Ipskamp Drukkers, Enschede

The research presented in this thesis was performed at the department of Biochemistry, Radboud University Medical Centre, Nijmegen, the Netherlands and financially supported by the Radboud University, Nijmegen, the Netherlands.

Financial support for the printing of this thesis by the Radboud University, Nijmegen, the Netherlands is gratefully acknowledged.

DEVELOPMENT OF **ALBUMIN-BASED LYOPHILISOMES** AS **DRUG DELIVERY CAPSULE** FOR CANCER THERAPY

Proefschrift

ter verkrijging van de graad van doctor
aan de Radboud Universiteit Nijmegen
op gezag van de rector magnificus prof. dr. Th.L.M. Engelen
volgens besluit van het college van decanen
in het openbaar te verdedigen op woensdag 17 juni 2015
om 14.30 uur precies

door

Etienne van Bracht
geboren op 11 november 1984
te Nijmegen

Promotor
Prof. dr. R. Brock

Copromotoren
Dr. ir. W.F. Daamen
Dr. T.H. van Kuppevelt

Manuscriptcommissie
Prof. dr. O.C. Boerman (*voorzitter*)
Prof. dr. ir. J. Van Hest
Prof. dr. G. Storm (*UU*)

Paranimfen
T.V.R. van Bracht
Drs. R. Raavé

CONTENTS

1

General introduction & aims and outline of this thesis

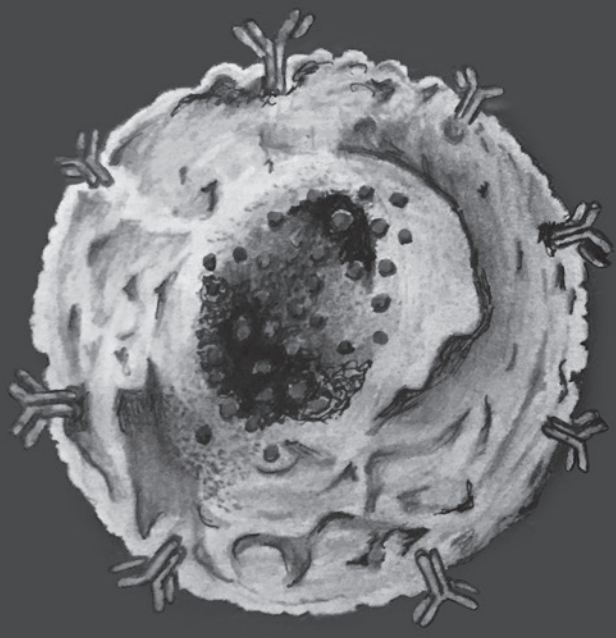

GENERAL INTRODUCTION

Cancer is a leading cause of death around the world. The World Health Organization estimates that without intervention 84 million people will die of cancer between 2005 and 2015 [1]. For effective cancer therapy, it is necessary to improve our knowledge of cancer physiopathology, discover new anti-cancer drugs and develop novel biomedical technologies. Cancer therapy has become a multidisciplinary challenge requiring close collaboration among clinicians, biological researchers, material scientists, and biomedical engineers [2]. Cancer therapeutics aim to prevent tumor progression, improve the quality of life and expand the time of survival, with the ultimate goal to cure the patient. The potency of a cancer therapeutic is determined by its ability to eliminate cancerous tissue without damaging surrounding healthy tissue [3]. However, pharmacological agents are usually non-specifically distributed throughout the body and their efficacy is often limited due to severe side effects, indicating that tissue selectivity is a major problem. To overcome problems associated with conventional (chemo)-therapeutics and improve their pharmacological properties, antibody-drug conjugates have been developed. The first concept was already described in the early 20th century by Paul Ehrlich, while the first credible experiments were performed in 1958 [4,5]. Currently, only four antibody-drug conjugates have been approved by the FDA, of which the first antibody-drug conjugate (Rituximab) in oncology was approved in 1997 [4]. The antibody-drug conjugate concept combines a tumor-specific antibody with a cytotoxic drug to specifically target this drug to the tumor [6]. After binding, certain antibodies -not all- trigger internalization into the target cell together with the anti-tumor drug. Subsequently, the drug is released and the tumor cell eliminated. To increase the anti-tumor drug concentration, researchers pursued new drug delivery systems [7–10]. Drug delivery systems are carrier materials of which polymer-drug conjugates were first described in 1955 by Jatzkewitz that led to the discovery of multiple drug delivery systems in the following years [11]. In 1990, the first polymer-drug conjugate (Adagen) was approved by the FDA [12] and in 1995, the first liposomal formulations were approved by the FDA (Doxil and Abelcet) [13]. Drug delivery systems are able to transport higher quantities of anti-tumor drug molecules. By delivering pharmacologically high concentrations of active agents more selectively to pathological sites, drug delivery systems aim to improve the balance between efficacy and toxicity of systemically administered therapeutics. To design a novel drug delivery system that can efficiently deliver anti-tumor therapeutics to the targeted site via intravenous injection, various specifications need to prevail, as summarized in Table 1. Currently, a variety of drug delivery systems has been designed and characterized including liposomes [14–16], polymer-based drug delivery systems [17–19], and protein-based drug delivery systems [20–22].

Table 1 Goals and specifications of drug delivery systems [2]

1.	Increase drug concentrations in the tumor through:
	(a) passive targeting
	(b) active targeting
2.	Decrease drug concentration in healthy tissue
3.	Improve pharmacokinetic and pharmacodynamic profiles
4.	Improve drug solubility to allow intravenous administration
5.	Release a minimum of drug during transit
6.	Release a maximum of drug at the target site
7.	Increase drug stability and reduce drug degradation
8.	Improve internalization and intracellular delivery
9.	Improve biocompatibility and biodegradability

TUMOR MICROENVIRONMENT

The tumor microenvironment differs considerably from normal tissue, with regard to vascular structure, oxygenation, perfusion, pH, and metabolic state. To probe the possibility to utilize drug delivery systems for cancer therapy, researchers can employ different therapeutic strategies based on these differences. Here, differences in terms of tumor vasculature will be described, as they are most relevant for the design of tumor targeted drug delivery systems.

Angiogenesis

Angiogenesis is the physiological process involved in the formation of new blood vessels from pre-existing vessels and is a vital process in the development of a solid tumor. Once a tumor size has reached a diameter of 1 – 2 mm^3, simple diffusion of oxygen and nutrients from the microvasculature becomes insufficient [23]. Tumors larger than 2 mm^3 require angiogenesis to generate their own blood supply. Angiogenesis can be divided into five stages: 1. endothelial cell activation, 2. basement membrane degradation, 3. endothelial cell activation, 4. vessel formation, and 5. angiogenic remodeling. All these stages are regulated by a fine balance of activators, such as the growth factors vascular endothelial growth factor (VEGF) and platelet derived growth factor (PDGF), and inhibitors, like the statins angiostatin and endostatin [24,25]. Immature vasculature structures undergo extensive remodeling during which the vessels are stabilized by pericytes and smooth muscle cells. In tumors, often aberrant and immature vascular structures are present with altered endothelial cell-pericyte ratios, resulting in irregularly shaped and leaky tumor blood

vessels [26]. The ability of tumors to progress from a non-angiogenic to an angiogenic phenotype, also called the "angiogenic switch", is central to progression of cancer and allows the spreading of cancer cells throughout the body, leading to metastasis [27].

Enhanced Permeability and Retention effect

Structural changes in vascular pathophysiology could provide opportunities for the use of drug delivery systems, in particular nano-sized particles. Before such nanoparticles reach the target site, they need to travel through the vascular bed. For cancer, an effective strategy is based on the enhanced permeability effect (EPR) associated with hyperpermeability of tumor vasculature and lack of lymphatic drainage (Fig. 1) [28–30]. Nanoparticles entered into the tumor are not efficiently removed and thus retained in the tumor. Nanoparticles do not extravasate through normal endothelium since tight endothelial

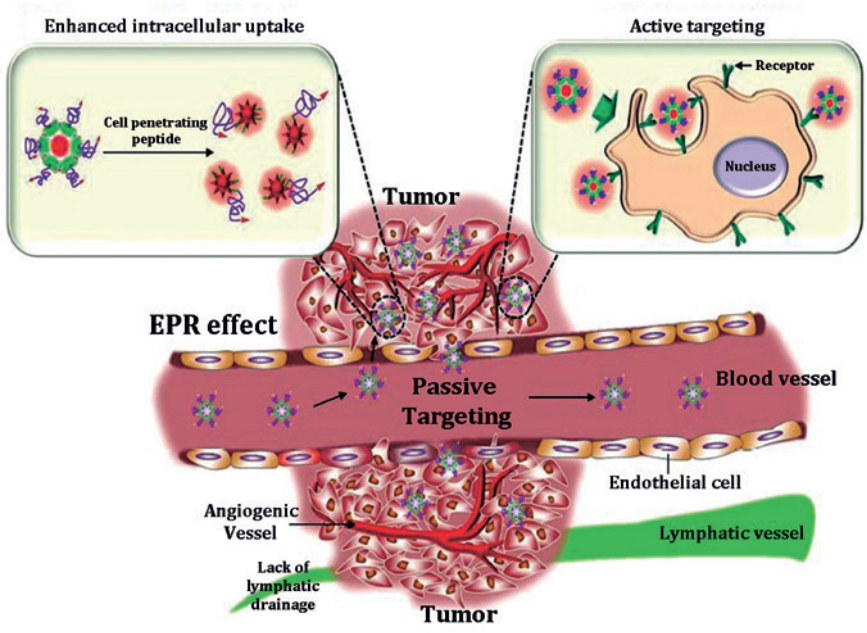

Figure 1 Passive and active targeting approaches of nanocarriers in cancer. Passive tumor targeting is achieved by extravasation of nanocarriers through increased permeability of the tumor vasculature and ineffective lymphatic drainage (EPR effect). Cell penetrating peptides (left inset) can be used in passive targeting devices to facilitate intracellular uptake of nanocarriers. Active tumor targeting (right inset) can be achieved by functionalization of nanocarriers with targeting ligands that promote cell specific recognition and binding to tumor cells. Antibodies and CPPs may also be combined. Figure was adapted from Park [35].

junctions (5 – 10 nm) between endothelial cells prevent extravasations of small particles [31]. However, the cut-off size for permeability in individual tumors varies between 200 – 800 nm [32]. Therefore, particle size has a fundamental effect on biodistribution [33]. Due to this EPR effect, drug delivery systems (<800 nm) can extravasate from the blood vessels to the tumor and accumulate, thereby creating high local drug concentrations [34].

PRINCIPLES OF DRUG TARGETING TO TUMORS

Drug delivery refers to administration of an active pharmaceutical compound to achieve an increased drug accumulation at the tumor site compared to other tissues and organs. Current chemotherapy still fails in many cases because the drug concentration at the tumor site is too low and the drug is usually distributed nonspecifically throughout the body, thereby affecting healthy tissue as well. In this section, we will concentrate on nanoparticulate drug targeting systems to tumors based on the EPR effect (passive targeting), on the use of targeting moieties (active targeting), and enhanced intracellular delivery by cell penetrating peptides (Fig. 2).

Passive targeting

The passive targeting concept utilizes the transport of nanocarriers through (leaky) tumor capillary fenestrations into the tumor interstitium, facilitated by long systemic circulation times, as nanocarriers are more likely to reach the tumor site through the EPR effect when circulating for a longer period of time in the circulation (Fig. 1). This is accompanied with changes in the tumor microenvironment, as described in section 'tumor microenvironment'. The concept of the EPR effect was first described by Matsumura and Maeda by using one of the first protein-polymer conjugates (smancs) [29]. The enhanced drug-carrier system effect was achieved due to decreased systemic drug elimination through renal excretion, prolonged circulation, low tumor lymphatic drainage, and tumor hyperpermeability, currently known as the passive targeting phenomenon. Due to these features, drug delivery systems can reach levels 10 to 100 times higher in tumor tissue in comparison with classical chemotherapeutics [35].

Passive targeting approaches using nanoparticles have been largely used in clinical setting as the treatment results in fewer side effects compared to classical chemotherapeutics. However, delivery of the 'nanomedicine' to the interstitial fluid through the EPR effect does not guarantee *intracellular* delivery of the therapeutic drug. For optimal drug delivery to tumors, drug carriers must deliver their payload into the tumor cells [36]. Due to the non-specific process of passive targeting, drug carriers deliver their payload not only to (tumor) cells, but also in the interstitial fluid in the vicinity of tumor tissue. The consequence of drug release in the interstitium can result in multidrug resistance [37,38], because anti-tumor drug concentrations are too low which allows resistant tumor cells to

remove the drug by an efflux pump [39]. To overcome these limitations and to achieve enhanced drug delivery, the active targeting approach is being developed.

Active targeting

The opposite of passive targeting, 'active targeting', relies on the use of components such as antibodies and peptides with specific binding affinities for tumor targets such as receptors, and that are bound to the drug carrier systems. This approach also takes advantage of the EPR effect for accumulation of the drug carrier system into the interstitial fluid of the tumor. However, a certain class of ligands can facilitate the entry of nanoparticles to tumor cells via receptor-mediated endocytosis, after which they can release their drug payload to provide a therapeutic effect [40]. Examples of potential targets for actively targeted nanomedicine formulation to tumor cells are folate [41,42], transferrin [43,44], and mucin-1 [45,46].

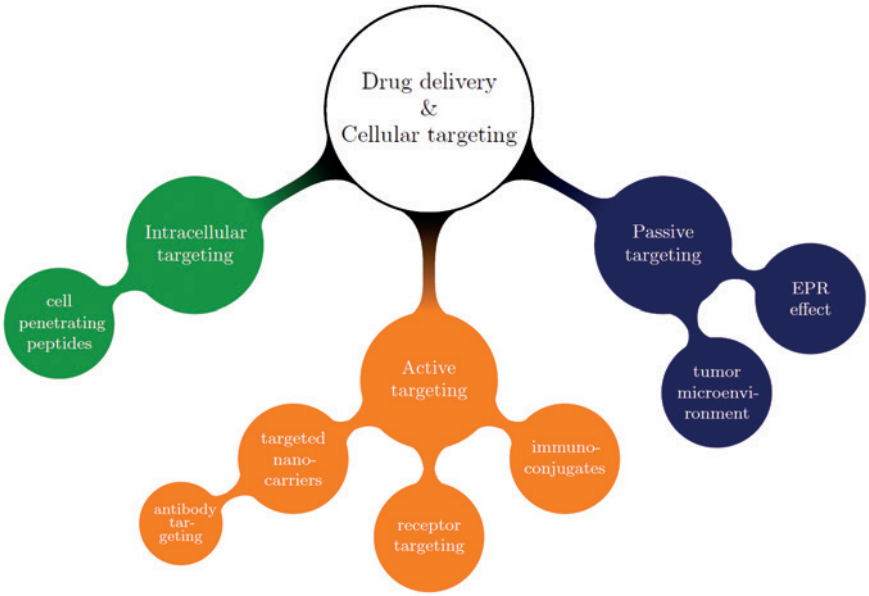

Figure 2 Current approaches in drug delivery can be divided into passive, active, and intracellular targeting mechanisms. To employ passive targeting, the tumor microenvironment and enhanced permeability (EPR) effect are important parameters for nanoparticles to extravagate to the tumor site. In order to actively target tumor cells, this can be performed by targeted nanocarriers (antibody targeting), receptor targeting or by using immunoconjugates. To enhance intracellular drug delivery cell penetrating peptides can be employed.

Enhanced intracellular uptake by cell penetrating peptides

The inability of therapeutics to reach their designated intracellular target site is one of the main obstacles for administering active molecules, particularly where cell membranes prevent nanoparticulate drug delivery systems from entering the cell in the absence of active transport [47]. In order to overcome these limitations, cell penetrating peptides (CPPs) have been used for intracellular delivery of a broad variety of cargos including multiple nanoparticulate drug delivery systems [48]. Amongst all CPPs, transactivator of transcription (TAT) peptide has been the most widely exploited CPP for the intracellular delivery of different sized cargoes and/or drug delivery systems [49].

Although of considerable potential, CPPs also have some limitations. CPPs have the undesirable characteristic of non-specificity and can enter any cell they come into contact with [50]. This lack of selectivity can induce toxic effects in normal tissues. In addition, the stability of the peptide in biological systems is not optimal, since peptides can be enzymatically cleaved by plasma enzymes [51,52]. In order to prevent cleavage of the peptide, a protease-resistance D-form of the peptide is developed, instead of the naturally occurring L-amino acid form, that cannot be degraded by these enzymes [53]. This approach could overcome the cleavage of the peptide during circulation, however, non-specificity is still an obstacle. To overcome the non-specificity problem, CPPs may be incorporated in so called 'smart' drug delivery systems [54]. These comprise nanocarriers were CPPs are shielded by a polymer or antibody until arrival at the target site. The targeted antibodies provide specificity and via a stimulus-sensitive bond, protective moieties will be detached due to local environmental conditions (*e.g.* pH change) in order to achieve cellular uptake by the active CPP [47].

NANOPARTICLE PLATFORMS

Over the past three decades, considerable research efforts were put in the development of drug delivery systems using nanoparticles. Nanomedical approaches to drug delivery involve the development of nanoscale particles or macromolecules to improve the biological activity and pharmacokinetic profile of various drugs [55]. In recent years, a large variety of drug delivery systems have been developed. These classes of nanoparticles are discussed in more detail with the emphasis on protein-based nanoparticles.

Liposomes

Liposomes were first described in 1965 and are one of the first nanoparticle platforms to be applied in medicine [56]. Liposomes are spherical vesicles with an aqueous core and a single or multiple bilayered membrane structure composed of natural or synthetic lipids [14]. Lipids are characterized by their hydrophilic head and hydrophobic tail (Fig. 3). Depending on their design, they can range in size from tens of nanometers to several

micrometers [57]. For biomedical applications, liposomes have proven to be biocompatible, biodegradable, show low toxicity, can be manipulated with regard to liposomal size and can be modified to alter surface characteristics [58–60]. Liposomes are quickly removed from the circulation after administration. To improve the circulation half-life, liposomes need to be coated with polymers such as polyethylene glycol (PEG) to avoid recognition as foreign bodies by the immune system [61,62]. Furthermore, a wide range of therapeutics can be encapsulated in their internal aqueous compartment or embedded within the phospholipid bilayer. Currently, some liposomal formulations are in clinical use. Examples are Doxil, Caelyx, and Myocet, all nanometer-sized liposomes with encapsulated doxorubicin which are used to treat Kaposi's sarcoma, ovarian cancer, breast cancer and multiple myeloma [63–65]. However, the limited chemical and physical stability of liposomes during manufacturing and storage still poses a challenge [66].

Polymer-based nanoparticles

Polymeric nanoparticles can be produced from both natural and synthetic polymers. The most widely used polymers for nanoparticles are polylactic acid (PLA), polyglycolic acid (PGA), poly(lactide-co-glycolic) acid copolymer (PLGA), and [*N*-(2-hydroxypropyl)-methacrylamide copolymer (HPMA) [68,69]. For polymer-based nanoparticles for drug delivery, size generally ranges between 10 – 400 nm [70]. However, depending on the methodology, polymeric particles can be prepared up to hundreds of micrometers. Besides the variety in polymers, many different compositions of polymer-based nanoparticles are developed, including polymersomes, polymeric nanoparticles, dendrimers, polymeric micelles, and

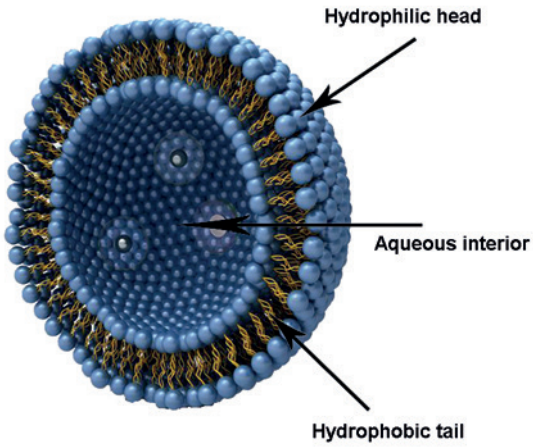

Figure 3 Schematic representation of a liposome formed by phospholipids in an aqueous solution. Figure was adapted from Izon [67]

polymer-drug conjugates (Fig. 4) [71]. Depending on their amphiphilicity, polymer-based nanoparticles can encapsulate hydrophilic or hydrophobic drug molecules and macromolecules such as proteins and nucleic acids [72,73]. Polymeric nanoparticles can be easily manipulated, without the loss of their physical, chemical, and biological properties.

This characteristic can be exploited to enhance the function of the nanoparticles in cancer therapy. For instance, attachment of tumor-specific targeting moieties and PEGylation is needed to improve residence time in the blood and reduce nonspecific distribution, transforming them into so called 'stealth' nanoparticles [74–76]. A well-known issue with biodegradable polymers is uncertainty with regard to the safety, as they may give harmful degradation products [21]. Because degradation often results in a range of fragment sizes, toxicity is challenging to determine experimentally. Currently, many polymer-based nanoparticles for drug delivery are under development and several are being evaluated in clinical trials [18,71]. Among these, Genexol-PM, (polymeric micelle with paclitaxel) is already approved for use in metastatic breast cancer patients in South Korea.

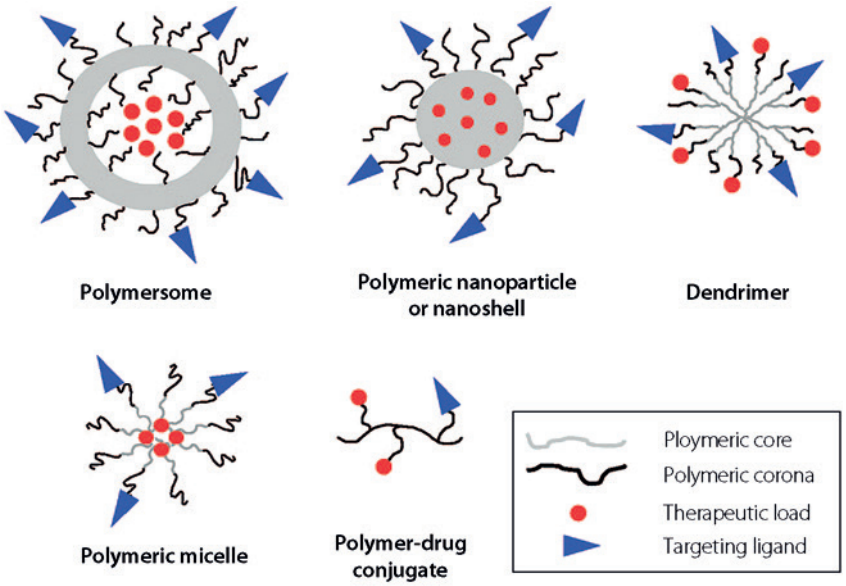

Figure 4 Polymeric nanoparticles platform. Schematic representation of different types of polymeric nanoparticles for drug delivery. Polymeric nanoparticles consist more or less of similar core materials. They can be used in different settings to prepared variety of nanoparticles, such as polymersomes, polymeric nanoparticles or nanoshells, dendrimers, polymeric micelles, and polymer-drug conjugates. Figure was adapted from Alexis *et al.* [71].

Protein-based drug delivery systems

In recent years, more research has focused on protein-based drug delivery systems due to their bioavailability, biocompatibility, and biodegradability coupled with low toxicity of their degradation products [77]. A variety of proteins has been used and characterized for drug delivery, such as albumin, gelatin, collagen, elastin, and casein [20]. Proteins are a class of natural molecules that have unique functionalities and potential applications in both biological as well as material fields and there are many different sizes and types of protein-based drug delivery systems, such as nanoparticles, microparticles, hydrogels, and films. Here, we will focus on the preparation of albumin-based nanoparticles.

Albumin nanoparticles

Albumin is a versatile protein carrier for drug delivery and an interesting material, because of its biodegradability, biocompatibility and its lack of toxicity [78]. Therefore, it is an ideal molecule to fabricate nanoparticles for drug delivery. Albumin-based nanoparticles are well tolerated by the body, as indicated by clinical studies with FDA approved albumin nano/micro particle formulations such as Albunex [79,80] and Abraxane [81,82]. Moreover, albumin drug delivery systems offer possibilities for surface modification due to the natural occurrence of functional groups (i.e. carboxylic and amine groups) enabling specific drug targeting to the site of action [83]. Albumin-based systems are considered safe since they are metabolizable *in vivo* by digestive enzymes into innocuous peptides [21]. In addition, albumin is thought to facilitate endothelial transcytosis of unbound and albumin-bound plasma constituents into the extravascular space. This process is initiated by binding of albumin to a cell surface, 60 kDa glycoprotein (gp60) receptor, to extravagate from the circulation as demonstrated for Abraxane [84].

Albumin-based lyophilisomes

Lyophilisomes are a novel class of proteinaceous biodegradable nano/micro drug delivery capsules prepared by freezing, annealing and lyophilization [85]. This methodology results in globular structures ranging in the nano- and micro size range. The proposed mechanism of capsule formation comprises a three step procedure (freezing – annealing – lyophilization).
Fast-freezing of biomolecules in solution (Fig. 5, step 1) results in phase separation between water (the main solvent) and biomolecule, which become organized into sheets (Fig. 5, step 2). Annealing (heating the preparation, but keeping the mixture under 0° C) rearranges the sheets into spheres and lyophilization transforms spheres into capsules, most likely through a 3D analogy of the coffee-stain mechanism (Fig. 5, step 3).
The system is highly flexible, allowing the incorporation of virtually any biomolecule in the wall and/or lumen. For instance, enzymes incorporated in the capsule wall and the lumen still exerted their biological activity, partly due to mild preparation conditions applied [85]. Lyophilisomes made of albumin may show potential as a carrier system to be used as a delivery system for anti-tumor drugs.

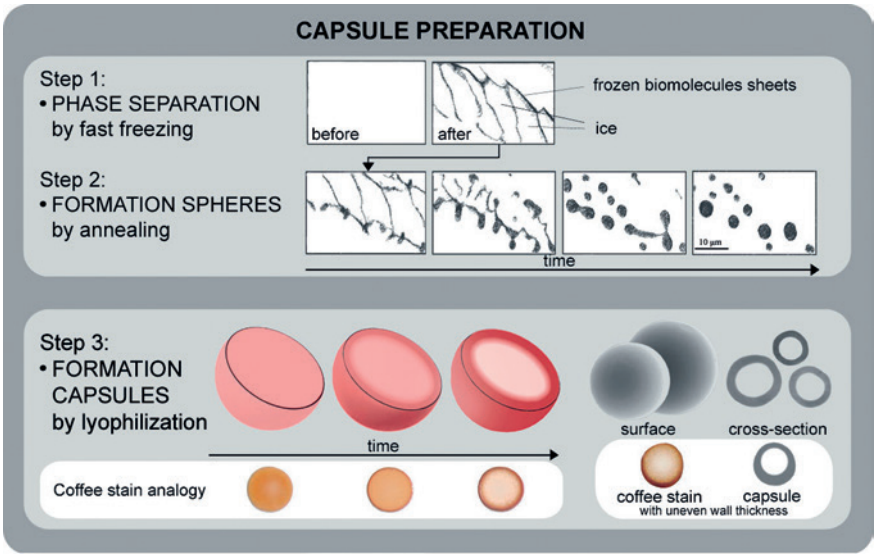

Figure 5 Cartoon of the proposed lyophilisome capsule formation. Capsule formation comprises a three-step procedure (freezing–annealing–lyophilization). Fast-freezing of biomolecules in solution (left upper panel) results in phase separation between water (the main solvent) and biomolecules, which become organized into sheets (right upper panel). Annealing rearranges the sheets into spheres and lyophilization transforms spheres into capsules, most likely due to a 3D analogy of the coffee-stain mechanism. Figure was adapted from Daamen *et al.* [85]. Copyright Wiley-VCH Verlag GmbH & Co. KGaA. Reproduced with permission.

AIMS AND OUTLINE OF THESIS

Nanotechnology is a field of research at the crossroads of biology, chemistry, physics, engineering, and medicine. Design of multifunctional nanoparticles capable of targeting cancer cells, and delivering and releasing drugs in a regulated manner are the future application of nanotechnology to oncological diseases. The aim of the research described in this thesis is to prepare and functionalize lyophilisomes made from albumin in order to obtain albumin-based nanoparticles that can act as a drug delivery system and eliminate ovarian tumor cells. In **chapter 1**, an overview of the most commonly used drug delivery systems is given and different strategies to target tumors more efficiently are discussed. **Chapter 2** demonstrates that lyophilisomes show potential to act as a drug delivery system, as they were internalized by tumor cells and doxorubicin and curcumin loaded lyophilisomes were able to eliminated ovarian tumor cells *in vitro*. In addition, an adjusted lyophilisome methodology is described that results in a more monodisperse particle

population. In **chapter 3**, lyophilisomes were modified with hKC4-antibodies against mucin-1 (MUC1) and shown to specifically target ovarian tumor cells overexpressing MUC1 antigen. In **Chapter 4**, lyophilisomes were modified with cell penetrating peptides to facilitate their cellular uptake, which may result in a more efficient therapeutic outcome. Moreover, an additional technique (fluorescent activated cell sorting) is described to select lyophilisomes below 1,000 nm. **Chapter 5** describes the biodistribution of albumin-based lyophilisomes intravenously injected in mice. In addition, a new methodology to size-select lyophilisomes more precisely and with a higher absolute yield is given. **Chapter 6** concludes this thesis with a summary and future prospective.

REFERENCES

1. World Health Organization (2007) Cancer Control: Knowledge into Action. WHO Guide for Effective Programmes. Palliative Care.
2. Danhier F, Feron O, Preat V (2010) To exploit the tumor microenvironment: Passive and active tumor targeting of nanocarriers for anti-cancer drug delivery. J Control Release 148: 135-146.
3. Byrne JD, Betancourt T, Brannon-Peppas L (2008) Active targeting schemes for nanoparticle systems in cancer therapeutics. Adv Drug Deliv Rev 60: 1615-1626.
4. Feld J, Barta SK, Schinke C, Braunschweig I, Zhou Y, *et al.* (2013) Linked-in: design and efficacy of antibody drug conjugates in oncology. Oncotarget 4: 397-412.
5. Mathe G, Tran Ba LO, Bernard J (1958) Effect on mouse leukemia 1210 of a combination by diazo-reaction of amethopterin and gamma-globulins from hamsters inoculated with such leukemia by heterografts. C R Hebd Seances Acad Sci 246: 1626-1628.
6. Carter PJ, Senter PD (2008) Antibody-drug conjugates for cancer therapy. Cancer J 14: 154-169.
7. De Jong WH, Borm PJ (2008) Drug delivery and nanoparticles:applications and hazards. Int J Nanomedicine 3: 133-149.
8. Cho K, Wang X, Nie S, Chen ZG, Shin DM (2008) Therapeutic nanoparticles for drug delivery in cancer. Clin Cancer Res 14: 1310-1316.
9. Sanvicens N, Marco MP (2008) Multifunctional nanoparticles--properties and prospects for their use in human medicine. Trends Biotechnol 26: 425-433.
10. Fadeel B, Garcia-Bennett AE (2009) Better safe than sorry: Understanding the toxicological properties of inorganic nanoparticles manufactured for biomedical applications. Adv Drug Deliv Rev 62: 362-374.
11. Petros RA, Desimone JM (2010) Strategies in the design of nanoparticles for therapeutic applications. Nat Rev Drug Discov 9: 615-627.
12. Felice B, Prabhakaran MP, Rodriguez AP, Ramakrishna S (2014) Drug delivery vehicles on a nano-engineering perspective. Mater Sci Eng C Mater Biol Appl 41: 178-195.
13. Zhang Y, Chan HF, Leong KW (2013) Advanced materials and processing for drug delivery: the past and the future. Adv Drug Deliv Rev 65: 104-120.
14. Torchilin VP (2005) Recent advances with liposomes as pharmaceutical carriers. Nat Rev Drug Discov 4: 145-160.
15. Al-Jamal WT, Kostarelos K (2011) Liposomes: from a clinically established drug delivery system to a nanoparticle platform for theranostic nanomedicine. Acc Chem Res 44: 1094-1104.
16. Mikhaylov G, Mikac U, Magaeva AA, Itin VI, Naiden EP, *et al.* (2011) Ferri-liposomes as an MRI-visible drug-delivery system for targeting tumours and their microenvironment. Nat Nanotechnol 6: 594-602.
17. Mora-Huertas CE, Fessi H, Elaissari A (2010) Polymer-based nanocapsules for drug delivery. Int J Pharm 385: 113-142.
18. Duncan R (2006) Polymer conjugates as anticancer nanomedicines. Nat Rev Cancer 6: 688-701.
19. Vaidya A, Agarwal A, Jain A, Agrawal RK, Jain SK (2011) Bioconjugation of polymers: a novel platform for targeted drug delivery. Curr Pharm Des 17: 1108-1125.
20. Maham A, Tang Z, Wu H, Wang J, Lin Y (2009) Protein-based nanomedicine platforms for drug delivery. Small 5: 1706-1721.
21. Elzoghby AO, Samy WM, Elgindy NA (2012) Protein-based nanocarriers as promising drug and gene delivery systems. J Control Release 161: 38-49.
22. Neumann E, Frei E, Funk D, Becker MD, Schrenk HH, *et al.* (2010) Native albumin for targeted drug delivery. Expert Opin Drug Deliv 7: 915-925.
23. Folkman J (1971) Tumor angiogenesis: therapeutic implications. N Engl J Med 285: 1182-1186.
24. Bergers G, Benjamin LE (2003) Tumorigenesis and the angiogenic switch. Nat Rev Cancer 3: 401-410.
25. Carmeliet P (2000) Mechanisms of angiogenesis and arteriogenesis. Nat Med 6: 389-395.
26. Stollman TH, Ruers TJ, Oyen WJ, Boerman OC (2009) New targeted probes for radioimaging of angiogenesis. Methods 48: 188-192.
27. Baeriswyl V, Christofori G (2009) The angiogenic switch in carcinogenesis. Semin Cancer Biol 19: 329-337.
28. Torchilin V (2011) Tumor delivery of macromolecular drugs based on the EPR effect. Adv Drug Deliv Rev 63: 131-135.

29. Matsumura Y, Maeda H (1986) A new concept for macromolecular therapeutics in cancer chemotherapy: mechanism of tumoritropic accumulation of proteins and the antitumor agent smancs. Cancer Res 46: 6387-6392.
30. Maeda H, Wu J, Sawa T, Matsumura Y, Hori K (2000) Tumor vascular permeability and the EPR effect in macromolecular therapeutics: a review. J Control Release 65: 271-284.
31. Hofheinz RD, Gnad-Vogt SU, Beyer U, Hochhaus A (2005) Liposomal encapsulated anti-cancer drugs. Anticancer Drugs 16: 691-707.
32. Gaumet M, Vargas A, Gurny R, Delie F (2008) Nanoparticles for drug delivery: the need for precision in reporting particle size parameters. Eur J Pharm Biopharm 69: 1-9.
33. Decuzzi P, Godin B, Tanaka T, Lee SY, Chiappini C, *et al.* (2010) Size and shape effects in the biodistribution of intravascularly injected particles. J Control Release 141: 320-327.
34. Torchilin VP (2010) Passive and active drug targeting: drug delivery to tumors as an example. Handb Exp Pharmacol 3-53.
35. Park K (2012) Polysacharide-based near-infrared fluorescence nanoprobes for cancer diagnosis. Quant Imaging Med Surg 2: 106-113.
36. Tang J, Zhang L, Liu Y, Zhang Q, Qin Y, *et al.* (2013) Synergistic targeted delivery of payload into tumor cells by dual-ligand liposomes co-modified with cholesterol anchored transferrin and TAT. Int J Pharm 454: 31-40.
37. Gottesman MM (1993) How cancer cells evade chemotherapy: sixteenth Richard and Hinda Rosenthal Foundation Award Lecture. Cancer Res 53: 747-754.
38. Simon SM, Schindler M (1994) Cell biological mechanisms of multidrug resistance in tumors. Proc Natl Acad Sci U S A 91: 3497-3504.
39. Ullah MF (2008) Cancer multidrug resistance (MDR): a major impediment to effective chemotherapy. Asian Pac J Cancer Prev 9: 1-6.
40. Kirpotin DB, Drummond DC, Shao Y, Shalaby MR, Hong K, *et al.* (2006) Antibody targeting of long-circulating lipidic nanoparticles does not increase tumor localization but does increase internalization in animal models. Cancer Res 66: 6732-6740.
41. Wang S, Low PS (1998) Folate-mediated targeting of antineoplastic drugs, imaging agents, and nucleic acids to cancer cells. J Control Release 53: 39-48.
42. Wang X, Li J, Wang Y, Cho KJ, Kim G, *et al.* (2009) HFT-T, a targeting nanoparticle, enhances specific delivery of paclitaxel to folate receptor-positive tumors. ACS Nano 3: 3165-3174.
43. Qian ZM, Li H, Sun H, Ho K (2002) Targeted drug delivery via the transferrin receptor-mediated endocytosis pathway. Pharmacol Rev 54: 561-587.
44. Anabousi S, Bakowsky U, Schneider M, Huwer H, Lehr CM, *et al.* (2006) In vitro assessment of transferrin-conjugated liposomes as drug delivery systems for inhalation therapy of lung cancer. Eur J Pharm Sci 29: 367-374.
45. Savla R, Taratula O, Garbuzenko O, Minko T (2011) Tumor targeted quantum dot-mucin 1 aptamer-doxorubicin conjugate for imaging and treatment of cancer. J Control Release 153: 16-22.
46. Yu C, Hu Y, Duan J, Yuan W, Wang C, *et al.* (2011) Novel aptamer-nanoparticle bioconjugates enhances delivery of anticancer drug to MUC1-positive cancer cells in vitro. PLoS One 6: e24077.
47. Koren E, Torchilin VP (2012) Cell-penetrating peptides: breaking through to the other side. Trends Mol Med 18: 385-393.
48. Torchilin VP (2008) Tat peptide-mediated intracellular delivery of pharmaceutical nanocarriers. Adv Drug Deliv Rev 60: 548-558.
49. Sawant R, Torchilin V (2010) Intracellular transduction using cell-penetrating peptides. Mol Biosyst 6: 628-640.
50. Martin I, texeidó M, Giralt E (2010) Building Cell Selectivity into CPP-Mediated Strategies. Pharmaceuticals 3: 1456-1490.
51. Grunwald J, Rejtar T, Sawant R, Wang Z, Torchilin VP (2009) TAT peptide and its conjugates: proteolytic stability. Bioconjug Chem 20: 1531-1537.
52. Koren E, Apte A, Sawant RR, Grunwald J, Torchilin VP (2011) Cell-penetrating TAT peptide in drug delivery systems: proteolytic stability requirements. Drug Deliv 18: 377-384.
53. Verdurmen WP, Bovee-Geurts PH, Wadhwani P, Ulrich AS, Hallbrink M, *et al.* (2011) Preferential uptake of L- versus D-amino acid cell-penetrating peptides in a cell type-dependent manner. Chem Biol 18: 1000-1010.

54. Torchilin V (2009) Multifunctional and stimuli-sensitive pharmaceutical nanocarriers. Eur J Pharm Biopharm 71: 431-444.
55. Davis ME, Chen ZG, Shin DM (2008) Nanoparticle therapeutics: an emerging treatment modality for cancer. Nat Rev Drug Discov 7: 771-782.
56. Bangham AD (1993) Liposomes: the Babraham connection. Chem Phys Lipids 64: 275-285.
57. Lelkes PI (1990) Liposomes: a practical approach. New RRC 49.
58. Torchilin VP (2006) Multifunctional nanocarriers. Adv Drug Deliv Rev 58: 1532-1555.
59. Gómez-Hens A, Fernández-Romero JM (2012) Analytical methods for the control of liposomal delivery systems. Trends in Analytical Chemistry 25: 167-178.
60. Bae SJ, Jung S, Um SH (2011) Budding dynamics of the lipid membrane. J Nanosci Nanotechnol 11: 6172-6176.
61. Romberg B, Hennink WE, Storm G (2008) Sheddable coatings for long-circulating nanoparticles. Pharm Res 25: 55-71.
62. Moghimi SM, Hunter AC, Murray JC (2001) Long-circulating and target-specific nanoparticles: theory to practice. Pharmacol Rev 53: 283-318.
63. Allen TM, Cullis PR (2004) Drug delivery systems: entering the mainstream. Science 303: 1818-1822.
64. Duggan ST, Keating GM (2011) Pegylated liposomal doxorubicin: a review of its use in metastatic breast cancer, ovarian cancer, multiple myeloma and AIDS-related Kaposi's sarcoma. Drugs 71: 2531-2558.
65. Slingerland M, Guchelaar HJ, Gelderblom H (2012) Liposomal drug formulations in cancer therapy: 15 years along the road. Drug Discov Today 17: 160-166.
66. Zhang JA, Pawelchak J (2000) Effect of pH, ionic strength and oxygen burden on the chemical stability of EPC/cholesterol liposomes under accelerated conditions. Part 1: Lipid hydrolysis. Eur J Pharm Biopharm 50: 357-364.
67. 2014) Izon website. http://www.izon.com/media/webinars/.
68. Hans ML, Lowman AM (2002) Biodegradable nanoparticles for drug delivery and targeting. Curr Opin Solid State Mater Sci 6: 319-327.
69. Tian H, Tang Z, Zhuang X, Chen X, Jing X (2011) Biodegradable synthetic polymers: Preparation, functionalization and biomedical application. Prog Polym Sci 37: 237-280.
70. Rao JP, Geckeler EG (2011) Polymer nanoparticles: Preparation techniques and size-control parameters. Prog Polym Sci 36: 887-913.
71. Alexis F, Pridgen E, Molnar LK, Farokhzad OC (2008) Factors affecting the clearance and biodistribution of polymeric nanoparticles. Mol Pharm 5: 505-515.
72. Amjadi I, Rabiee M, Hosseini MS, Mozafari M (2012) Synthesis and Characterization of Doxorubicin-Loaded Poly(Lactide-co-glycolide) Nanoparticles as a Sustained-Release Anticancer Drug Delivery System. Appl Biochem Biotechnol 168: 1434-1447.
73. Park JH, Lee S, Kim JH, Park K, Kim K, *et al.* (2007) Ploymeric nanomdicine for cancer therapy. Prog Polym Sci 33: 113-137.
74. Jokerst JV, Lobovkina T, Zare RN, Gambhir SS (2011) Nanoparticle PEGylation for imaging and therapy. Nanomedicine (Lond) 6: 715-728.
75. Cardoso MM, Peca IN, Roque AC (2012) Antibody-conjugated nanoparticles for therapeutic applications. Curr Med Chem 19: 3103-3127.
76. van Vlerken LE, Amiji MM (2006) Multi-functional polymeric nanoparticles for tumour-targeted drug delivery. Expert Opin Drug Deliv 3: 205-216.
77. Jahanshahi M, Babaei Z (2008) Protein nanoparticle: A unique system as drug delivery vehicles. Afr J Biotechnol 7: 4926-4934.
78. Kratz F (2008) Albumin as a drug carrier: design of prodrugs, drug conjugates and nanoparticles. J Control Release 132: 171-183.
79. Feinstein SB, Cheirif J, Ten Cate FJ, Silverman PR, Heidenreich PA, *et al.* (1990) Safety and efficacy of a new transpulmonary ultrasound contrast agent: initial multicenter clinical results. J Am Coll Cardiol 16: 316-324.
80. Geny B, Mettauer B, Muan B, Bischoff P, Epailly E, *et al.* (1993) Safety and efficacy of a new transpulmonary echo contrast agent in echocardiographic studies in patients. J Am Coll Cardiol 22: 1193-1198.
81. Ibrahim NK, Desai N, Legha S, Soon-Shiong P, Theriault RL, *et al.* (2002) Phase I and pharmacokinetic study of ABI-007, a Cremophor-free, protein-stabilized, nanoparticle formulation of paclitaxel. Clin Cancer Res 8: 1038-1044.

82. Ibrahim NK, Samuels B, Page R, Doval D, Patel KM, *et al.* (2005) Multicenter phase II trial of ABI-007, an albumin-bound paclitaxel, in women with metastatic breast cancer. J Clin Oncol 23: 6019-6026.
83. Elzoghby AO, Samy WM, Elgindy NA (2011) Albumin-based nanoparticles as potential controlled release drug delivery systems. J Control Release 157: 168-182.
84. Hawkins MJ, Soon-Shiong P, Desai N (2008) Protein nanoparticles as drug carriers in clinical medicine. Adv Drug Deliv Rev 60: 876-885.
85. Daamen WF, Geutjes PJ, Nillesen STM, Van Moerkerk HTB, Wismans R, *et al.* (2007) Lyophilisomes: A new type of (bio)capsules. Adv Mater 19: 673-677.

2

Lyophilisomes as a new generation of drug delivery capsules

Etienne van Bracht, René Raavé, Wouter P.R. Verdurmen,
Ronnie G. Wismans, Paul J. Geutjes, Roland E. Brock,
Egbert Oosterwijk, Toin H. van Kuppevelt, Willeke F. Daamen

International Journal of Pharmaceutics, Volume 439, Issue 1-2, Page: 127-135, 2012

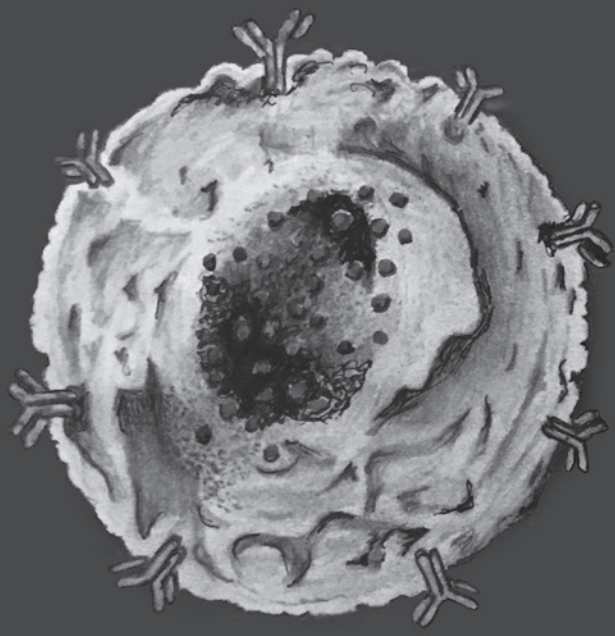

ABSTRACT

Nanoparticulate drug delivery systems are currently explored to overcome critical challenges associated with classical administration forms. In this study, we present a drug delivery system based on a novel class of proteinaceous biodegradable nano/micro capsules, lyophilisomes. Lyophilisomes can be prepared from biomolecules without the need for amphiphilicity. Albumin-based lyophilisomes were prepared by freezing, annealing and lyophilizing, resulting in capsules ranging from 100 to 3,000 nm. Lyophilisomes were loaded with the anti-tumor drugs doxorubicin and curcumin using different concentrations and time/temperature regimes. Incubation in 0.1 mg/ml doxorubicin or 1.0 mg/ml curcumin resulted in an entrapment efficiency of 95±1% and 4±1%, respectively. This corresponds to a drug loading of 0.24 mg doxorubicin per milligram albumin and 0.10 mg curcumin per milligram albumin. Drug release profiles from doxorubicin and curcumin-loaded lyophilisomes were studied in culture medium and showed slow release for doxorubicin (2.7% after 72 h), and rapid release for curcumin (55% after 72 h). When applied to cells, non-loaded lyophilisomes did not influence cell viability, even at high concentrations (1 mg/ml). Lyophilisomes were internalized by cells. When loaded with doxorubicin and curcumin, lyophilisomes strongly reduced cell proliferation and viability of SKOV-3 and HeLa cells, respectively, to a level similar or better compared to an equal amount of free drugs. In conclusion, albumin lyophilisomes show potential as (nano)carriers of drugs for tumor cell elimination.

INTRODUCTION

The potency of a cancer therapeutic is determined by its ability to eliminate cancerous tissue without damaging surrounding healthy tissue. Anti-tumor drugs are usually distributed non-specifically throughout the body, thereby affecting healthy tissues as well. To generate a successful therapeutic device, it is essential to develop systems which increase drug concentrations in a site-specific manner [1]. Nano/micro carrier drug delivery systems including polymeric particles and liposomes protect the drug from the environment, and may prolong drug retention time, reduce clearance and minimize side effects [2–4]. For biomedical applications, it would be advantageous if capsules could be prepared from a wide repertoire of natural (proteinaceous) macromolecules, to address the variety of medical demands, such as site-specific delivery, receptor-mediated cellular uptake and physicochemical parameters such as pI and serum interaction.

Previously, our group described a new type of nano/micro biocapsule called "lyophilisome", which can be prepared from a diversity of water-soluble macromolecules, including proteins, without the need for amphiphilicity [5]. The use of proteins for fabrication of drug delivery systems is well described in literature, which has resulted in a growing interest in protein delivery carriers as they are generally regarded as safe [6]. Using this methodology, the composition of the capsule wall can be modified and additional components can be incorporated into the wall (*e.g.* enzymes) with preserved biological activity, enabling an adaption to various applications [5]. In tumor targeting, albumin is an interesting material for carrier-mediated drug delivery, because of its biodegradability, biocompatibility, its lack of toxicity and of immunogenicity [7]. Lyophilisomes made of albumin may therefore show potential as a carrier system to be used as a delivery system for anti-tumor drugs such as doxorubicin and curcumin.

Doxorubicin is widely used in cancer chemotherapy and has a broad range of reactivity, showing anti-neoplastic activity against a number of human cancers [8,9]. The drug acts as an DNA intercalating agent that inhibits the enzyme topoisomerase II essential for DNA replication, resulting in cell death [10]. However, its clinical use is seriously hampered due to severe side effects [11–13].

Curcumin is used for its anti-tumor, anti-oxidant, and anti-inflammatory properties [14–18]. It affects cell proliferation, differentiation and apoptosis and the anti-carcinogenic properties are most likely due to effects on multiple molecular targets [19,20]. However, the water solubility of free curcumin is poor (maximally 11 ng/ml) [21]. It is therefore not possible to administer curcumin systemically.

In this study, we formulate a new protein-based drug delivery system consisting of lyophilisomes prepared from albumin using a freezing, annealing and lyophilization regime, followed by drug-loading. The loading and release characteristics of doxorubicin and curcumin are studied, and cytotoxicity and cellular uptake are evaluated. Finally, the tumor cell eliminating potential of drug-loaded lyophilisomes is described.

MATERIALS & METHODS

Materials

Bovine serum albumin (BSA) was purchased from PAA Laboratories (Linz, Austria). Doxorubicin, curcumin, and fluorescein isothiocyanate (FITC) conjugated bovine albumin were purchased from Sigma Aldrich (Steinheim, Germany). Dylight 633 (amine reactive) was purchased from Pierce (Rockford, IL, USA). CellMask orange was purchased from Invitrogen (Breda, Netherlands). Glutaraldehyde and formaldehyde were obtained from Merck (Darmstadt, Germany).

Methods

Preparation of lyophilisomes

A solution of 0.25% (w/v) BSA in 0.01 M acetic acid (20 µl droplets) was frozen in liquid nitrogen (-196°C). Generally, we use 40 ml corresponding to 100 mg albumin (2.5 mg/ml). In order to visualize the lyophilisomes, FITC-conjugated albumin was added to non-labeled albumin (1:10) in the starting solution prior to the preparation of lyophilisomes. The frozen albumin preparation was incubated at -10 to -20°C for 3 h (annealing step), and subsequently lyophilized [5]. This procedure results in hollow nano/micro spheres ("lyophilisomes"). The exact conditions of the freeze drying program are presented in more detail in Table S1 (Supplementary data). To stabilize the lyophilisomes, vapor crosslinking was performed using a 1:1 mixture of 25% glutaraldehyde and 37% formaldehyde for 2 h. To quench free aldehydes, 3.5 mg lyophilisomes were incubated in 1 ml 1% (w/v) glycine (Scharlau, Barcelona, Spain) in phosphate buffered saline (PBS, pH 7.4). Using gentle sonication (Branson Sonifier 250, 10 s, output 20) lyophilisomes were separated, washed three times in combination with three to four low-speed centrifugation steps (60x *g*; Thermo, Heraeus Fresco 17; Newport Pagnell, Great Britain) to remove large lyophilisomes and sheet-like structures, until no pellet was observed. After this procedure, about 30% of the original weight of lyophilisomes remained. One fifth of this preparation (200 µg) was used for loading experiments and taken up in 500 µl of drug solution (see section 'Loading and visualization of doxorubicin and curcumin lyophilisomes').

In order to produce red fluorescent lyophilisomes, Dylight 633 was activated by a *N*-hydroxysuccinimide ester and conjugated to the free amine groups in albumin (according to the manufacturer's protocol), and subsequently dialyzed in 0.01 M acetic acid and mixed with non-labeled albumin in a 1:4 ratio, followed by lyophilisome preparation as earlier described.

Scanning electron microscopy

Lyophilisomes were deposited on poly-D-lysine coated cover slips or mounted on carbon tape, sputtered with gold, and analyzed using a JEOL JSM-6310 scanning electron microscope (Tokyo, Japan) at an accelerating voltage of 15 kV.

Transmission electron microscopy

Lyophilisomes were embedded in 1.5% (w/v) agarose, fixed in 2% (v/v) glutaraldehyde in 0.1 M phosphate buffer (pH 7.4), post-fixed with 1% (w/v) osmium tetroxide, dehydrated in an ascending series of ethanol, and embedded in Epon 812. Ultrathin sections (60 nm) were cut and picked up on Formvar-coated grids, post-stained with lead citrate and uranyl acetate, and examined in a JEOL 1010 transmission electron microscope (Tokyo, Japan).

Dynamic light scattering

Dynamic light scattering (DLS, Zetasizer Nano-S, Malvern Instruments Ltd., Malvern, UK) was used to measure particle size of lyophilisomes. Stabilized lyophilisomes were dispersed in 0.1% (v/v) Tween-20 (Sigma Aldrich, Steinheim, Germany) in PBS (PBS-T, pH 7.4) and analyzed by DLS.

Particle size measurements by qNano

The qNano was used to measure particle size of lyophilisomes [22]. Fluid cells were washed with de-izonized water and dried with a tissue. In the center of the lower fluid cell 80 µl standard electrolyte buffer, provided by manufacturer (Izon, Science Ltd., Burnside, New Zealand), was placed avoiding air bubbles. The membrane was mounted on the instrument. The upper fluid cell was placed into position and 50 µl of standard electrolyte buffer was added. Pore width was controlled by adjusting the arm of the tunable nanopore onto the holding stage, and voltage was controlled by the connected computer. To ensure a continuous flow of particles, a pore size of approximately 700 to 1,600 nm was used. At constant voltage (0.2 V), the pore was open when a direct correlation could be observed between ionic current and adjustment of the tunable arms of the nanopore. Finally, particles were added on the upper fluid cell for measurements. Data was analyzed with Izon Control Suite 2.1 software.

Loading and visualization of doxorubicin and curcumin lyophilisomes

Lyophilisomes (200 µg) were incubated overnight in 500 µl 0.1 and 1.0 mg/ml doxorubicin in 10 mM 4-(2-hydroxyethyl)-1-piperazineethanesulfonic acid (HEPES) buffer (pH 7.4; Promega, Madison, WI, USA), and 0.1 and 1.0 mg/ml curcumin in 100% (v/v) ethanol at either 4°C, room temperature or 37°C. Subsequently, they were centrifuged (17,000x *g*), washed three times in 1.0 ml 0.1% PBS-T and stored at 4°C. Loaded capsules were deposited on poly-D-lysine coated cover slips and the location of doxorubicin and curcumin in lyophilisomes was studied using confocal laser scanning microscopy (Olympus FV1000, Olympus GmbH, Hamburg, Germany) and analyzed with FV 10-ASW 1.6 Viewer software. FITC-lyophilisomes and curcumin were visualized with an argon laser at 488 nm, Dylight 633 lyophilisomes and doxorubicin with a diode laser at 559 and 635 nm, respectively.

Entrapment efficiency

The entrapment efficiency of doxorubicin and curcumin in lyophilisomes was determined as follows: lyophilisomes were separated from the free drug using centrifugation (17,000x *g*) and washed three times in 1.0 ml PBS-T. The supernatant with free drug was collected and absorbance was measured spectrophotometrically using a Synergy 2 plate reader at 490 nm for doxorubicin and 420 nm for curcumin (Biotek, Winooski, VT) assuming that drug not present in the supernatant was entrapped in lyophilisomes [23,24]. The concentration was calculated using a calibration curve of doxorubicin and curcumin in HEPES buffer and ethanol respectively and all measurements were performed in triplicate. Entrapment efficiency was calculated as follows:

$$\text{Entrapment efficiency (\%)} = \frac{[\text{Drug}]_{\text{total}} - [\text{Drug}]_{\text{free}}}{[\text{Drug}]_{\text{total}}} \times 100$$

Drug release from doxorubicin and curcumin loaded lyophilisomes

Drug release from loaded lyophilisomes was examined at three temperatures (4°C, room temperature, and 37°C), at three time points (24, 48, and 72 h) and both in PBS and culture medium. Lyophilisomes (200 µg) were loaded with 500 µl of 0.1 mg/ml doxorubicin and 1.0 mg/ml curcumin at room temperature as described above. Subsequently, samples were centrifuged (17,000x *g*, 5 min, 4°C) and washed three times in 1.0 ml PBS. Pellets were resuspended in 500 µl PBS or culture medium (RPMI 1640 + L-glutamine without phenol red, Gibco Karlsruhe, Germany). Culture medium was supplemented with 10% (v/v) heat-inactivated fetal calf serum (FCS; PAA Laboratories, Pasching, Austria). In this study, curcumin was dissolved in ethanol prior to loading. Released curcumin precipitated in the medium and was dissolved in ethanol and measured spectrophotometrically. Release was determined spectrophotometrically at 490 nm for doxorubicin and 420 nm for curcumin, and calculated as follows:

$$\text{Release (\%)} = \frac{[\text{Drug}]_{\text{released}}}{[\text{Drug}]_{\text{total}}} \times 100$$

Cell culture

All culture media were purchased from Gibco (Karlsruhe, Germany) unless indicated otherwise. The human ovarian cancer cell line SKOV-3 was cultured in McCoy 5A GlutaMAX medium supplemented with 10% (w/v) FCS. HeLa cells were cultured in RPMI 1640 GlutaMAX supplemented with 10% (w/v) FCS. The cells were cultured in a humidified atmosphere with 5% CO_2 at 37°C. Subconfluent cells were dissociated with 0.05% (w/v) trypsin and 0.02% (w/v) ethylenediaminetetraacetic acid (EDTA) in Dulbecco's-PBS (PAA Laboratories, Pasching, Austria) and were maintained as proliferating cultures.

Cytotoxicity studies

To investigate the cell viability of cancer cells exposed to lyophilisomes with and without doxorubicin or curcumin, the 4-[3-(4-iodophenyl)-2-(4-nitrophenyl)-2H-5-tetrazolio]-1,3-benzene disulfonate (WST-1, Roche Diagnostics, Mannheim, Germany) cell proliferation assay was performed. SKOV-3 cells were chosen to analyze the cell eliminating potential of doxorubicin loaded lyophilisomes because this drug is frequently used to treat ovarian cancer [25,26]. HeLa cells were used to examine the effect of curcumin-loaded lyophilisomes, since this tumor cell line is susceptible to the cytotoxic effect of curcumin [23,27]. To access the efficiency of doxorubicin or curcumin on SKOV-3 and HeLa cells, free doxorubicin or curcumin was added to cells in an ascending concentration (0, 1, 5, 10, 20 and 50 µM). To efficiently eliminate SKOV-3 and HeLa cells, 20 µM of free doxorubicin or curcumin was required. For curcumin, a stock solution (2 mM) was prepared in ethanol. This was further diluted in medium before adding to the cell culture. As a control, ethanol only was added in equal concentration to cells and this did not affect cell viability (results not shown). Cells were seeded into 96-well plates at a concentration of 2,000 cells per well. On the next day, equivalent amounts of free and lyophilisome-incorporated doxorubicin/curcumin were added corresponding to 20 µM of the drug. As a control, a similar concentration of empty lyophilisomes was added. After 24, 48, and 72 h, medium was replaced, WST-1 reagent was added and incubated for 2 – 4 h at 37°C. Absorbance was analyzed using a Synergy 2 plate reader at 410 nm. Untreated cells served as a control. All experiments were performed in triplicate.

Intracellular uptake study

To study internalization of lyophilisomes, confocal microscopy was performed on living cells. Cells were cultured up to 80% confluency and incubated with 50 µl of lyophilisome suspension (lyophilisome content 125 µg/ml) for 24 h in RPMI medium containing 10% FCS. After incubation, cells were washed once, incubated for 5 min with CellMask orange (5 µg/ml) to visualize the cell membranes and then washed again, all with the same medium. Cells were kept at 37°C on a temperature controlled microscope stage and living cells were imaged immediately with a Leica SP5 confocal microscope (Leica Microsystems, Mannheim, Germany). FITC was excited at 488 nm and emission was collected between 500 and 550 nm. CellMask orange was excited at 561 nm and emission was collected between 570 and 650 nm. Images were recorded sequentially using Leica Application Suite Software (Advanced Fluorescence Lite, 2.3.0. build 5131).

Statistical analysis

Data are presented as mean with standard deviation. Drug entrapment experimental data were analyzed using two-tailed Student's *t*-tests. Cell eliminating potential assays were analyzed using two way Anova Bonferroni post tests. All statistical analyses were performed in Graphpad Prism 5.0 (Graphpad, San Diego, CA, USA).

RESULTS

Characterization of lyophilisomes

Lyophilisomes were prepared by a freezing, annealing and lyophilization regime, and analyzed by dynamic light scattering (DLS), qNano, scanning and transmission electron microscopy (SEM, TEM).

The size distribution of lyophilisomes is summarized in table 1. Using DLS, the mean particle diameter of lyophilisomes was measured 1,695±55 nm with a polydispersity index of 0.726±0.035. This indicates a rather heterogeneous particle size distribution. For DLS it is known that larger particles will dominate smaller particles during measurement, resulting in a larger mean particle size. When measuring the lyophilisomes using qNano, a mean particle size of 1,214±79 nm was found. Using this instrument, particles smaller than 700 nm were not detected with the specific pore used for our experiments (700 – 1,600 nm), since they were eliminated against background levels. To investigate the lyophilisome preparation further, SEM was used and revealed globular structures ranging from 100 nm up to 3,000 nm (Fig. 1a) and TEM verified that capsules indeed contained a lumen (Fig. 1b). Besides capsules, sheet-like structures were formed. In order to use lyophilisomes as a drug delivery system they were stabilized by crosslinking in the vapor of a mixture of glutaraldehyde and formaldehyde. Particles thus prepared did not coagulate and no aggregation was observed in buffer or culture medium.

Table 1 Size distribution of lyophilisomes

Stabilized lyophilisomes	DLS	qNano
Particle diameter (nm)	1,695 ± 55	1,214 ± 79
Polydispersity index	0.726 ± 0.035	N.A.[a]

[a]N.A. = Not available

Loading and visualization of doxorubicin and curcumin in lyophilisomes

To visualize entrapment of doxorubicin and curcumin within lyophilisomes and to demonstrate the drug distribution within the lyophilisomes, FITC- and Dylight 633 labeled lyophilisomes were used, respectively. For doxorubicin loaded FITC-lyophilisomes confocal microscopy showed red auto-fluorescence of doxorubicin within green-fluorescent lyophilisomes (Fig. 2a). Curcumin loaded Dylight 633 lyophilisomes (Fig. 2b) showed green auto-fluorescence of curcumin within the red-fluorescent Dylight 633 lyophilisomes. Both doxorubicin and curcumin showed a homogeneous distribution throughout the capsule lumen, but they were also visible in the capsule wall (Fig. 2a and b). The merged image

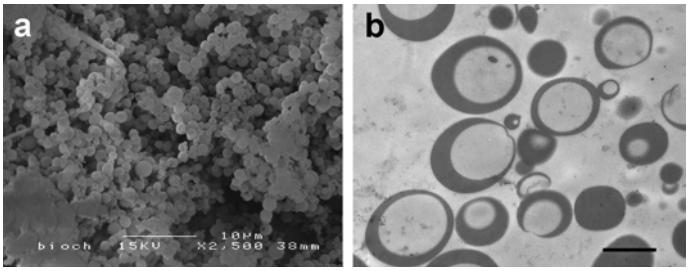

Figure 1 Scanning electron microscopical image (**a**) and transmission electron microscopical image (**b**) of lyophilisomes, showing spherical capsules ranging from 100 up to 3000 nm. Bar represents 10 µm in (**a**) and 1 µm in (**b**).

(Fig. 2a3 and b3) is an overlay of doxorubicin and curcumin in lyophilisomes (Fig. 2a2 and b2) and the corresponding lyophilisome image (Fig. 2a1 and b1).

For the loading of doxorubicin and curcumin in lyophilisomes, two concentrations were used at room temperature, *i.e.* 0.1 and 1.0 mg/ml. For doxorubicin, 0.1 mg/ml resulted in an entrapment efficiency of 95±1%. With 1.0 mg/ml, an entrapment efficiency of 48±2% was obtained (Fig. 2c). Despite this lower entrapment efficiency, the absolute amount of doxorubicin was 5 x higher when incubated at the higher concentration. This corresponds to a drug loading of 0.24 and 1.2 mg doxorubicin per milligram albumin (Table 2). For curcumin, an entrapment efficiency of 5±2% was achieved using 0.1 mg/ml curcumin. Using 1.0 mg/ml, entrapment was 4±1% resulting in an 8 x higher loading of curcumin (Fig. 2d). This corresponds to a drug loading of 0.01 and 0.10 mg curcumin per milligram albumin (Table 2). As an alternative to establish the amount of doxorubicin in lyophilisomes, they were digested using papain resulting in the liberation of the encapsulated doxorubicin that was measured spectrophotometrically. Using this method, a loading efficiency of 95% was calculated. To verify that the anti-tumor drugs were entrapped in lyophilisomes, bare lyophilisomes and doxorubicin and curcumin loaded lyophilisomes were centrifuged. Results show clear supernatants and colored pellets for doxorubicin and curcumin, indicating the absence of free anti-tumor drug (Fig. 2e). Use of other temperatures (4°C, 37°C) did not influence entrapment efficiency, which was 92 – 96% for doxorubicin and 3 – 5% for curcumin.

Drug release studies

The drug release of doxorubicin and curcumin from lyophilisomes was studied both in PBS and medium supplemented with 10% FCS, for a time period up to 72 h at 4°C, room temperature and 37°C. The release of doxorubicin from loaded lyophilisomes was limited, both for PBS and medium (Fig. 3a and b). The highest release was observed at 37°C, *i.e.*

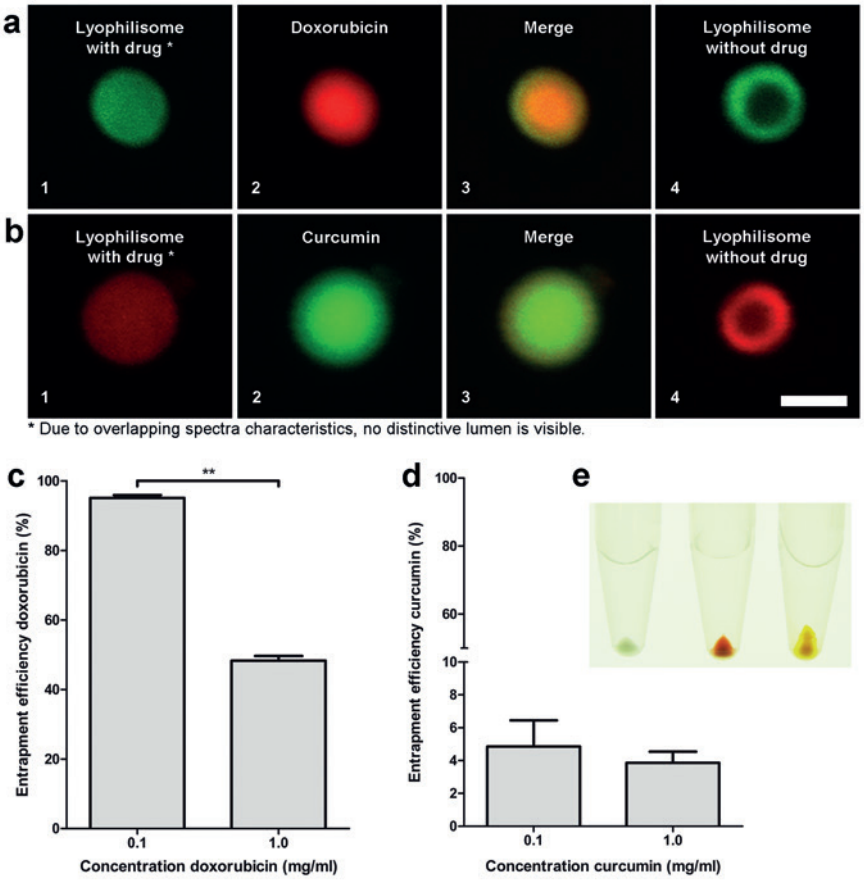

Figure 2 Visualization and loading efficiency of doxorubicin and curcumin in lyophilisomes. (**a** and **b**) Lyophilisomes after incubation in doxorubicin containing HEPES buffer (**a**) or curcumin in ethanol (**b**) result in entrapment of the drug. In a4 and b4, lyophilisomes are depicted without drug to show their lumen. Note that since both anti-tumor drugs are also visible at wavelengths used to visualize lyophilisomes the lumen cannot be visualized in the presence of the drugs. The merge image (a3 and b3) is an overlay of image (a1 and b1) and (a2 and b2). Bar represents 1 µm. c and d) Entrapment efficiency in lyophilisomes of doxorubicin (**c**) and curcumin (**d**) after overnight incubation of lyophilisomes in 0.1 and 1.0 mg/ml drug; **p<0.001. (**e**) Centrifuged lyophilisome suspensions (1: without drug; 2: with doxorubicin; 3: with curcumin) show a clear supernatant and white, red, and yellow pellet, indicating entrapment of the drugs.

Table 2 Drug entrapment in lyophilisomes

Drug	Content used for loading experiments (mg drug/ml)	Drug loading (mg drug/mg albumin)
Doxorubicin	0.1 mg/ml	0.24
	1.0 mg/ml	1.20
Curcumin	0.1 mg/ml	0.01
	1.0 mg/ml	0.10

2.4±0.4% and 2.7±0.3% after 72 h in PBS and medium, respectively. In contrast, curcumin-loaded lyophilisomes showed a much higher release, *i.e.* in PBS 42±5% at 24 h, 50±2% at 48 h, and 56±2% at 72 h (Fig. 3c and d). Similar releases were obtained for medium (46±4% at 24 h, 52±6% at 48 h, and 55±8% at 72 h). Temperature did not influence the release profile of curcumin loaded lyophilisomes.

Cell viability in the presence of lyophilisomes

In order to investigate whether lyophilisomes are cytocompatible, empty lyophilisomes were administered to cells in ascending concentrations, ranging from 0 to 1,000 µg/ml. Cell viability was not compromised as indicated by a WST-1 proliferation assay showing comparable values for SKOV-3 and HeLa cells with and without lyophilisomes (Fig. 4). Despite coverage of cells by lyophilisomes, also no detectable morphological changes were visible at the light microscopical level (data not shown).

Intracellular uptake of lyophilisomes

The ability of lyophilisomes to be internalized by cells was studied by confocal microscopy. HeLa cells were incubated with lyophilisomes and after 24 h uptake of lyophilisomes was observed (Fig. 5). When incubated with lyophilisomes, cells clearly contained green fluorescent hollow spheres at 24 h, representing the lyophilisomes (Fig. 5b). The plasma membrane dye CellMask further indicated that the lyophilisomes were indeed internalized and not merely associated with the plasma membrane. In addition, the corresponding bright field image showed that lyophilisomes did not lead to detectable morphological changes of the cells (Figure 5c and d), further corroborating the absence of cytotoxic effects.

Cell eliminating potential of lyophilisomes loaded with doxorubicin or curcumin

To compare the cell eliminating potential of both anti-tumor drug loaded lyophilisomes, a WST-1 proliferation assay was used. A concentration of 20 µM of free doxorubicin or free curcumin was required to eliminate SKOV-3 and HeLa cells, respectively. To assess the

effect of doxorubicin and curcumin loaded lyophilisomes on tumor cells, equivalent amounts of free and drug loaded lyophilisomes were used. As a control, a similar concentration of empty lyophilisomes was employed. Due to the high entrapment efficiency, doxorubicin loaded lyophilisomes with 0.1 mg/ml loading concentration were used. Since curcumin had a lower entrapment efficiency, lyophilisomes loaded with a 1.0 mg/ml curcumin solution were applied. Lyophilisome contents correspond to 50 – 100 µg/ml lyophilisomes, a concentration at which cell viability is ensured (Fig. 4).

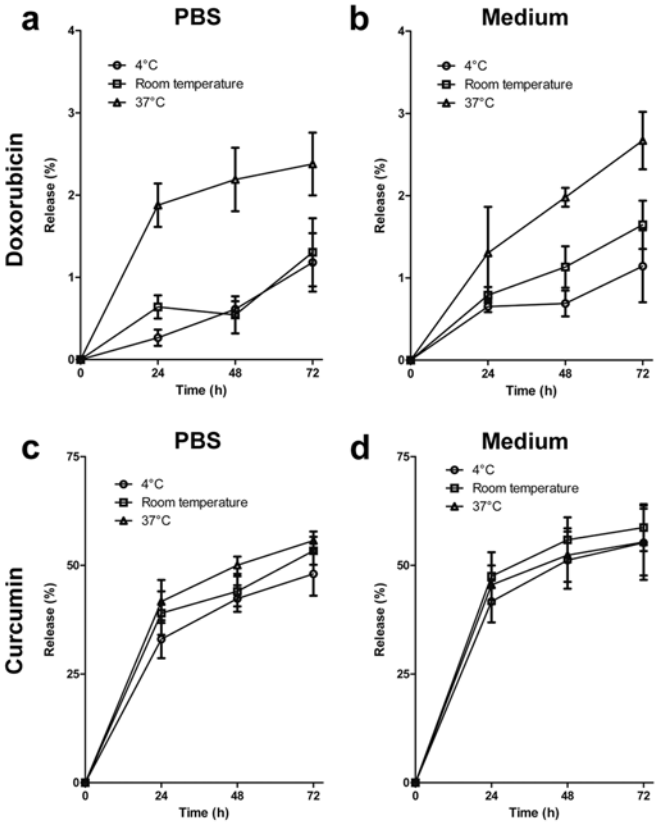

Figure 3 Drug release from doxorubicin and curcumin loaded lyophilisomes in PBS and medium. (**a** and **b**) Lyophilisomes were incubated in 0.1 mg/ml doxorubicin in HEPES buffer, washed three times, and release was analyzed in PBS and medium. A similar release profile was obtained for PBS (**a**) and medium (**b**) with a maximum release of 2.4±0.4% and 2.7±0.3% after 72 h. (**c** and **d**) Curcumin release profiles of loaded lyophilisomes after incubation in 1.0 mg/ml curcumin in ethanol and washing three times. Curcumin release was 56±2% and 55±8% after 72 h in PBS and medium, respectively. Note variation in the range of y-axis.

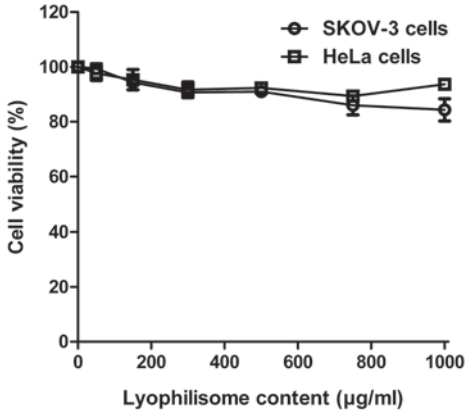

Figure 4 Cell viability of SKOV-3 and HeLa cells after incubation with lyophilisomes. Cells were exposed to various contents of empty lyophilisomes and cell viability assays (WST-1) were performed after 72 h. Cell viability was not affected by the presence of lyophilisomes.

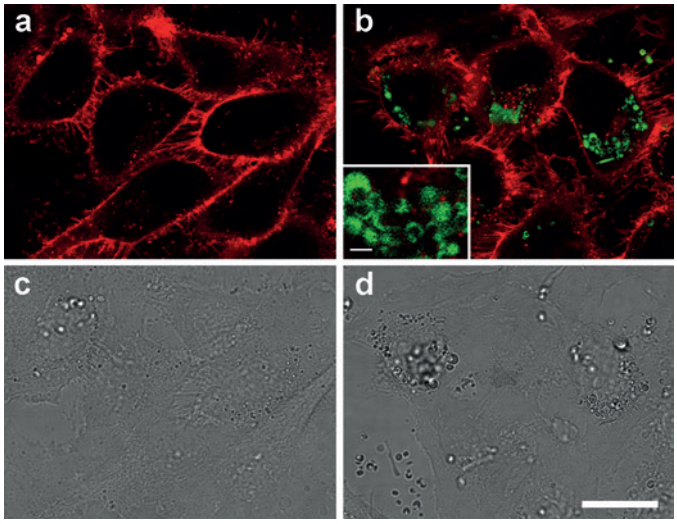

Figure 5 Cellular uptake of lyophilisomes studied by confocal laser scanning microscopy. HeLa cells were cultured in an 8-well microscopy chamber to 80% confluency and treated without (**a** and **c**) and with (**b** and **d**) lyophilisomes for 24 h. Note internalization of lyophilisomes (**b**). Inset: magnification of internalized lyophilisomes. Green fluorescence corresponds with FITC-lyophilisomes and fluorescence of CellMask orange is shown in red. Bright field images (**c** and **d**) show general morphology of the cells. The scale bar represents 20 µm in (**a**-**d**) and 2 µm in inset (b).

Exposure to doxorubicin-loaded lyophilisomes (corresponding to 20 µM free doxorubicin) inhibited SKOV-3 ovarian cancer cell growth in a time-dependent manner (Fig. 6a). Similar inhibition of cell proliferation was observed for free doxorubicin and entrapped doxorubicin, where entrapped doxorubicin only resulted in lower SKOV-3 cell viability at 24 h ($p<0.05$). After 72 h of culture, cell viability had decreased to 6% in comparison to cells treated with non-loaded lyophilisomes.

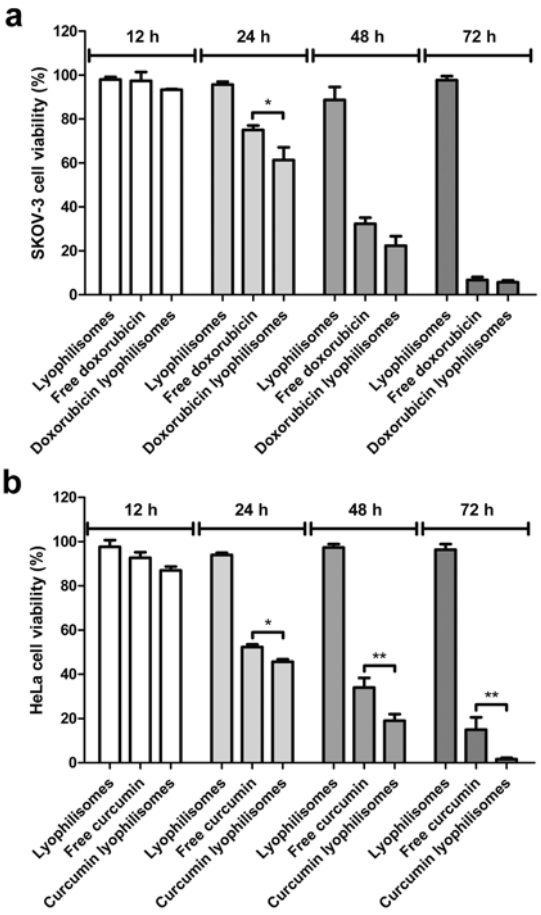

Figure 6 Time dependent effect of doxorubicin and curcumin loaded lyophilisomes on cell viability of SKOV-3 (**a**) and HeLa cells (**b**). Similar dosages of free doxorubicin/curcumin and doxorubicin/curcumin containing lyophilisomes were used, and cell viability was assayed using WST-1. (**a**) SKOV-3 cells generally responded to doxorubicin loaded lyophilisomes in a similar fashion as free doxorubicin. (**b**) HeLa cells showed a more pronounced response to curcumin loaded lyophilisomes compared to free curcumin at later time points. *$p<0.05$ **$p<0.001$.

When HeLa cells were incubated with curcumin loaded lyophilisomes (corresponding to 20 μM free curcumin) also a decrease in cell viability was observed. Curcumin loaded lyophilisomes exerted a more pronounced effect on the cancer cells as compared to free curcumin after 24 h ($p<0.05$), 48 h and 72 h ($p<0.001$; Fig. 6b). After 72 h of culture, cell viability had decreased to 2% in comparison to cells treated with non-loaded lyophilisomes. The low cell viability results for both SKOV-3 and HeLa cells after incubation with loaded lyophilisomes were consistent with the small remaining number of cells observed by light microscopy (data not shown).

DISCUSSION

In the past decade, the field of drug delivery for cancer has been revolutionized with the advent of nanotechnology, and biocompatible nanoparticles have been developed as systemic carriers for therapeutic compounds to target specific cells and tissues. Numerous investigations have been conducted to develop more efficient systems for drug delivery. The most important challenge in the formulation of drug delivery systems involves the preparation of carrier systems that are capable of encapsulating the desired drug and deliver it to the tumor tissue in its active form. Liposomes constitute an effective drug delivery system, as exemplified by Doxil [28]. However, their chemical and physical instability during manufacturing and storage still poses a challenge [29]. In a quest for stable and efficient carrier systems for anti-tumor agents, we have developed a drug delivery system named 'lyophilisomes' [5]. The process to produce lyophilisomes is physical rather than chemical in nature, and allows for the use of biological macromolecules, including proteins, as the wall material. Nanoparticles made from albumin are well tolerated by the body, as indicated by clinical studies with FDA approved albumin nano/micro particle formulations such as Albunex [30,31] and Abraxane [32,33].

Albumin is the main protein in the plasma and is best known for its remarkable ligand binding capacity, providing an arsenal of compounds with favorable, noncovalent reversible binding characteristics for transport in the body and release at the cell surface [34,35]. Potential drug loading mechanisms include electrostatic attraction and hydrophobic interactions. Moreover, albumin drug delivery systems offer possibilities for surface modification due to the presence of functional groups (i.e. carboxylic and amino groups) enabling specific drug targeting to the site of action [35]. Albumin-based systems are considered safe since they are metabolizable *in vivo* by digestive enzymes into innocuous peptides whereas synthetic polymers may give harmful degradation products [6]. In addition, albumin is thought to facilitate endothelial transcytosis of unbound and albumin-bound plasma constituents into the extravascular space. This process is initiated by binding of albumin to a cell surface, 60-kDa glycoprotein (gp60) receptor [36].

In this study we prepared albumin-based lyophilisomes. Even large numbers of lyophilisomes did not affect SKOV-3 and HeLa cell viability. After 24 h lyophilisomes were internalized by HeLa cells, without changes in proliferation or morphology, indicating that they are non cytotoxic. Quite interestingly, this uptake occurred in the absence of an internalization signal such as a receptor ligand or a cell-penetrating peptide. It remains to be shown in which way such modifications would modulate uptake kinetics and/or efficiency. To investigate whether lyophilisomes could be used for drug delivery, we used doxorubicin and curcumin as model drugs and analyzed their incorporation into lyophilisomes. This procedure was based on diffusion of the drug into the capsule. Interestingly, doxorubicin loaded lyophilisomes resulted in a high entrapment efficiency (95%) together with a very low release (2 – 3% after 72 h). This effect cannot be explained by the process of simple diffusion. Albumin is known as an important transport protein and has several binding sites for hydrophobic compounds, which may explain the affinity of albumin for doxorubicin, maintaining the drug within lyophilisomes [37,38]. Albumin-based lyophilisomes may be a suitable delivery system for this drug and doxorubicin loaded lyophilisomes may be prepared upfront and stored at 4°C or in a lyophilized state. Next to doxorubicin, we also analyzed the drug curcumin. The entrapment efficiency of curcumin was quite low (4%) and release was rather fast (±55% after 72 h). Similar release profiles have been observed for curcumin in other nanoparticle systems, e.g. alginate-chitosan-pluronic composite, PLGA, and polymeric nanoparticles [23,39,40]. To retain the drug within the lyophilisomes for a longer time, lyophilisomes may be further crosslinked after loading which will make the capsule's wall less porous and may result in a better retention of curcumin.

In order to investigate the cell eliminating potential of our formulations, SKOV-3 and HeLa cells were treated with lyophilisomes loaded with doxorubicin or curcumin, respectively. Doxorubicin-loaded lyophilisomes showed a profound cytotoxic effect similar to free doxorubicin (20 μM in culture medium). This activity was contrasted with the low release of the drug from doxorubicin-loaded lyophilisomes in PBS or medium (3% of 20 μM is 0.6 μM). This concentration is likely not sufficient to induce cell death. An explanation for the efficacy of loaded lyophilisomes may be their internalization into the cell, followed by drug release inside the cell, which may be assisted by the action of endogenous proteinases. Alternatively, the albumin wall of lyophilisomes attached to the outside of the cell may be damaged (*e.g.* by excreted enzymes) to locally release high doses of doxorubicin resulting in elimination of cells. For curcumin-loaded lyophilisomes, which are more effective than free curcumin, a similar effect may be put forward: local release of curcumin and internalization of drug-loaded lyophilisomes. It should be noted that the wall of the lyophilisomes can be made from any protein, and can be adapted to the type of drug and the proteases / microenvironment of specific tumor cells.

Before drug delivery systems reach the target site, they need to travel through the vascular bed. Particle size has a fundamental effect on biodistribution [41]. For cancer, an effective strategy is based on the enhanced permeability effect (EPR) associated with hyper-

permeability of tumor vasculature and lack of lymphatic drainage [42]. Nanoparticles usually do not extravasate through normal endothelium since tight endothelial junctions (5 – 10 nm) between endothelial cells prevent extravasations of small particles [43]. However, due to the EPR effect, nanoparticles (<500 nm) can extravasate from the blood vessels to the tumor and accumulate, creating high local drug concentrations [44]. The cut-off size for permeability in individual tumor varies between 200 and 800 nm [45]. Lyophilisomes have a rather large size distribution, ranging from 100 to 3,000 nm. A next step is therefore to size them to appropriate diameters to make them more suitable to employ the enhanced permeability effect in tumors and functionalize the capsules with targeting molecules to increase specificity.

CONCLUSIONS

This study demonstrates the potential of albumin-based lyophilisomes as a drug delivery system. Both doxorubicin and curcumin-loaded lyophilisomes were capable of efficiently eliminating tumor cells *in vitro*.

Table S1 Specifics on freeze drying program.

Step 1	Freeze / ℃	-10	
	Freeze / min	60	
	Freeze / mbar	-	Lyophilisomes are put in the freeze dryer
Step 2	Freeze / ℃	-13	
	Freeze / min	60	
	Freeze / mbar	-	
Step 3	Freeze / ℃	-16	
	Freeze / min	60	Annealing step
	Freeze / mbar	-	
Step 4	Freeze / ℃	-20	
	Freeze / min	60	
	Freeze / mbar	-	
Step 5	Product 1 / ℃	-20	
	Product 2 / min	-20	
	Product 3 / mbar	-20	Start lyophilization
Step 6	Heating / ℃	-20	
	Heating / min	30	
	Heating / mbar	0.8	
Step 7	Heating / ℃	-20	
	Heating / min	300	
	Heating / mbar	0.8	
Step 8	Heating / ℃	-20	
	Heating / min	180	
	Heating / mbar	0.8	Lyophilization
Step 9	Heating / ℃	-0.1	
	Heating / min	1	
	Heating / mbar	0.8	
Step 10	Heating / ℃	-0.1	
	Heating / min	210	
	Heating / mbar	0.8	
Step 11	Heating / ℃	20	
	Heating / min	90	
	Heating / mbar	0.8	End lyophilization
Step 12	Heating / ℃	0	
	Heating / min	0	
	Heating / mbar	0	
Step 13	Drying / ℃	20	

REFERENCES

1. Byrne JD, Betancourt T, Brannon-Peppas L (2008) Active targeting schemes for nanoparticle systems in cancer therapeutics. Adv Drug Deliv Rev 60: 1615-1626.
2. Lammers T, Hennink WE, Storm G (2008) Tumour-targeted nanomedicines: principles and practice. Br J Cancer 99: 392-397.
3. Moghimi SM, Hunter AC, Murray JC (2005) Nanomedicine: current status and future prospects. FASEB J 19: 311-330.
4. Moghimi SM, Hunter AC, Murray JC (2001) Long-circulating and target-specific nanoparticles: theory to practice. Pharmacol Rev 53: 283-318.
5. Daamen WF, Geutjes PJ, Nillesen STM, Van Moerkerk HTB, Wismans R, *et al.* (2007) Lyophilisomes: A new type of (bio)capsules. Adv Mater 19: 673-677.
6. Elzoghby AO, Samy WM, Elgindy NA (2012) Protein-based nanocarriers as promising drug and gene delivery systems. J Control Release 161: 38-49.
7. Kratz F (2008) Albumin as a drug carrier: design of prodrugs, drug conjugates and nanoparticles. J Control Release 132: 171-183.
8. Young RC, Ozols RF, Myers CE (1981) The anthracycline antineoplastic drugs. N Engl J Med 305: 139-153.
9. Bellarosa D, Ciucci A, Bullo A, Nardelli F, Manzini S, *et al.* (2001) Apoptotic events in a human ovarian cancer cell line exposed to anthracyclines. J Pharmacol Exp Ther 296: 276-283.
10. Osheroff N, Corbett AH, Robinson MJ (1994) Mechanism of action of topoisomerase II-targeted antineoplastic drugs. Adv Pharmacol 29B: 105-126.
11. Lowenthal RM, Eaton K (1996) Toxicity of chemotherapy. Hematol Oncol Clin North Am 10: 967-990.
12. Klein-Szanto AJ (1992) Carcinogenic effects of chemotherapeutic compounds. Prog Clin Biol Res 374: 167-174.
13. Bouma J, Beijnen JH, Bult A, Underberg WJ (1986) Anthracycline antitumour agents. A review of physicochemical, analytical and stability properties. Pharm Weekbl Sci 8: 109-133.
14. Shishodia S, Sethi G, Aggarwal BB (2005) Curcumin: getting back to the roots. Ann N Y Acad Sci 1056: 206-217.
15. Maheshwari RK, Singh AK, Gaddipati J, Srimal RC (2006) Multiple biological activities of curcumin: a short review. Life Sci 78: 2081-2087.
16. Duvoix A, Blasius R, Delhalle S, Schnekenburger M, Morceau F, *et al.* (2005) Chemopreventive and therapeutic effects of curcumin. Cancer Lett 223: 181-190.
17. Aggarwal BB, Kumar A, Bharti AC (2003) Anticancer potential of curcumin: preclinical and clinical studies. Anticancer Res 23: 363-398.
18. Brouet I, Ohshima H (1995) Curcumin, an anti-tumour promoter and anti-inflammatory agent, inhibits induction of nitric oxide synthase in activated macrophages. Biochem Biophys Res Commun 206: 533-540.
19. Hatcher H, Planalp R, Cho J, Torti FM, Torti SV (2008) Curcumin: from ancient medicine to current clinical trials. Cell Mol Life Sci 65: 1631-1652.
20. Li L, Braiteh FS, Kurzrock R (2005) Liposome-encapsulated curcumin: in vitro and in vivo effects on proliferation, apoptosis, signaling, and angiogenesis. Cancer 104: 1322-1331.
21. Kaminaga Y, Nagatsu A, Akiyama T, Sugimoto N, Yamazaki T, *et al.* (2003) Production of unnatural glucosides of curcumin with drastically enhanced water solubility by cell suspension cultures of Catharanthus roseus. FEBS Lett 555: 311-316.
22. Garza-Licudine E, Deo D, Yu S, Uz-Zaman A, Dunbar WB (2010) Portable nanoparticle quantization using a resizable nanopore instrument - the IZON qNano. Conf Proc IEEE Eng Med Biol Soc 2010: 5736-5739.
23. Das RK, Kasoju N, Bora U (2010) Encapsulation of curcumin in alginate-chitosan-pluronic composite nanoparticles for delivery to cancer cells. Nanomedicine 6: 153-160.
24. Fritze A, Hens F, Kimpfler A, Schubert R, Peschka-Suss R (2006) Remote loading of doxorubicin into liposomes driven by a transmembrane phosphate gradient. Biochim Biophys Acta 1758: 1633-1640.
25. Yousefpour P, Atyabi F, Vasheghani-Farahani E, Movahedi AA, Dinarvand R (2011) Targeted delivery of doxorubicin-utilizing chitosan nanoparticles surface-functionalized with anti-Her2 trastuzumab. Int J Nanomedicine 6: 1977-1990.
26. Savla R, Taratula O, Garbuzenko O, Minko T (2011) Tumor targeted quantum dot-mucin 1 aptamer-doxorubicin conjugate for imaging and treatment of cancer. J Control Release 153: 16-22.

27. Nair KL, Thulasidasan AK, Deepa G, Anto RJ, Kumar GS (2012) Purely aqueous PLGA nanoparticulate formulations of curcumin exhibit enhanced anticancer activity with dependence on the combination of the carrier. Int J Pharm 425: 44-52.
28. Barenholz YC (2012) Doxil(R) - The first FDA-approved nano-drug: Lessons learned. J Control Release 160: 117-34.
29. Zhang JA, Pawelchak J (2000) Effect of pH, ionic strength and oxygen burden on the chemical stability of EPC/cholesterol liposomes under accelerated conditions. Part 1: Lipid hydrolysis. Eur J Pharm Biopharm 50: 357-364.
30. Feinstein SB, Cheirif J, Ten Cate FJ, Silverman PR, Heidenreich PA, *et al.* (1990) Safety and efficacy of a new transpulmonary ultrasound contrast agent: initial multicenter clinical results. J Am Coll Cardiol 16: 316-324.
31. Geny B, Mettauer B, Muan B, Bischoff P, Epailly E, *et al.* (1993) Safety and efficacy of a new transpulmonary echo contrast agent in echocardiographic studies in patients. J Am Coll Cardiol 22: 1193-1198.
32. Ibrahim NK, Desai N, Legha S, Soon-Shiong P, Theriault RL, *et al.* (2002) Phase I and pharmacokinetic study of ABI-007, a Cremophor-free, protein-stabilized, nanoparticle formulation of paclitaxel. Clin Cancer Res 8: 1038-1044.
33. Ibrahim NK, Samuels B, Page R, Doval D, Patel KM, *et al.* (2005) Multicenter phase II trial of ABI-007, an albumin-bound paclitaxel, in women with metastatic breast cancer. J Clin Oncol 23: 6019-6026.
34. Fasano M, Curry S, Terreno E, Galliano M, Fanali G, *et al.* (2005) The extraordinary ligand binding properties of human serum albumin. IUBMB Life 57: 787-796.
35. Elzoghby AO, Samy WM, Elgindy NA (2011) Albumin-based nanoparticles as potential controlled release drug delivery systems. J Control Release 157: 168-182.
36. Hawkins MJ, Soon-Shiong P, Desai N (2008) Protein nanoparticles as drug carriers in clinical medicine. Adv Drug Deliv Rev 60: 876-885.
37. Sawaya A, Benoit JP, Benita S (1987) Binding mechanism of doxorubicin in ion-exchange albumin microcapsules. J Pharm Sci 76: 475-480.
38. Dreis S, Rothweiler F, Michaelis M, Cinatl J Jr., Kreuter J, *et al.* (2007) Preparation, characterisation and maintenance of drug efficacy of doxorubicin-loaded human serum albumin (HSA) nanoparticles. Int J Pharm 341: 207-214.
39. Mukerjee A, Vishwanatha JK (2009) Formulation, characterization and evaluation of curcumin-loaded PLGA nanospheres for cancer therapy. Anticancer Res 29: 3867-3875.
40. Bisht S, Feldmann G, Soni S, Ravi R, Karikar C, *et al.* (2007) Polymeric nanoparticle-encapsulated curcumin ("nanocurcumin"): a novel strategy for human cancer therapy. J Nanobiotechnology 5: 3.
41. Decuzzi P, Godin B, Tanaka T, Lee SY, Chiappini C, *et al.* (2010) Size and shape effects in the biodistribution of intravascularly injected particles. J Control Release 141: 320-327.
42. Torchilin V (2011) Tumor delivery of macromolecular drugs based on the EPR effect. Adv Drug Deliv Rev 63: 131-135.
43. Hofheinz RD, Gnad-Vogt SU, Beyer U, Hochhaus A (2005) Liposomal encapsulated anti-cancer drugs. Anticancer Drugs 16: 691-707.
44. Torchilin VP (2010) Passive and active drug targeting: drug delivery to tumors as an example. Handb Exp Pharmacol 3-53.
45. Gaumet M, Vargas A, Gurny R, Delie F (2008) Nanoparticles for drug delivery: the need for precision in reporting particle size parameters. Eur J Pharm Biopharm 69: 1-9.

3

Specific targeting of tumor cells by lyophilisomes functionalized with antibodies

Etienne van Bracht, Sarah Stolle, Theo G. Hafmans, Otto C. Boerman, Egbert Oosterwijk, Toin H. van Kuppevelt, Willeke F. Daamen

European Journal of Pharmaceutics and Biopharmaceutics, Volume 87, Issue 1, Page: 80-89, 2014

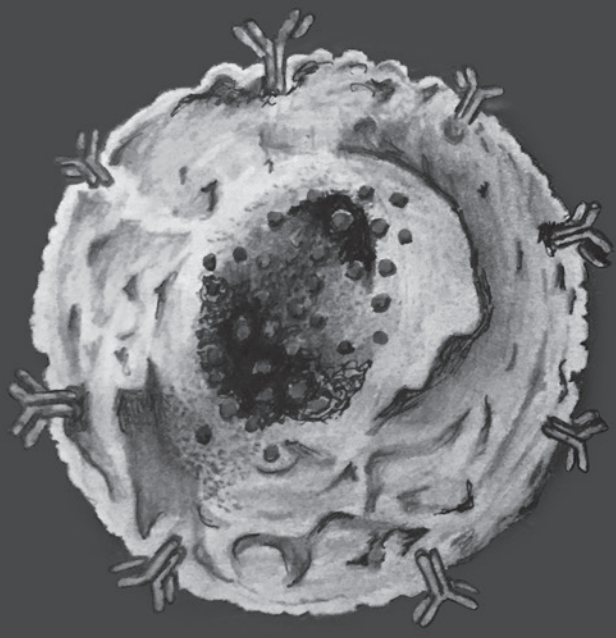

ABSTRACT

Lyophilisomes are a novel class of proteinaceous biodegradable nano/micro drug delivery capsules prepared by freezing, annealing and lyophilization. In the present study, lyophilisomes were functionalized for active targeting by antibody conjugation in order to obtain a selective drug-carrier system. Lyophilisomes were vapor crosslinked for 2 h, resulting in stable capsules, while leaving sufficient primary amines for further modification. The humanized KC4 (hKC4) antibody was conjugated to lyophilisomes to achieve specific targeting to mucin 1 (MUC1)-overexpressing tumor cells. For this, thiolated antibodies were conjugated to maleimide-activated lyophilisomes, resulting in an hKC4 specific drug targeting system towards MUC1-overexpressing human ovarian and cervical tumor cells. FACS analysis demonstrated that hKC4-conjugated lyophilisomes bound specifically to MUC1-overexpressing tumor cells (HeLa, OVCAR-3, and SKOV-3 cells), compared to MUC1-negative cells (LS174T). In addition, control non-specific IgG-conjugated lyophilisomes did not bind to MUC1-overexpressing tumor cells. When MUC1- positive and -negative cells were combined in one culture, hKC4-conjugated lyophilisomes specifically targeted MUC1-positive cells, whereas negative cells showed merely background levels. Transmission electron micro- scopy showed uptake of hKC4-conjugated lyophilisomes via phagocytosis or macro- pinocytosis. In conclusion, hKC4-conjugated albumin-based lyophilisomes represent a potential drug delivery system for targeted drug transport to MUC1-overexpressing tumor cells.

INTRODUCTION

Chemotherapy is a standard treatment for cancer, but its efficacy is often limited due to associated adverse effects. In recent years, new strategies for cancer treatment have emerged which are based on drug delivery systems. These systems include drug carriers for specific transport of anti-cancer drugs to the tumor site, such as liposomes and polymersomes [1,2]. However, the limited chemical and physical stability of such capsules during manufacturing and storage still pose a challenge [3,4]. Besides optimizing current nanoparticle systems, research on new drug delivery systems continues. The abundant interest shown in the field of drug delivery is illustrated by the development of numerous drug delivery systems over the last decade [5]. Lyophilisomes, a novel drug delivery capsule in the nano/micrometer range, may become a new generation of drug delivery systems [6].

Lyophilisomes can be prepared from a diversity of water-soluble macromolecules (*e.g.* albumin, elastin, and heparin) by freezing, annealing, and lyophilization regimens. This makes it possible to manufacture lyophilisomes with different properties, resulting in an adaptable carrier system towards various applications. The system is highly flexible, allowing the incorporation of virtually any biomolecule in the wall and/or lumen. For instance, enzymes incorporated in the capsule wall and the lumen demonstrated they could still exert their biological activity, partly due to mild preparation conditions [7]. We have already shown that lyophilisomes can be efficiently loaded with doxorubicin, resulting in tumor cell elimination [6]. Drugs can be entrapped by diffusional loading after preparation of the capsules, thus separating the crosslinking step from the drug loading step. Using this procedure, biomolecules are not exposed to harsh conditions, such as an acid environment preventing deactivation of biomolecules. Furthermore, lyophilisomes possess a relatively thick wall that can be loaded with enzymes that upon degradation may activate a prodrug in the lumen at the site of interest. Due to these properties, lyophilisomes can be utilized to design multifunctional systems for the delivery of therapeutic agents.

In this study, albumin-based lyophilisomes were used. Albumin has been used as a drug carrier because of its ample availability, its lack of toxicity and immunogenicity, and its biodegradability [8,9]. In addition, it is likely that albumin, with a half-life of 19 days in circulation, may play an important role for improving the pharmacokinetics and targeting properties of drugs, for instance because of its preferential uptake in tumors [8]. In contrast to nanoparticulate systems from *e.g.* polymers, albumin offers the benefit of carrying natural functional groups (*e.g.* amine and carboxylic groups) that can be used for surface modification [10,11]. In a previous study we noticed that albumin-based lyophilisomes did not affect cell viability [6]. The FDA-approved products, Albunex [12,13] and Abraxane [14,15], demonstrate that albumin nano/micro particles are well-tolerated in humans.

The potential of nanoparticles to act as a drug delivery system mainly comprises passive tumor targeting. Passive targeting results from the "enhanced permeability and retention (EPR) effect" characterized by enhanced accumulation of nanoparticles in tumors due to leaky tumor vasculature in combination with impaired lymphatic drainage [16]. An active targeting effect can be achieved if a targeting ligand is conjugated to the surface of the drug delivery carrier. Specific targeting can improve binding kinetics and result in a more efficient uptake of the anti-cancer drug [17–19].
To probe the possibility of using lyophilisomes for specific tumor targeting, antibodies to mucin 1 (MUC1) were conjugated to lyophilisomes. MUC1 is a highly glycosylated type 1 transmembrane glycoprotein that functions as a signal transducer and is involved in cancer progression [20,21]. Cancer cells of various origin express high levels of MUC1, such as cancers of the ovary, cervix, colon, prostate, breast, lung, and pancreas, making it a suitable target for chemotherapeutics, while expression on healthy cells is low [22–24]. In this study, antibody-conjugated lyophilisomes were prepared to investigate the specific targeting potential towards MUC1-overexpressing human ovarian and cervical tumor cells.

MATERIALS & METHODS

Materials

Bovine serum albumin was purchased from PAA Laboratories (Linz, Austria). Fluorescein isothiocyanate (FITC)-conjugated bovine albumin and non-specific human IgG from human serum were purchased from Sigma Aldrich (Steinheim, Germany). Sulfo-*N*-[g-maleimidobutyryloxy]sulfosuccinimide ester (sulfo-GMBS) and 2-iminothiolane reagent were purchased from Pierce Biotechnology (Rockford, IL, USA). Glutaraldehyde and formaldehyde were obtained from Merck (Darmstadt, Germany).

Methods

Preparation of lyophilisomes

Albumin lyophilisomes were prepared as described [6]. Briefly, droplets of a solution of 0.25% (w/v) bovine serum albumin (BSA) in 0.01 M acetic acid were frozen in liquid nitrogen (-196°C). The frozen albumin preparation was incubated at -10 to -20°C for 3 h (annealing step), and subsequently lyophilized. This procedure results in hollow nano/micro spheres ("lyophilisomes"). In order to visualize the lyophilisomes, FITC-conjugated albumin was added to non-labeled albumin (1:10) in the starting solution. To obtain stabilized lyophilisomes, they were vapor crosslinked with glutaraldehyde and formaldehyde. Generally we use 40 ml of a 0.25 % BSA solution, which corresponds to 100 mg albumin (2.5 mg/ml). The final lyophilisome population was centrifuged three of four times at low speed (60x *g*; Thermo, Heraeus Fresco 17; Newport Pagnell, Great Britain) to remove large lyophilisomes and sheet-like structures, until no pellet was observed. After this procedure, about 30% of the original weight of lyophilisomes remained. Lyophilisomes (1 mg/ml)

were stored in 0.1% (v/v) Tween-20 (Sigma Aldrich, Steinheim, Germany) in phosphate buffered saline (PBS-T, pH 7.4).

Particle size measurements

Two methods were used to determine lyophilisome size: dynamic light scattering (DLS) and qNano [6,25]. For DLS, stabilized lyophilisomes were dispersed in 0.1% (v/v) PBS-T (pH 7.4) and analyzed using a Zetasizer Nano-S (Malvern Instruments Ltd, Malvern, UK). For qNano (Izon, Science Ltd., Burnside, New Zealand), a pore size of 600 – 2,000 nm was used to ensure a continuous flow of particles. Data were analyzed with Izon Control Suite 2.1 software.

Quantification of amine group content on lyophilisomes

Primary amine groups were utilized in the vapor crosslinking step to stabilize the lyophilisomes. Primary amines are also necessary to conjugate antibodies to the lyophilisomes. To determine the amount of remaining primary amines after stabilization, a 2,4,6-trinitrobenzene sulfonic acid (TNBS) assay was performed. The amine group content of lyophilisomes was determined spectrophotometrically at 420 nm with a standard curve of glycine [26].

Optimization and quantification of thiol groups on antibodies

In order to conjugate antibodies to lyophilisomes, a sulfhydryl group was introduced on the antibody that can react with maleimide-modified lyophilisomes. To determine the amount of reactive sulfhydryl groups on antibodies, Ellman's reagent was used [27,28]. The quantification was performed immediately after modifying the antibodies to prevent dimerization by oxidative disulfide bridge formation.

One ml of 1 mg/ml antibody solution in 2 mM ethylenediaminetetraacidic acid (EDTA) in phosphate-buffered saline (PBS; pH 8.0) was incubated with 4.7 µl (10-fold molar excess), 11.9 µl (25-fold molar excess), 23.8 µl (50-fold molar excess), or 47.6 µl (100-fold molar excess) of 2 mg/ml 2-iminothiolane (Traut's reagent), for 2, 5 and 16 h under rotation (36 rpm, "Assistant" Rotating mixer, Karl Hecht, Sondheim, Germany) at room temperature. The antibody was purified on Sephadex™ G-25M desalting columns (GE Healthcare, Buckinghamshire, UK) using 2 mM EDTA in PBS (pH 8.0) as eluent. The protein-containing fractions were identified spectrophotometrically at 280 nm with the NanoDrop 2000c (Thermo Scientific, Wilmington, DE, USA) and pooled. This solution was concentrated to approximately 1 mg/ml using Amicon Ultra 5k centrifugal filter devices (Millipore, Darmstadt, Germany). Aliquots (250 µl) of concentrated antibody were incubated in 6.25 µl of Ellman's reagent (4 mg/ml in sodium phosphate buffer, pH 8.0) for 15 min at room temperature and measured spectrophotometrically using a Synergy 2 plate reader at 412 nm (Biotek, Winooski, VT) with a calibration curve of L-cysteine. For antibody conjugations at pH 7.2, a 50-fold molar excess of Traut's reagent was tested after incubation for 2, 5 and 16 h.

Antibody conjugation to lyophilisomes

A schematic representation of the reactions is depicted in figure 1.

Reaction 1: Activation of lyophilisomes. A suspension of 1 ml lyophilisomes (1 mg/ml) in 0.1% (v/v) PBS-T (pH 7.4) was centrifuged (5 min, 17,000x *g*, 4°C). To obtain maleimide-activated lyophilisomes, 1 mg lyophilisomes was resuspended in 1 ml PBS-T and incubated overnight with 31.1 µl of 10 mM sulfo-GMBS in PBS-T (pH 8.0) at 4°C on a rotator (36 rpm), resulting in a 20-fold molar excess of sulfo-GMBS in relation to albumin. Excess sulfo-GMBS was removed by centrifugation using three washing steps in PBS-T (pH 7.4).

Reaction 2: Thiolation of antibodies. To introduce sulfhydryl groups on hKC4 antibodies and non-specific control IgG antibodies, 1 ml of 1 mg/ml antibody solution was incubated in PBS (pH 7.2) with a 50-molar excess of Traut's reagent and incubated for 5 h at room temperature on a rotator (36 rpm). Antibodies were purified using a Sephadex™ G-25M desalting column. The protein-containing fractions were measured spectrophotometrically with the NanoDrop at 280 nm and pooled. This solution was concentrated using Amicon Ultra 5k centrifugal filter devices to a final concentration of approximately 1 mg-ml in 2 mM EDTA in PBS (pH 6.5). This procedure generates a thiolated antibody reactive towards a maleimide crosslinker. Thiolated antibodies were immediately used for the conjugation reaction to lyophilisomes to prevent dimerization.

Reaction 3: Conjugation of antibodies to lyophilisomes. For the coupling reaction, 1 ml of 1 mg/ml sulfhydryl-reactive lyophilisomes was centrifuged and conjugated in 1 ml to thiolated hKC4 or non-specific IgG control antibody (both 1 mg/ml) in 2 mM EDTA in PBS (pH 6.5). Non-coupled antibodies were removed by centrifugation (5 min, 17,000x *g*, 4°C) using three washing steps in PBS-T (pH 7.4). Antibody-conjugated lyophilisomes were stored at 4°C in the dark.

To verify antibody conjugation, antibody-conjugated lyophilisomes were incubated with a goat-anti-human fluorescent IgG (Alexa 594 nm; 10 µg/ml) for 1 h at room temperature under rotation (36 rpm) in the dark, and subsequently washed three times with 0.2% BSA in PBS. Lyophilisomes were deposited on poly-D-lysine-coated cover slips and analyzed by fluorescent microscopy (Leica DM 6000 B, Leica Microsystems, Wetzler, Germany).

Cell culture

All culture media were purchased from Gibco (Karlsruhe, Germany) unless indicated otherwise. The human ovarian cancer cell lines OVCAR-3 and SKOV-3 were cultured in DMEM GlutaMAX and McCoy's 5A GlutaMAX, respectively, supplemented with 10% (v/v) fetal calf serum (FCS; PAA Laboratories, Pasching, Austria). The human cervical tumor cell line, HeLa, and the human colon adenocarcinoma cell line, LS174T, were cultured in RPMI 1640 GlutaMAX medium supplemented with 10% (v/v) FCS. The cells were cultured in a humidified atmosphere with 5% CO_2 at 37°C. Subconfluent cells were dissociated with 0.05% (w/v) trypsin in 0.02% (w/v) EDTA in PBS (PAA Laboratories) and were maintained as proliferating cultures.

For FACS analysis, cells were stained with the cell membrane dye PKH26 (Sigma Aldrich, Missouri, USA) [29,30]. One million cells were incubated in 2 µM PKH26 dye in 500 µl buffer (Diluent C, provided by manufacturer) for 5 min. To stop the staining reaction, 500 µl FCS was added and incubated for 5 min. Subsequently, cells were washed three times with culture medium and cultured for one day prior to experiments.

MUC1 expression of ovarian and cervix tumor cell lines

In order to investigate the MUC1 antigen expression of OVCAR-3, SKOV-3, HeLa, and LS174T tumor cell lines, 60,000 cells were incubated with 10 µg/ml hKC4 antibody in an Eppendorf tube for 1 h at room temperature under rotation (36 rpm) in the dark. Subsequently, cells were washed three times with 0.2% BSA in PBS and incubated with a goat-anti-human fluorescent IgG (Alexa 594 nm; 10 µg/ml) for 1 h at room temperature under rotation (36 rpm) in the dark and subsequently washed three times with 0.2% BSA in PBS and analyzed with the FACScaliber (Becton Dickinson, Breda, Netherlands) and Flowjo software (FlowJo, Ashland, OR, USA).

Binding of antibody-conjugated lyophilisomes

To investigate the binding of hKC4-conjugated lyophilisomes, MUC1 overexpressing OVCAR-3, SKOV-3 and HeLa cells were used. The MUC1-negative cell line, LS174T, served as a control. An aliquot of 25 µl of lyophilisomes (lyophilisome content 40 µg/ml) conjugated to (non-)specific antibody was added to 60,000 PKH26 stained cells in an Eppendorf tube and incubated for 1 h at room temperature under rotation (36 rpm). In addition, an excess of free MUC1 antibody (10 µg/ml) was added to the cells 1 h prior to the incubation with hKC4-conjugated lyophilisomes. Cells were washed three times with 0.2% BSA in PBS and analyzed with the FACScaliber (Becton Dickinson, Breda, Netherlands) and Flowjo software (FlowJo, Ashland, OR, USA). FACS settings were determined so that cells not associated with lyophilisomes were depicted below a fluorescent signal of 10^1 and regarded as negative. When lyophilisomes were associated with cells, the fluorescent signal became higher than 10^1 and these cells were regarded as positive. Data were analyzed by GraphPad Software 5.0 (Graphpad, San Diego, CA, USA).

Binding of antibody-conjugated lyophilisomes to mixed cell cultures

In order to examine whether hKC4-conjugated lyophilisomes bound specifically to MUC1 expressing tumor cells, both MUC1-positive and -negative cells were mixed (1:1) before exposure to lyophilisomes. To visualize cells, all nuclei were stained with 4',6-diamidino-2-phenylindole (DAPI) [31]. To differentiate between both cell lines, MUC1-positive cells were stained with PKH26. 25 µl of lyophilisomes (40 µg/ml) conjugated with specific and non-specific antibody were incubated with 60,000 cells (30,000 MUC1-positive cells and 30,000 MUC1-negative cells) for 1 h at room temperature under rotation (36 rpm). Subsequently, cells were fixed in 4% paraformaldehyde and cytospins were made. FACS

analysis was performed using FACScaliber and Flowjo software. Confocal images were obtained using an Olympus FV-1000 confocal microscope (Olympus GmbH, Hamburg, Germany) and analyzed with FV 10-ASW 1.6 viewer software. Data were analyzed by GraphPad Software 5.0.

Cell binding and uptake of antibody-conjugated lyophilisomes visualized by transmission electron microscopy

MUC1-positive and -negative cells were incubated with 25 µl of lyophilisomes (lyophilisome content 40 µg/ml) conjugated with (non-)specific antibody for 1 h under rotation (36 rpm). Subsequently, cells were embedded in 1.5% (w/v) agarose, fixed in 2% (v/v) glutaraldehyde in 0.1 M phosphate buffer (pH 7.4), post-fixed with 1% (w/v) osmium tetroxide, dehydrated in an ascending series of ethanol, and embedded in Epon 812. Ultrathin sections (60 nm) were cut and picked up on Formvar-coated grids, post-stained with lead citrate and uranyl acetate, and examined in a JEOL 1010 transmission electron microscope (Tokyo, Japan).

Statistical analyses

Data are presented as mean with standard deviation. Data of sections 'Particle size measurements of lyophilisomes', 'Optimizing vapor crosslinking on lyophilisomes for antibody conjugation', 'Thiolation of IgG antibody' and 'Binding of antibody-conjugated lyophilisomes' were analyzed using two-tailed Student's t-tests. All statistical analyses were performed in Graphpad Prism 5.0 (Graphpad, San Diego, CA, USA).

RESULTS

To probe the possibility of using lyophilisomes for specific tumor targeting, lyophilisomes were modified with antibodies using the heterobifunctional crosslinker sulfo-GMBS in combination with Traut's reagent (Fig. 1).

Particle size measurements of lyophilisomes

The size distribution of lyophilisomes is summarized in Table 1. Using DLS, the mean particle diameter of lyophilisomes was measured 1,561±49 nm with a polydispersity index of 0.7±0.03. This indicates a rather heterogeneous particle size distribution. For DLS, it is known that larger particles will dominate smaller particles in the measurement, resulting in an overestimated mean particle size. When measuring the lyophilisomes using qNano, a mean particle size of 1,160±75 nm was found. With this instrument, particles smaller than 600 nm were not detected with the specific pore used for our experiments (600 – 2,000 nm), as they became background signal. The standard deviations in Table 1 are rather small since the data are determined using the absolute mean value of multiple experiments. To visualize the size range of lyophilisomes in more detail, a typical size distribution measured by qNano is depicted in figure 2.

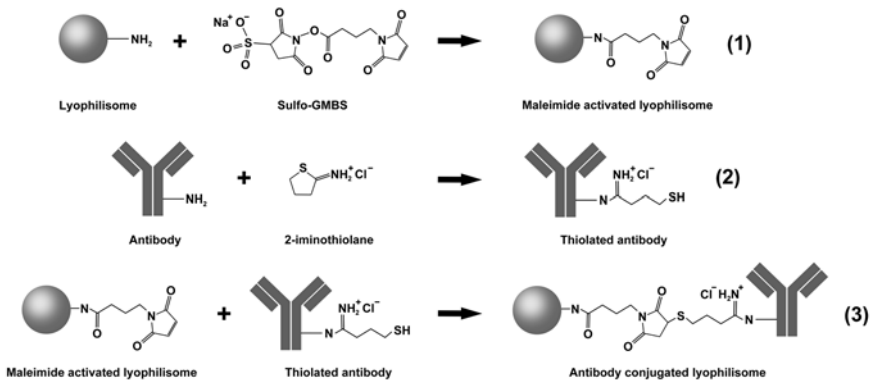

Figure 1 Schematic illustration of lyophilisome conjugation with antibody. (**1**) Free amine groups of lyophilisomes react with sulfo-GMBS introducing reactive maleimide groups. (**2**) Antibodies are modified with 2-iminothiolane (Traut's reagent) introducing reactive sulfhydryl groups, resulting in thiolated antibodies. (**3**) Thiolated antibodies are conjugated to pre-activated maleimide-lyophilisomes, resulting in stable antibody conjugation to lyophilisomes. In this study, hKC4 antibodies were used to actively target cancers overexpressing MUC1 antigen, using non-specific human IgG's as a control antibody.

Antibody conjugation did not influence mean particle diameter, as DLS measured a mean particle diameter of 1,426±68 with a polydispersity index of 0.8±0.04 and qNano measured a mean particle diameter of 1,256±84 (Table 1).

Table 1 Size distribution of lyophilisomes before and after antibody conjugation

Stabilized lyophilisomes	DLS	qNano	DLS	qNano
	Before Ab conjugation		After Ab conjugation	
Mean Particle diameter (nm)	1,561 ± 49	1,160 ± 75	1,426 ± 68	1,306 ± 84
Polydispersity index	0.698 ± 0,029	N.A.[a]	0.784 ± 0,042	N.A.[a]

[a]N.A. = Not available

Optimizing vapor crosslinking on lyophilisomes for antibody conjugation

Albumin contains approximately 1,000 nmol amine groups/mg. In lyophilisomes, these functional groups were partially used to stabilize lyophilisomes by vapor crosslinking with glutaraldehyde and formaldehyde. The percentages of primary amines that remained on lyophilisomes were 66±7%, 58±9%, and 37±7% after vapor crosslinking for 2, 8, and 16 h, respectively (Fig. 3).

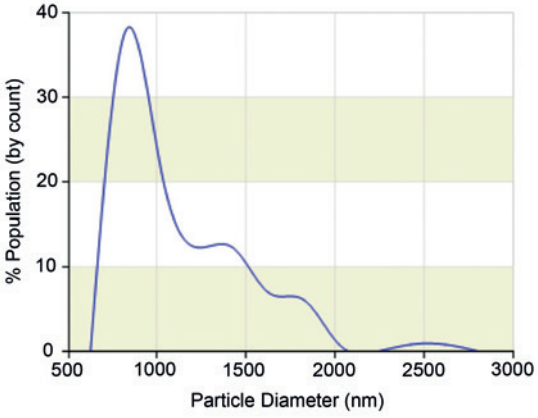

Figure 2 Size distribution of non-modified lyophilisomes as measured by qNano.

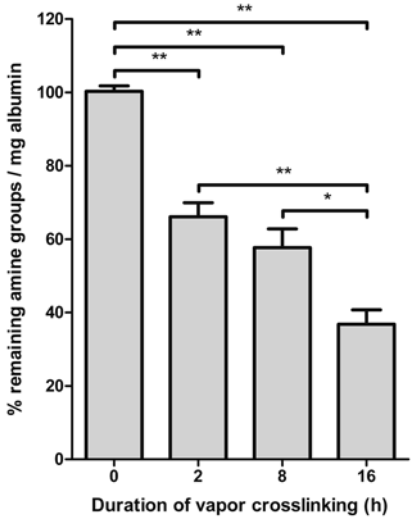

Figure 3 Effect of vapor crosslinking on the percentage of remaining primary amine groups on lyophilisomes. Lyophilisomes were crosslinked in a vapor mixture of glutaraldehyde and formaldehyde for 2, 8, and 16 h. The number of primary amine groups was spectrophotometrically detected using a TNBS assay. The absolute amine group content of albumin is 1061±78 nmol/mg. After vapor crosslinking for 2, 8, and 16 h, 66±7%, 58±9%, and 37±7% of the amine groups remained available, respectively. *p<0.05 **p<0.01.

Stabilized lyophilisomes -independent of time of stabilization- did not dissolve upon wetting. For this study, we chose to use a 2 h vapor crosslinking step for lyophilisomes, since most amine groups were preserved using this incubation time, allowing further modification.

Thiolation of IgG antibody

To conjugate hKC4 anti-MUC1 antibodies to lyophilisomes, sulfhydryl groups were introduced on the antibody by Traut's reagent. Non-specific human IgG's were used to determine the optimal conditions to introduce sulfhydryl groups. As depicted in figure 4, increasing the molar excess of Traut's reagent resulted in a significantly increased number of thiol groups per antibody. Similar results were obtained for longer incubation times. However, no differences were observed between 5 and 16 h incubation, possibly due to an increase in disulfide bridging. Ideally, the number of thiol groups should range between one and two per antibody to allow efficient conjugation and preserve antibody function [17]. Therefore, the optimal incubation conditions were 50-fold molar excess for 2 h, which resulted in 2.0±0.3 thiol groups per antibody.

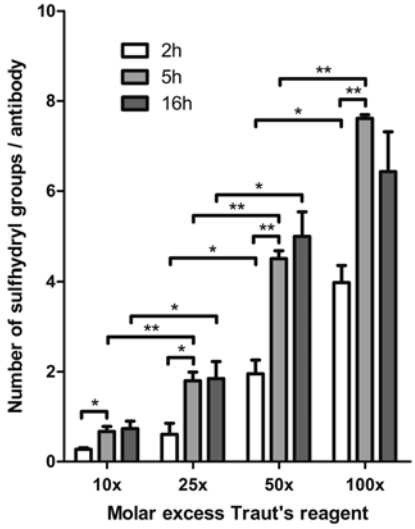

Figure 4 The number of sulfhydryl groups introduced on non-specific human IgG's by 2-iminothiolane (Traut's reagent) using different incubation times and different amounts of Traut's reagent. With increased molar excess of Traut's reagent and longer incubation time, the number of thiol groups on non-specific human IgG's increased, with the exception of the 16 h incubation time, possibly due to disulfide bridging. *p<0.01 **p<0.001.

These experiments were performed at pH 8.0. However, our antibody was dissolved in PBS with a pH of 7.2. The thiolation reaction occurred less efficient at pH 7.2, resulting in fewer sulfhydryl groups introduced per antibody. Reaction with a 50-fold molar excess of Traut's reagent for 2, 5 and 16 h resulted in 0.5±0.1, 1.3±0.2 and 1.5±0.4 thiol groups per antibody, respectively. For further experiments, the antibody conjugation conditions at pH 7.2 were therefore altered to 50-fold molar excess for 5 h.

Antibody conjugation to lyophilisomes

hKC4 is a humanized monoclonal antibody directed against MUC1, which is overexpressed by several tumor cells. To show that antibody conjugation was successful, lyophilisomes were studied with fluorescent microscopy. Unmodified lyophilisomes were green without

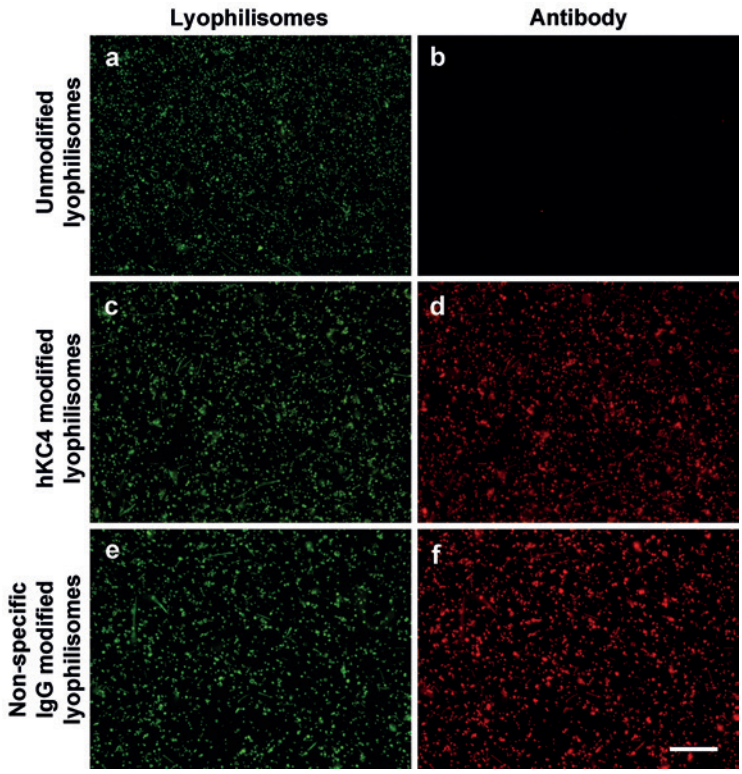

Figure 5 Antibody conjugation to lyophilisomes visualized by fluorescence microscopy. Green fluorescence corresponds to FITC-labeled lyophilisomes. Red fluorescence corresponds to antibodies conjugated to lyophilisomes. **a** and **b**) Unmodified lyophilisomes without antibody. **c** and **d**) Lyophilisomes conjugated with hKC4 antibody. **e** and **f**) Lyophilisomes conjugated with non-specific human IgG as a control antibody. The scale bar represents 10 µm.

red fluorescence, indicating the absence of antibodies (Fig. 5a and b). hKC4-conjugated lyophilisomes showed both green and red fluorescence, confirming the presence of hKC4 antibodies to lyophilisomes (Fig. 5c and d). As a control antibody, a non-specific human IgG antibody was conjugated to lyophilisomes and its presence was also confirmed by fluorescent microscopy (Fig. 5e and f).

Binding of antibody-conjugated lyophilisomes

MUC1 overexpressing tumor cell lines, OVCAR-3, SKOV-3 and HeLa, showed MUC1 antigen expression with a mean fluorescence value of 805±188, 232±112, and 228±56, respectively. The MUC1-negative tumor cell line (LS174T) only gave a mean fluorescence value of 5±1 (Table 2).

Table 2 MUC1 expression of ovarian and cervix tumor cell lines

Cell line	MUC1 expression	Mean Fluorescence Intensity (N=3 ± SD)
OVCAR-3	+	805 ± 188
SKOV-3	+	232 ± 112
HeLa	+	228 ± 56
LS174T	-	5 ± 1

MUC1-positive and -negative cell lines were incubated with hKC4-conjugated lyophilisomes or lyophilisomes conjugated with a non-specific human IgG control antibody. As shown in figure 6, hKC4-conjugated lyophilisomes showed significant binding to OVCAR-3, SKOV-3, and HeLa cells compared to non-specific IgG-conjugated lyophilisomes. To confirm the findings of specific targeting to MUC1-overexpressing tumor cells, a competition experiment was carried out. Excess of free MUC1 antibody (10 µg/ml) was added to the cells 1 h prior to the incubation with antibody-conjugated lyophilisomes. Theoretically, MUC1 binding sites on the cell surface will be blocked by the excess of hKC4 antibody, resulting in control levels after incubation with hKC4-conjugated lyophilisomes. When SKOV-3 and HeLa cells were pre-incubated with an excess of hKC4 antibody, binding indeed decreased to baseline levels similar to controls and non-specific IgG-conjugated lyophilisomes (Fig. 6b and c). For OVCAR-3 cells, decreased binding was observed after pre-incubation with hKC4 antibody, but residual lyophilisome binding was above background levels (Fig. 6a). The high antigen expression (Table 2) of OVCAR-3 cells compared to other MUC1-positive cell lines and/or rapid re-expression of the antigen may be responsible for the binding being not fully blocked. The negative cell line, LS174T, did not show specific binding of lyophilisome preparations (Fig. 6d). Results were quantified using the percentage of cells associated with one or more lyophilisomes (Fig. 6e). OVCAR-3,

SKOV-3, and HeLa cells all showed significantly more binding of hKC4-conjugated lyophilisomes, compared to non-specific IgG-lyophilisomes (75±7% *vs.* 9±2%; 61±4% *vs.* 13±5%; 60±3% *vs.* 4±0%, respectively). For LS174T cells, increased binding was observed between IgG-conjugated lyophilisomes and hKC4-conjugated lyophilisomes. However, this was non-specific, as a pre-incubation with excess of hKC4 did not significantly decrease the binding of hKC4-conjugated lyophilisomes.

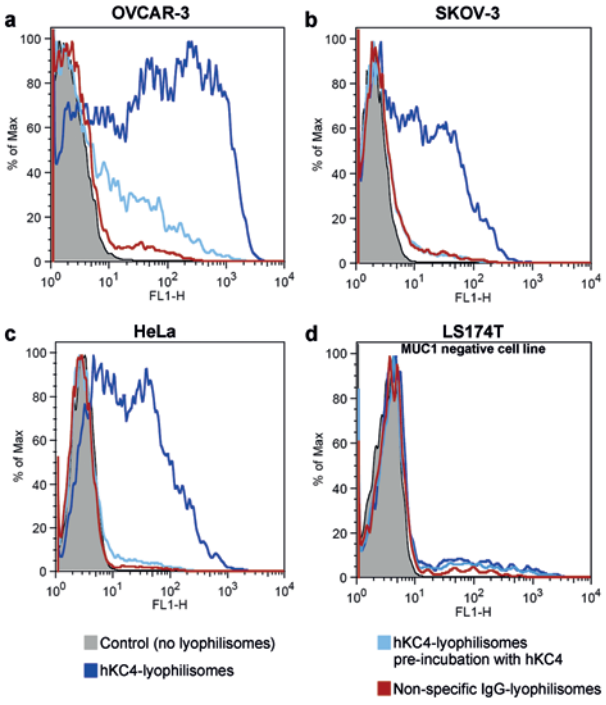

Figure 6 Cellular binding of various lyophilisome formulations to MUC1 overexpressing and MUC1 negative cancer cells. All cell lines were incubated either with hKC4-conjugated lyophilisomes, with and without a pre-incubation of excess hKC4 antibody, or non-specific IgG-conjugated lyophilisomes (control antibody). **a**-**c**) OVCAR-3, SKOV-3, and HeLa cells showed a significant shift to the right in the histogram, indicating increased binding of hKC4-conjugated lyophilisomes, whereas non-specific IgG-conjugated lyophilisomes showed background binding levels. Binding decreased to background levels after pre-incubation with hKC4 for SKOV-3 and HeLa cells. Binding to OVCAR-3 cell did not completely decrease to the level of the control antibody. **d**) The negative cell line LS174T did not show specific binding for lyophilisome preparations.

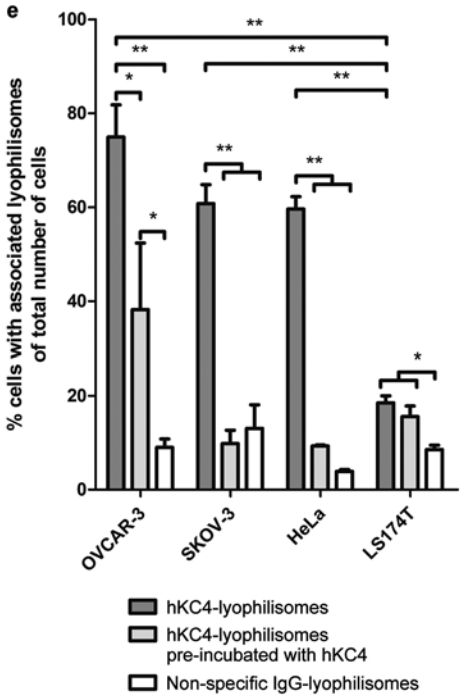

Figure 6 Continued. **e**) Quantified results of a-d. *p<0.05 **p<0.001.

Binding of antibody-conjugated lyophilisomes in mixed cell culture

To investigate whether hKC4-conjugated lyophilisomes specifically target tumor cells that express MUC1 antigens, MUC1-positive cells were mixed with MUC1-negative cells in a 1:1 ratio (Fig. 7). Positive (PHK26 stained) and negative cells (unstained) were analyzed in separate histograms. hKC4-conjugated lyophilisomes bound to cells that expressed MUC1 antigen, whereas little binding was observed to LS174T cells. Non-specific IgG-conjugated lyophilisomes showed no preferential binding to either MUC1-positive or -negative cells. Confocal laser scanning microscopy confirmed these results. hKC4-conjugated lyophilisomes specifically targeted MUC-1-positive red cells compared to MUC-1 negative tumor cells (Fig. 7).

Cellular uptake of antibody-conjugated lyophilisomes

TEM was used to investigate the internalization of lyophilisomes. After a 1 h incubation of hKC4-conjugated lyophilisomes to OVCAR-3 cells, lyophilisomes bound to the cell membrane (Fig. 8a). However, after a 4 h incubation time, lyophilisomes were also internalized by

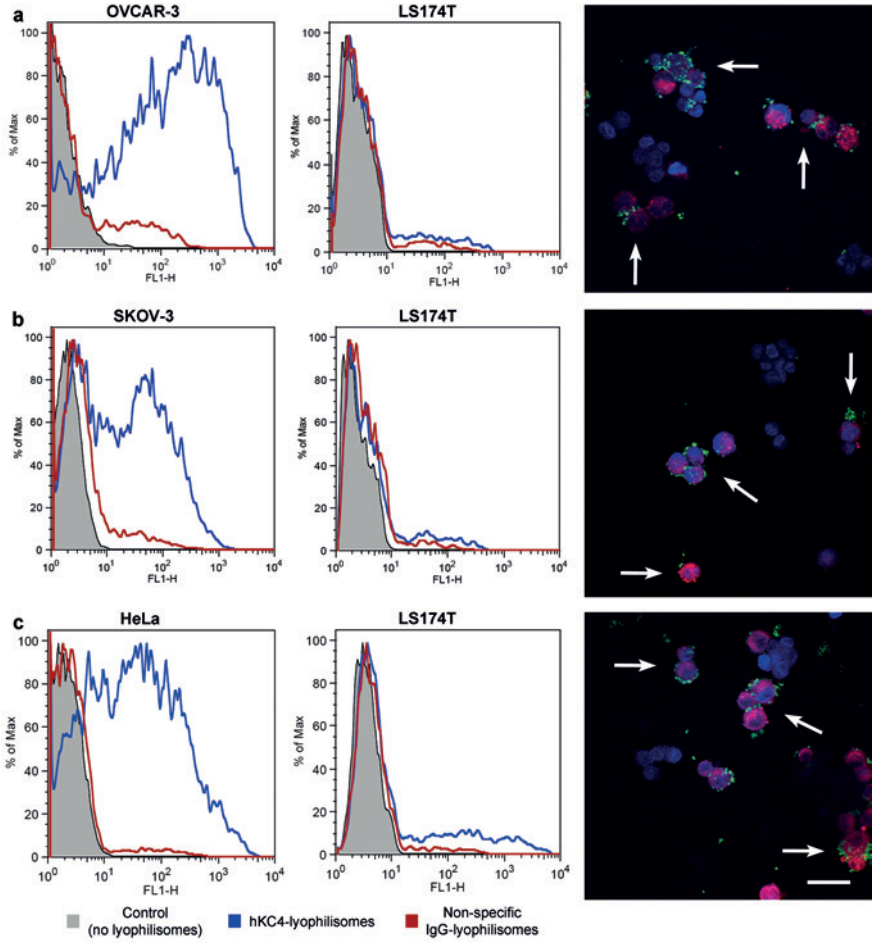

Figure 7 Specific targeting of cancer cells in a combination culture of MUC1 positive and negative cells. MUC1 positive and negative cells were mixed in a 1:1 ratio. To distinguish between both cell types, MUC1 positive cells were stained red by PKH26 membrane dye. For evaluation, positive and negative cells were plotted in separate histograms. **a**-**c**) OVCAR-3 (**a**), SKOV-3 (**b**), and HeLa (**c**) cells showed binding of hKC4 conjugated lyophilisomes when compared to LS174T cells. The non-specific IgG-conjugated lyophilisomes did not show a preferential binding to either cell type. Confocal laser scanning microscopy confirmed these results, where MUC1 positive cells could be distinguished from negative cells by their red fluorescence. hKC4-conjugated lyophilisomes showed specific targeting to MUC1 positive red cells (arrows) in contrast to MUC1 negative cells. Scale bar represents 60 µm.

the tumor cells (Fig. 8b). The same phenomenon was observed for SKOV-3 and HeLa cells (results not shown). For non-specific IgG-conjugated lyophilisomes, almost no binding was observed and lyophilisomes were not taken up by the cell (Fig. 8c). The cell membrane of OVCAR-3 cells was rather undisturbed after incubation with IgG-conjugated lyophilisomes. However, hKC4-conjugated lyophilisomes triggered membrane ruffling, most likely to internalize attached hKC4-conjugated lyophilisomes (Fig. 8b).

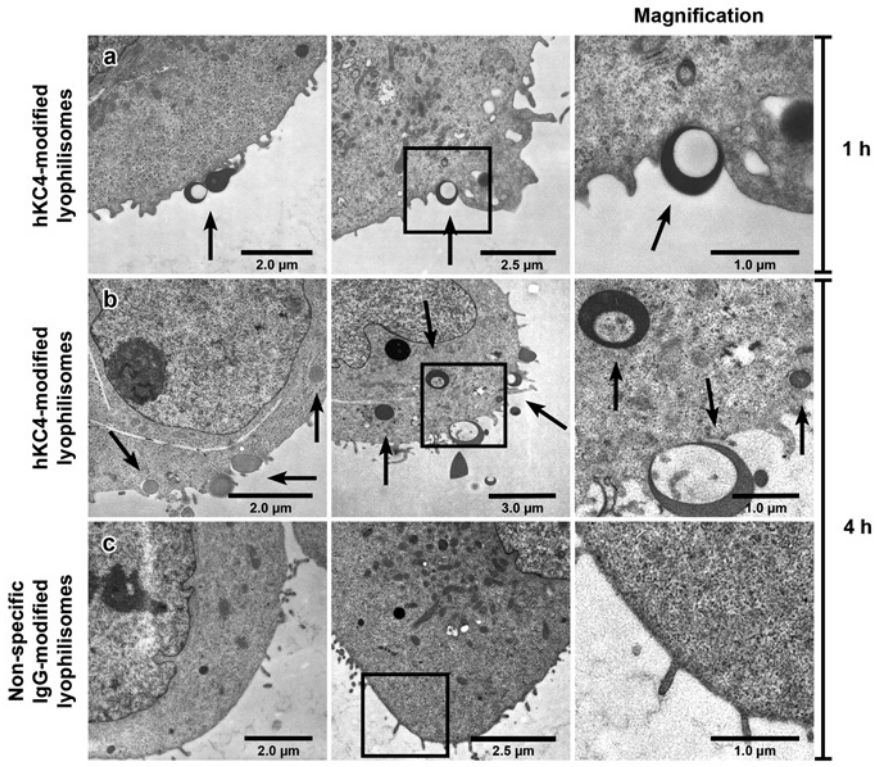

Figure 8 Cellular uptake of lyophilisomes as analyzed by transmission electron microscopy. OVCAR-3 cells were incubated with both hKC4-conjugated (**a** and **b**) and non-specific IgG-conjugated (**c**) lyophilisomes for one (**a**) and four (**b** and **c**) hours. **a**) hKC4-conjugated lyophilisomes bound to OVCAR-3 cells after one hour incubation. **b**) After an incubation time of four hours, internalized hKC-4-conjugated lyophilisomes were observed in OVCAR-3 tumor cells. **c**) No uptake was observed using non-specific IgG-conjugated lyophilisomes after a 4 h incubation.

DISCUSSION

A major goal in cancer research is to achieve high drug levels in target cells, without affecting healthy cells. Drug delivery systems have the advantage of guiding drugs to the tumor tissue, as they protect the drug until it reaches the target site. In order to achieve higher drug levels in the target cells, drug delivery systems can be designed with ligands or antibodies for active targeting [32,33]. In this study, we designed a MUC1 lyophilisome-based targeted delivery system to enhance binding in MUC1 overexpressing tumor cells.
Current nano/micro drug delivery systems for cancer therapeutic applications include liposomes, dendrimers, micelles, nanoconjugates, and (protein-based) nanoparticles [2,34,35]. Among the available drug carrier systems, protein-based nanoparticles are particularly interesting as they hold certain advantages such as increased stability during storage, non-toxicity, biocompatibility, and biodegradability *in vivo* [36,37]. Lyophilisomes can be prepared from a large variety of water-soluble macromolecules including proteins (*e.g.* albumin and elastin). In fact, virtually any biomolecule can be incorporated into the wall/lumen of the capsule, resulting in a highly flexible carrier system with multiple applications. Recently we showed that lyophilisomes have been efficiently loaded with doxorubicin resulting in tumor cell elimination *in vitro* [6].
In order to use lyophilisomes for active targeting of tumor cells, a MUC1-reactive hKC4 antibody was conjugated to lyophilisomes. First, maleimide groups were introduced on lyophilisomes whereas sulfhydryl groups were created on the antibody. In lyophilisomes, primary amine groups in albumin have already been partially used for stabilization of the capsules, but a 2 h vapor fixation left sufficient amines for conjugation. For the antibody, one to two thiol groups would be ideal for conjugation, since it ensures an efficient reaction while preserving the immunoreactivity of the antibody [17]. When introducing thiol groups, long incubations come with the risk of dimerization of sulfhydryl groups [11,17]. Similar to other studies, our results indicate that incubations longer than 5 h are therefore not optimal. Antibody conjugation to lyophilisomes proved to be reproducible when using a 5 h incubation with a 50-fold molar excess of Traut's reagent at pH 7.2. Antibody conjugation did not influence the mean particle diameter, as demonstrated by DLS and qNano and the complex was stable and functional for at least three months when stored at 4°C (data not shown).
In this study, a MUC1 antibody (hKC4) was conjugated to lyophilisomes to actively target tumor cells. Mucins are expressed by various epithelial cell types and have a central role in maintaining homeostasis and, therefore, promoting cell survival [38]. These characteristics also contribute to tumor cell survival when expressing mucins on their cellular membrane. Mucins are also able to bind growth factors to further stimulate the proliferation of tumor cells [38]. Since many tumors show high expression of MUC1, whereas it is expressed to a limited extent in normal cells, it is a good candidate to specifically target cancer cells [38].

When studying specificity of tumor cell targeting *in vitro*, hKC4-conjugated lyophili-somes showed an increased tumor targeting specificity. The relative fluorescent values obtained by FACS for the single cell experiments are in good correspondence with other MUC1 targeting drug delivery systems studies [10,11,39]. Dinauer *et al.* described their results by absolute gain in specific targeting [10]. Their group achieved a 16-fold gain in specific targeting compared to IgG-nanoparticles. Our findings showed a 15- fold, 8-fold, and 5-fold gain for respectively HeLa, OVCAR-3, and SKOV-3 cells. IgG-conjugated lyophilisomes showed an average background around 9%, compared to 6% measured by Dinauer *et al.* Furthermore, Steinhauser *et al.* showed that cellular association can be time dependent [11]. In our study, an incubation time of only 1 h was used whereas other studies incubated for a longer period of time up to 4 h, emphasizing on the rapid binding of hKC4-conjugat-ed lyophilisomes to MUC1 overexpressing tumor cells [10,17,40]. Furthermore, the incubation method (static *vs.* dynamic) is likely of importance. In this study, lyophilisomes were incubated with tumor cells under dynamic conditions, whereas other studies used static incubation conditions [17,40]. Even under dynamic conditions, hKC4-conjugated lyophilisomes specifically bound to MUC1-overexpressing tumor cells.

hKC4-conjugated lyophilisomes showed specific binding and uptake by MUC1-overexpressing tumor cells. To demonstrate the specificity of antibody-conjugated lyophilisomes, MUC1 positive and negative cells were mixed in culture. In this study, hKC4-conjugated lyophilisomes specifically bound to MUC1-overexpressing cells, whereas they did not bind to MUC1-negative LS174T cells. This observation held for all MUC1-positive cell lines used in this study (OVCAR-3, SKOV-3 and HeLa cells).

When examining the uptake, lyophilisomes specifically bound to MUC1-overexpressing tumor cells due to their specific antibody – antigen interaction. After binding, TEM results indicated the internalization of lyophilisomes modified with hKC4. Cells have a variety of endocytic mechanisms, including phagocytosis and pinocytosis, where pinocytosis occurs by at least four basic mechanisms (macropinocytosis, clathrin-mediated endocytosis, caveo-lae-mediated endocytosis, and clathrin- and caveolae-independent endocytosis) [41,42]. Phagocytosis and macropinocytosis (0.5 – 3 µm) are mechanisms for uptake of large particles whereas most mechanisms of pinocytosis internalize small particles (<200 nm) [42–44]. TEM images strongly suggest that lyophilisomes are internalized by phagocytosis or macropinocytosis, since intensive ruffling of the cell membrane was observed to the outside embracing the lyophilisome. In addition, the particle size of lyophilisomes ranges between 100 up to 3,000 nm, supporting uptake via phagocytosis or macropinocytosis [6,43]. However, lyophilisomes smaller than 200 nm could still be internalized by one of the other mechanisms of pinocytosis.

As demonstrated previously, lyophilisomes can be loaded with anti-tumor drugs, *e.g.* doxorubicin and curcumin [6]. In order to use antibody-modified lyophilisomes for the treatment of cancer, active tumor targeting can be combined with the drug delivery properties of lyophilisomes to establish a powerful system to selectively eliminate tumor cells.

CONCLUSION

Albumin-based lyophilisomes were functionalized with anti-MUC1 antibodies to obtain a selective drug carrier system specific towards cancers overexpressing MUC1. The lyophilisomes prepared specifically targeted MUC1 expressing tumor cell lines and were internalized. Functionalized lyophilisomes may present a novel strategy for the specific delivery of anti-tumor drugs to cancer cells.

Acknowledgements

The authors thank Dr. David M. Goldenberg (Immunomedics, Inc., Morris Plains, NJ, USA) for providing the hKC4 antibody. The research project was funded by the Radboud University Nijmegen Medical Centre.

REFERENCES

1. Wang AZ, Langer RS, Farokhzad OC (2012) Nanoparticle Delivery of Cancer Drugs. Annu Rev Med 63: 185-198.
2. Byrne JD, Betancourt T, Brannon-Peppas L (2008) Active targeting schemes for nanoparticle systems in cancer therapeutics. Adv Drug Deliv Rev 60: 1615-1626.
3. Zhang JA, Pawelchak J (2000) Effect of pH, ionic strength and oxygen burden on the chemical stability of EPC/cholesterol liposomes under accelerated conditions. Part 1: Lipid hydrolysis. Eur J Pharm Biopharm 50: 357-364.
4. Ahmed F, Discher DE (2004) Self-porating polymersomes of PEG-PLA and PEG-PCL: hydrolysis-triggered controlled release vesicles. J Control Release 96: 37-53.
5. Alexis F, Pridgen EM, Langer R, Farokhzad OC (2010) Nanoparticle technologies for cancer therapy. Handb Exp Pharmacol 55-86.
6. van Bracht E, Raave R, Verdurmen WP, Wismans RG, Geutjes PJ, *et al.* (2012) Lyophilisomes as a new generation of drug delivery capsules. Int J Pharm 439: 127-135.
7. Daamen WF, Geutjes PJ, Nillesen STM, Van Moerkerk HTB, Wismans R, *et al.* (2007) Lyophilisomes: A new type of (bio)capsules. Adv Mater 19: 673-677.
8. Kratz F (2008) Albumin as a drug carrier: design of prodrugs, drug conjugates and nanoparticles. J Control Release 132: 171-183.
9. Elsadek B, Kratz F (2012) Impact of albumin on drug delivery - New applications on the horizon. J Control Release 157: 4-28.
10. Dinauer N, Balthasar S, Weber C, Kreuter J, Langer K, *et al.* (2005) Selective targeting of antibody-conjugated nanoparticles to leukemic cells and primary T-lymphocytes. Biomaterials 26: 5898-5906.
11. Steinhauser I, Spankuch B, Strebhardt K, Langer K (2006) Trastuzumab-modified nanoparticles: optimisation of preparation and uptake in cancer cells. Biomaterials 27: 4975-4983.
12. Feinstein SB, Cheirif J, Ten Cate FJ, Silverman PR, Heidenreich PA, *et al.* (1990) Safety and efficacy of a new transpulmonary ultrasound contrast agent: initial multicenter clinical results. J Am Coll Cardiol 16: 316-324.
13. Geny B, Mettauer B, Muan B, Bischoff P, Epailly E, *et al.* (1993) Safety and efficacy of a new transpulmonary echo contrast agent in echocardiographic studies in patients. J Am Coll Cardiol 22: 1193-1198.
14. Ibrahim NK, Desai N, Legha S, Soon-Shiong P, Theriault RL, *et al.* (2002) Phase I and pharmacokinetic study of ABI-007, a Cremophor-free, protein-stabilized, nanoparticle formulation of paclitaxel. Clin Cancer Res 8: 1038-1044.
15. Ibrahim NK, Samuels B, Page R, Doval D, Patel KM, *et al.* (2005) Multicenter phase II trial of ABI-007, an albumin-bound paclitaxel, in women with metastatic breast cancer. J Clin Oncol 23: 6019-6026.
16. Maeda H, Wu J, Sawa T, Matsumura Y, Hori K (2000) Tumor vascular permeability and the EPR effect in macromolecular therapeutics: a review. J Control Release 65: 271-284.
17. Wagner S, Rothweiler F, Anhorn MG, Sauer D, Riemann I, *et al.* (2010) Enhanced drug targeting by attachment of an anti alphav integrin antibody to doxorubicin loaded human serum albumin nanoparticles. Biomaterials 31: 2388-2398.
18. Loomis K, Smith B, Feng Y, Garg H, Yavlovich A, *et al.* (2010) Specific targeting to B cells by lipid-based nanoparticles conjugated with a novel CD22-ScFv. Exp Mol Pathol 88: 238-249.
19. Van de BB, Devoogdt N, D'Hollander A, Gijs HL, Jans K, *et al.* (2011) Specific cell targeting with nanobody conjugated branched gold nanoparticles for photothermal therapy. ACS Nano 5: 4319-4328.
20. Levi E, Klimstra DS, Andea A, Basturk O, Adsay NV (2004) MUC1 and MUC2 in pancreatic neoplasia. J Clin Pathol 57: 456-462.
21. Singh PK, Hollingsworth MA (2006) Cell surface-associated mucins in signal transduction. Trends Cell Biol 16: 467-476.
22. Ferlay J, Shin HR, Bray F, Forman D, Mathers C, *et al.* (2010) Estimates of worldwide burden of cancer in 2008: GLOBOCAN 2008. Int J Cancer 127: 2893-2917.
23. Yu C, Hu Y, Duan J, Yuan W, Wang C, *et al.* (2011) Novel aptamer-nanoparticle bioconjugates enhances delivery of anticancer drug to MUC1-positive cancer cells in vitro. PLoS One 6: e24077.
24. Gendler SJ (2001) MUC1, the renaissance molecule. J Mammary Gland Biol Neoplasia 6: 339-353.
25. Garza-Licudine E, Deo D, Yu S, Uz-Zaman A, Dunbar WB (2010) Portable nanoparticle quantization using a resizable nanopore instrument - the IZON qNano. Conf Proc IEEE Eng Med Biol Soc 2010: 5736-5739.

26. Kakade ML, Liener IE (1969) Determination of available lysine in proteins. Anal Biochem 27: 273-280.
27. Riener CK, Kada G, Gruber HJ (2002) Quick measurement of protein sulfhydryls with Ellman's reagent and with 4,4'-dithiodipyridine. Anal Bioanal Chem 373: 266-276.
28. Simpson RJ (2008) Estimation of Free Thiols and Disulfide Bonds Using Ellman's Reagent. CSH Protoc 2008: db.
29. Tario JD Jr., Gray BD, Wallace SS, Muirhead KA, Ohlsson-Wilhelm BM, *et al.* (2007) Novel lipophilic tracking dyes for monitoring cell proliferation. Immunol Invest 36: 861-885.
30. Wallace PK, Tario JD Jr., Fisher JL, Wallace SS, Ernstoff MS, *et al.* (2008) Tracking antigen-driven responses by flow cytometry: monitoring proliferation by dye dilution. Cytometry A 73: 1019-1034.
31. Tanious FA, Veal JM, Buczak H, Ratmeyer LS, Wilson WD (1992) DAPI (4',6-diamidino-2-phenylindole) binds differently to DNA and RNA: minor-groove binding at AT sites and intercalation at AU sites. Biochemistry 31: 3103-3112.
32. Lammers T, Kiessling F, Hennink WE, Storm G (2012) Drug targeting to tumors: Principles, pitfalls and (pre-) clinical progress. J Control Release 161: 175-187.
33. Cardoso MM, Peca IN, Roque AC (2012) Antibody-conjugated nanoparticles for therapeutic applications. Curr Med Chem 19: 3103-3127.
34. Cho K, Wang X, Nie S, Chen ZG, Shin DM (2008) Therapeutic nanoparticles for drug delivery in cancer. Clin Cancer Res 14: 1310-1316.
35. De Jong WH, Borm PJ (2008) Drug delivery and nanoparticles:applications and hazards. Int J Nanomedicine 3: 133-149.
36. Langer K, Balthasar S, Vogel V, Dinauer N, von Briesen H, *et al.* (2003) Optimization of the preparation process for human serum albumin (HSA) nanoparticles. Int J Pharm 257: 169-180.
37. Elzoghby AO, Samy WM, Elgindy NA (2012) Protein-based nanocarriers as promising drug and gene delivery systems. J Control Release 161: 38-49.
38. Hollingsworth MA, Swanson BJ (2004) Mucins in cancer: protection and control of the cell surface. Nat Rev Cancer 4: 45-60.
39. Chen Y, Clark S, Wong T, Chen Y, Chen Y, *et al.* (2007) Armed antibodies targeting the mucin repeats of the ovarian cancer antigen, MUC16, are highly efficacious in animal tumor models. Cancer Res 67: 4924-4932.
40. Wartlick H, Michaelis K, Balthasar S, Strebhardt K, Kreuter J, *et al.* (2004) Highly specific HER2-mediated cellular uptake of antibody-modified nanoparticles in tumour cells. J Drug Target 12: 461-471.
41. Doherty GJ, McMahon HT (2009) Mechanisms of endocytosis. Annu Rev Biochem 78: 857-902.
42. Conner SD, Schmid SL (2003) Regulated portals of entry into the cell. Nature 422: 37-44.
43. Brandhonneur N, Chevanne F, Vie V, Frisch B, Primault R, *et al.* (2009) Specific and non-specific phagocytosis of ligand-grafted PLGA microspheres by macrophages. Eur J Pharm Sci 36: 474-485.
44. Hillaireau H, Couvreur P (2009) Nanocarriers' entry into the cell: relevance to drug delivery. Cell Mol Life Sci 66: 2873-2896.

4

Enhanced cellular uptake of albumin-based lyophilisomes when functionalized with cell-penetrating peptide TAT in HeLa cells

Etienne van Bracht, Luuk R.M. Versteegden, Sarah Stolle,
Wouter P.R. Verdurmen, Rob Woestenenk, René Raavé, Theo Hafmans,
Egbert Oosterwijk, Roland Brock, Toin H. van Kuppevelt, Willeke F. Daamen

PLoS ONE, Volume 9, Issue 11, e110813, 2014

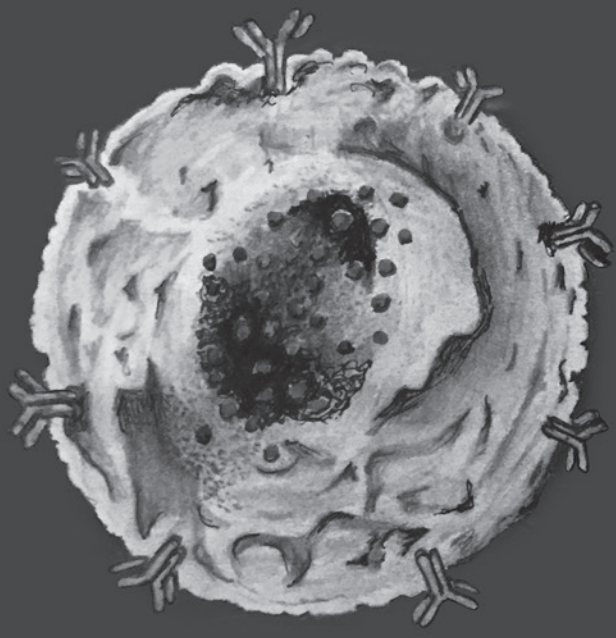

ABSTRACT

Lyophilisomes are a novel class of biodegradable proteinaceous nano/micrometer capsules with potential use as drug delivery carrier. Cell-penetrating peptides (CPPs) including the TAT peptide have been successfully implemented for intracellular delivery of a broad variety of cargos including various nanoparticulate pharmaceutical carriers. In the present study, lyophilisomes were modified using CPPs in order to achieve enhanced cellular uptake. Lyophilisomes were prepared by a freezing, annealing, and lyophilization method and a cystein-elongated TAT peptide was conjugated to the lyophilisomes using a hetero-bifunctional linker. Fluorescent-activated cell sorting (FACS) was utilized to acquire a lyophilisome population with a particle diameter smaller than 1,000 nm. Cultured HeLa, OVCAR-3, Caco-2 and SKOV-3 cells were exposed to unmodified lyophilisomes and TAT-conjugated lyophilisomes and examined with FACS. HeLa cells were investigated in more detail using a trypan blue quenching assay, confocal microscopy, and transmission electron microscopy. TAT-conjugation strongly increased binding and cellular uptake of lyophilisomes in a time-dependent manner *in vitro,* as assessed by FACS. These results were confirmed by confocal microscopy. Transmission electron microscopy indicated rapid cellular uptake of TAT-conjugated lyophilisomes via phagocytosis and/or macro-pinocytosis. In conclusion, TAT-peptides conjugated to albumin-based lyophilisomes are able to enhance cellular uptake of lyophilisomes in HeLa cells.

INTRODUCTION

An innovative strategy in cancer therapy utilizes drug delivery carriers to increase the therapeutic effect of anti-tumor drugs. The role of drug delivery carriers in this context is to improve pharmacokinetics and dynamics by protecting the drug from degradation [1–3]. Contemporary drug delivery systems include nanoparticulate systems loaded with anti-tumor drug and conjugates directly coupled to the drug. The unique property of nanoparticle carriers is their ability to encapsulate and deliver a high dose of anti-tumor drugs, including poorly soluble drugs, and to exploit the enhanced permeability and retention (EPR) effect for tumor targeting [4]. Because of these favorable characteristics, there has been intense interest in the development of nanoparticulate drug delivery systems.

Nanoparticles currently investigated for cancer therapeutic applications include liposomes, polymersomes, dendrimers, micelles, carbon nanotubes, nanoconjugates and (protein-based) nanospheres or capsules [5–7]. Among the available potential drug carrier systems, protein-based nanoparticles are particularly interesting as they hold certain advantages such as good stability during storage, non-toxicity, biocompatibility, and biodegradability *in vivo*[8,9]. Recently we showed that lyophilisomes, a novel class of proteinaceous biodegradable hollow nano/micrometer capsules, show potential as a drug delivery capsule [10,11]. Lyophilisomes can be prepared from a large variety of water-soluble macromolecules including proteins (*e.g.* albumin and elastin) but also polysaccharides (*e.g.* heparin). In fact, virtually any biomolecule can be incorporated into the wall/lumen of the capsule, resulting in a highly flexible carrier system with multiple applications. We previously demonstrated that enzymes introduced in the capsule's wall and in the lumen are bioactive and able to convert a substrate [10]. Furthermore, lyophilisomes have been efficiently loaded with doxorubicin resulting in tumor cell elimination *in vitro* [11]. In order to obtain a selective drug delivery system, lyophilisomes have also been modified with antibodies, resulting in specific targeting of the cell of interest *in vitro* [12]. Due to these properties, lyophilisomes can be deployed for the design of multifunctional targeting systems.

Lyophilisomes were prepared from albumin. Albumin is an attractive macromolecular carrier that has been shown to be non-toxic, non-immunogenic, biodegradable to produce innocuous degradation products, and easy to purify [13]. It is thus a suitable candidate for nanoparticle preparation, as demonstrated by FDA-approved products such as Abraxane [14,15] and Albunex [16,17].

Since delivery of nanocarriers is generally based on passive accumulation in pathological tissues, they do not efficiently deliver their cargo to specific cells. When drug delivery carriers arrive at the tumor site, they have to cross the plasma membrane in order to deliver the drug into the cell. The plasma membrane, however, prevent proteins, peptides, and nanoparticulate drug carriers from entering the cell in the absence of an active transport mechanism [18]. Cell-penetrating peptides (CPPs) have been successfully used to deliver a

large variety of cargos to the cell interior including proteins [19], peptides [20], nucleic acids [21] and pharmaceutical nanocarriers [22–24]. CPPs are short peptides consisting of up to 30 amino acids that are able to translocate across the cellular membrane [25]. When CPPs are conjugated to drug delivery carriers, efficient cellular uptake of the carriers can be achieved [26]. A representative CPP is the TAT peptide, derived from the TAT protein (trans-activation transcriptional activator) of the human immunodeficiency virus type 1 (HIV-1) [27,28]. The TAT peptide consists of 11 amino acids with the sequence YGRKKRRQRRR. The abundance of lysine and arginine residues makes it highly positively charged, important for the interaction with the plasma membrane. In this study, the TAT peptide was conjugated to lyophilisomes to investigate whether CPPs are able to enhance cellular uptake of lyophilisomes.

MATERIALS & METHODS

Materials

Bovine serum albumin was purchased from PAA Laboratories (Linz, Austria). FITC-conjugated bovine albumin was purchased from Sigma Aldrich (Steinheim, Germany). Sulfo-GMBS (sulfo-*N*-[γ-maleimidobutyryloxy]sulfosuccinimide ester) was purchased from Pierce Biotechnology (Rockford, IL, USA). Glutaraldehyde and formaldehyde were obtained from Merck (Darmstadt, Germany). Cysteine functionalized TAT peptide (C-Ahx-YGRKKRRQRRR) was purchased from EMC Microcollections GmbH (Tübingen, Germany), in which Ahx = aminohexanoic acid linker.

Methods

Preparation of lyophilisomes

Lyophilisomes were prepared from albumin as described previously [11]. Briefly, droplets of a solution of 0.25% (w/v) bovine serum albumin (BSA) in 0.01 M acetic acid were frozen in liquid nitrogen (-196°C). The frozen albumin preparation was incubated at -10 to -20°C for 3 h (annealing step), and subsequently lyophilized. This procedure results in hollow nano/micro spheres ("lyophilisomes"). In order to visualize the lyophilisomes, FITC-conjugated albumin was added to non-labeled albumin (1:10) in the starting solution. To obtain stabilized lyophilisomes, they were vapor crosslinked with glutaraldehyde and formaldehyde. Generally we prepare 40 ml of a 0.25 % BSA solution, which corresponds to 100 mg albumin (2.5 mg/ml). The final lyophilisome population was centrifuged three or four times at low speed (60x *g*; Thermo, Heraeus Fresco 17; Newport Pagnell, Great Britain) to remove large lyophilisomes and sheet-like structures, until no pellet was observed. After this procedure, about 30% of the original weight of lyophilisomes remained. Lyophilisomes (1 mg/ml) were stored in 0.1% (v/v) Tween-20 (Sigma Aldrich, Steinheim, Germany) in phosphate buffered saline (PBS-T, pH 7.4).

Conjugation of cell-penetrating peptide to lyophilisomes

A schematic representation of the conjugation reactions is depicted in figure 1.

Reaction 1: Activation of lyophilisomes. To obtain maleimide-activated lyophilisomes, 1 mg lyophilisomes were resuspended in 1 ml PBS-T and incubated overnight with 31 µl of 10 mM sulfo-GMBS in PBS-T (pH 8.0) at 4°C on a rotator (36 rpm, "Assistant" Rotating mixer, Karl Hecht, Sondheim, Germany), resulting in a 20:1 molar ratio of sulfo-GMBS:albumin. Excess sulfo-GMBS was removed by centrifugation (5 min, 17,000x *g*, 4°C) with three washing steps in PBS-T (pH 6.5).

Reaction 2: Conjugation of TAT peptide to lyophilisomes. For the coupling reaction, 1 ml of 1 mg/ml sulfhydryl-reactive lyophilisomes in 0.1% PBS-T was centrifuged and conjugated in 1 ml of cysteine functionalized TAT peptide (100 µM; C-Ahx-YGRKKRRQRRR) in 0.1% PBS-T (pH 6.5). Non-coupled TAT peptides were removed by centrifugation, using three washing steps in 0.1% PBS-T (pH 7.4). TAT-conjugated lyophilisomes were stored at 4°C in the dark.

Sorting of lyophilisomes by fluorescence-activated cell sorting

Fluorescence-activated cell sorting (FACS) was applied to select for small lyophilisomes (<1,000 nm) using a Coulter Epics Elite flow cytometer (BeckmanCoulter, Miami, FL, USA). Only small FITC-positive lyophilisomes were sorted (for settings, see figure 3). To achieve high sensitivity, gain was set at 20.

Particle size measurements by qNano

The qNano (Izon, Science Ltd., Burnside, New Zealand) was used to measure particle size distribution of lyophilisomes [11,29]. To ensure a continuous flow of particles, a pore size of 600 – 2,000 nm was used. Data were analyzed with Izon Control Suite 2.1 software.

Cell culture

HeLa (ACC 57, DSMZ, Braunschweig, Germany) and OVCAR-3 (#HTB-161, ATCC, LGC Standards GmbH, Wesel, Germany) cells were cultured in RPMI 1640 GlutaMAX medium Gibco (Karlsruhe, Germany) supplemented with 10% (v/v) fetal calf serum (FCS; PAA Laboratories, Pasching, Austria). Caco-2 cells (#HTB-37, ATCC) and SKOV-3 cells (#HTB-77, ATCC) were cultured in DMEM 1640 GlutaMAX medium Gibco supplemented with 20% (v/v) and 10% (v/v/) fetal calf serum, respectively. Cells were cultured in a humidified atmosphere with 5% CO_2 at 37°C. Subconfluent cells were dissociated with 0.05% trypsin (w/v) in 0.02% ethylenediaminetetraacetic acid (EDTA) (w/v) in PBS (PAA Laboratories) and were maintained as proliferating cultures.

For FACS, cells were stained with the plasma membrane dye PKH26 (Sigma Aldrich, Missouri, USA) [30,31]. One million cells were incubated in 2 µM PKH26 dye in 500 µl buffer (according to manufacturer's protocol) for 5 min. To stop the staining reaction, 500 µl FCS was added and incubated for 5 min. Subsequently, cells were washed three times with culture medium.

Cellular binding and internalization of lyophilisomes with and without TAT peptide

To determine whether the TAT peptide can promote the binding and internalization of lyophilisomes with HeLa, OVCAR-3, Caco-2 and SKOV-3 cells were seeded in a 24-well plate (30,000 cells/well in 1 ml medium). Cells were left to adhere overnight and subsequently incubated for 1 h with unsorted lyophilisomes with and without TAT peptide conjugated to them (25 µg/ml). After incubation, cells were washed three times with PBS to remove unbound lyophilisomes and harvested with enzyme-free EDTA solution (PAA Laboratories). Finally, cells were resuspended in 0.2% BSA in PBS and analyzed by FACS (FACSCalibur Becton Dickinson, Breda, Netherlands). Using the appropriate positive and negative controls FACS settings were adjusted. When lyophilisomes did not bind to cells, lyophilisomes were depicted at a fluorescent signal of 10^1 or below and cells were regarded negative. When lyophilisomes did bind to cells, they showed a fluorescent signal higher than 10^1. Data were analyzed by FlowJo software (Version 9.4, Treestar, Ashland, OR, USA).

Internalization studies of lyophilisomes by cells

FACS

In order to discriminate between attached and internalized lyophilisomes, a FITC quenching trypan blue assay was used [32–34]. Quenching of FITC signal occurs because trypan blue absorbs the light emitted by FITC-labeled lyophilisomes after excitation. The FITC signal of *internalized* lyophilisomes however, is not quenched since trypan blue cannot pass the plasma membrane. The fluorescence remaining after trypan blue quenching must therefore result from internalized lyophilisomes, as only extracellular fluorescence of FITC-lyophilisomes is quenched.

To investigate the cellular uptake of lyophilisomes, PKH26 stained HeLa cells were seeded in a 24-well plate (30,000 cells/well) and left to adhere overnight. Cells were incubated with 500,000 FACS-sorted lyophilisomes with and without TAT peptide for 1 and 4 h. After incubation, cells were washed three times with 0.2% (w/v) BSA in PBS, dissociated with enzyme-free EDTA dissociation buffer, resuspended in 1 ml culture medium and transferred to an eppendorf tube. Subsequently, cells were washed three times with 0.2% BSA-PBS by centrifugation (3 min, room temperature, 100x g) and incubated with 0.5% (w/v) trypan blue for 10 min and washed three times with 0.2% BSA-PBS. Cells were analyzed by FACSCalibur flowcytometry. Data were analyzed by FlowJo Software.

Confocal microscopy

To visualize cellular uptake of lyophilisomes, confocal microscopy was performed on living cells. HeLa cells were seeded in an 8-well microscopy chamber (Nunc; 30,000 cells/well) and left to adhere overnight. Cells were incubated with sorted lyophilisomes with and without TAT peptide using 0.8 and 3.5 million lyophilisomes in 200 µl per sample for 4 h in RPMI medium containing 10% FCS at 37°C. As a control, medium without lyophilisomes was used. After incubation, cells were washed three times, incubated for 5 min with

CellMask Orange (5 µg/ml) to visualize the plasma membranes and then washed again, all with the same medium. Cells were kept at 37°C on a temperature controlled microscope stage and living cells were imaged immediately with a Leica SP5 confocal microscope (Leica Microsystems, Mannheim, Germany). FITC was excited at 488 nm and emission was collected between 500-550 nm. CellMask orange was excited at 561 nm and emission was collected between 570-650 nm. Images were recorded sequentially using Leica Application Suite Software (Advanced Fluorescence Lite, 2.3.0. build 5131).

Transmission electron microscopy

Cells incubated with lyophilisomes with and without TAT peptide as described in the Materials and Methods section '*FACS*' were embedded in 1.5% (w/v) agarose, fixed in 2% (v/v) glutaraldehyde in 0.1 M phosphate buffer (pH 7.4), post-fixed with 1% (w/v) osmium tetroxide, dehydrated in an ascending series of ethanol, and embedded in Epon 812. Ultrathin sections (60 nm) were cut and picked up on Formvar-coated grids, post-stained with lead citrate and uranyl acetate, and examined with a JEOL 1010 transmission electron microscope (Tokyo, Japan).

Statistical Analysis

Data are presented as mean with standard deviation. Data of Results section '*Cellular binding and internalization of lyophilisomes with and without TAT peptide*' were analyzed using two-tailed Student's *t*-tests. Data of Results section '*Trypan blue assay and FACS*' were analyzed using two-way Anova Bonferroni post-hoc tests. All statistical analyses were performed in Graphpad Prism 5.0 (Graphpad, San Diego, CA, USA). P values <0.05 were considered significant.

RESULTS

Conjugation of TAT peptide to lyophilisomes

To probe the possibility of using CPP for enhanced intracellular delivery, lyophilisomes were modified with a cysteine-functionalized TAT peptide using the heterobifunctional linker sulfo-GMBS (Fig. 1). The succinimidyl ester functionality is conjugated to primary amine groups on the lyophilisome while the maleimide functionality is used for conjugation to the free thiol of the cysteine residue coupled to the TAT peptide.

Cellular binding and internalization of lyophilisomes with and without TAT peptide

To address the presence of the TAT peptide on TAT-conjugated lyophilisomes, unmodified lyophilisomes and TAT-conjugated lyophilisomes were administered to HeLa, OVCAR-3, Caco-2 and OVCAR-3 cells. Using standard FACS as a functional assay, it is not possible to

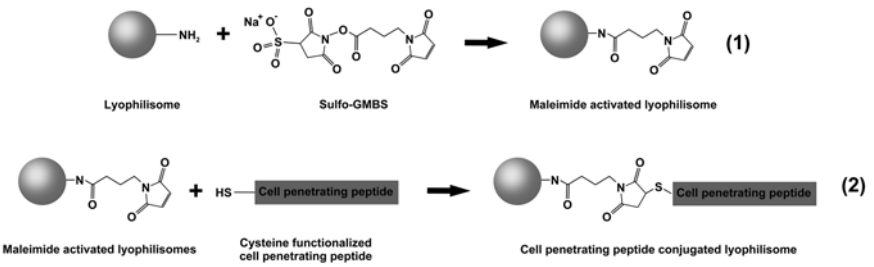

Figure 1 Schematic illustration of the conjugation of the cell-penetrating peptide (CPP) TAT to lyophilisomes. (**1**) Primary amine groups of lyophilisomes react with Sulfo-GMBS introducing reactive maleimide groups. (**2**) CPPs (cysteine-functionalized TAT-peptides; C-Ahx-YGRKKRRQRRR) are conjugated to maleimide-conjugated lyophilisomes, resulting in stable CPP-conjugated lyophilisomes. Sulfo-GMBS = sulfo-*N*-[γ-maleimidobutyryloxy]sulfo succinimide ester; Ahx = aminohexanoic acid; TAT = trans-activating transcriptional activator.

discriminate between cellular attachment and internalization. Instead, the total of cell binding and internalization is measured (Fig. 2). For HeLa cells, TAT-conjugated lyophilisomes showed an about 8-fold increase in lyophilisome-positive cells compared to lyophilisomes without the TAT peptide (86±3% and 12±4% lyophilisome-positive cells for TAT-conjugated and unmodified lyophilisomes, respectively. OVCAR-3 and Caco-2 cells showed about a 5-fold increase in lyophilisome-positive cells compared to lyophilisomes without the TAT peptide (lyophilisome-positive cells: 97±3% and 19±3% for OVCAR-3; 87±3% and 16±8% for Caco-2) for TAT-conjugated and unmodified lyophilisomes, respectively. SKOV-3 cells gave a high background value when incubated with lyophilisomes without TAT (67±20%), but still showed a 1.6 fold statistically significant increase with the presence of TAT peptide (95±10%).

Lyophilisomes sorted by fluorescence-activated cell sorting

When using lyophilisomes for tumor targeting, lyophilisomal size is an important parameter. The initial lyophilisome population included sizes up to 2.8 µm (Fig. 3a). To obtain a more monodisperse capsule population, lyophilisomes were sorted by FACS. Lyophilisomes were separated based on forward scatter and FITC fluorescence (FL1 channel; Fig. 3c). To verify the procedure, a rerun of sorted lyophilisomes was performed (Fig. 3d). Using this methodology, larger lyophilisomes as well as sheet-like structures (confirmed by scanning electron microscope) were separated from small lyophilisomes. These results were substantiated by qNano size analysis using a lyophilisome preparation before (Fig. 3a) and after (Fig. 3b) sorting (approximately 90% below 1 µm). Measurements using the qNano consisted of 200 – 250 particles. The size distribution contained multiple

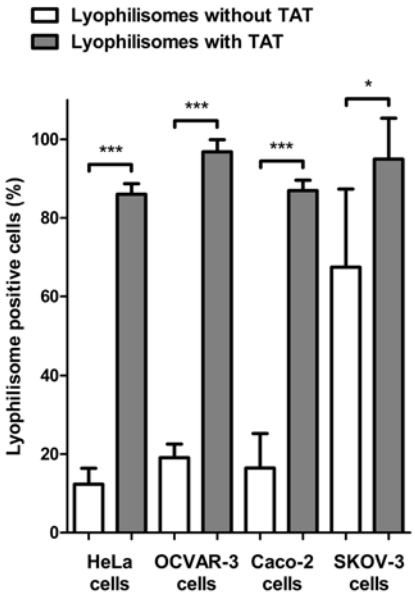

Figure 2 Cellular binding and internalization of unmodified lyophilisomes and TAT-conjugated lyophilisomes. HeLa, OVCAR-3, Caco-2 and SKOV-3 cells incubated with TAT-conjugated and unmodified lyophilisomes resulted in 86±3% and 12±4%, 87±3% and 16±8%, 97±3% and 19±3%, and 95±10% and 67±20% lyophilisome-positive cells, respectively.
TAT = trans-activating transcriptional activator. *p<0.01 ***p<0.0001.

peaks that can be explained by the low number of particles. Due to the limitations of the qNano instrument particles smaller than 600 nm could not be reliably detected which overestimates the average size of the lyophilisomes. Pilot experiments with a smaller qNano pore (200 – 800 nm) revealed the presence of lyophilisomes below 600 nm (results not shown), but larger lyophilisomes in the preparation frequently blocked this pore.

Cellular uptake of TAT-conjugated lyophilisomes

Trypan blue assay and FACS

To determine the internalization efficiency of sorted lyophilisomes with and without TAT peptide, a trypan blue quenching assay was used in order to distinguish between internalized and non-internalized (but plasma membrane-associated) lyophilisomes. This assay is based on the quenching of fluorescence of FITC-labeled lyophilisomes by the vital stain trypan blue (which does not penetrate plasma membranes). To validate that trypan blue also quenches fluorescence of FITC labeled lyophilisomes, lyophilisomes were incubated with trypan blue in the absence of cells and evaluated by FACS (Fig. 4).

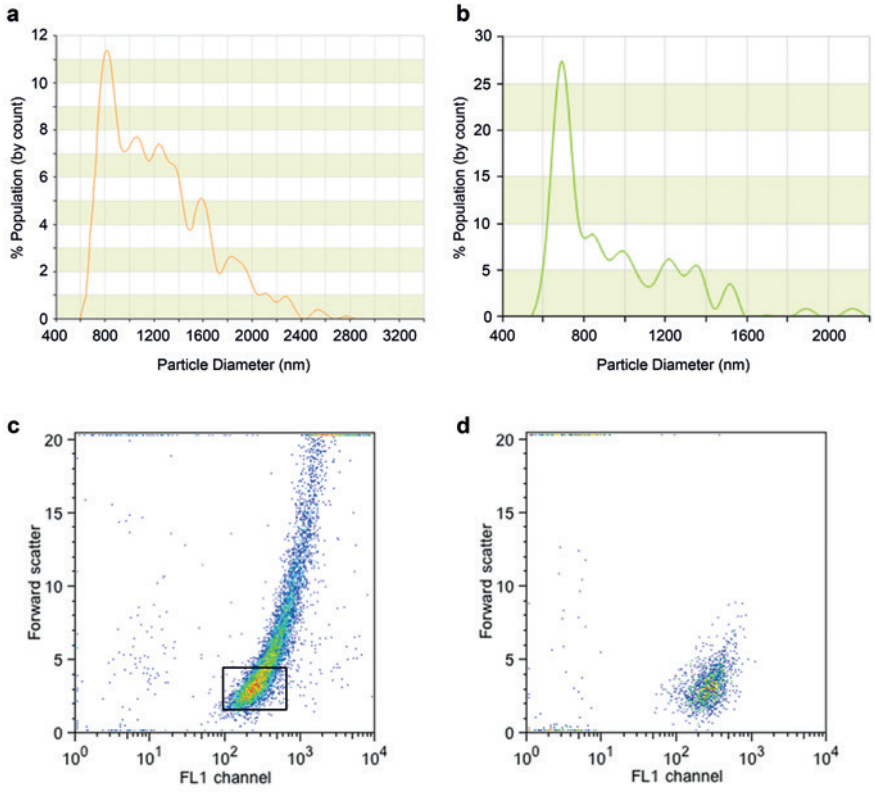

Figure 3 Sorting of lyophilisomes by fluorescence-activated cell sorting. **a** and **b**) A representative size distribution of the initial lyophilisome population (**a**) and sorted lyophilisomes (**b**) is depicted, showing smaller lyophilisomes after sorting. Note the difference in x and y axes. **c**) Initial lyophilisome population depicted in a FACS dot plot with forward (size) / FITC-positive lyophilisome (FL1 channel) scatter where gated FITC-positive lyophilisomes were sorted. **d**) After sorting, the scatter showed merely small lyophilisomes, as large lyophilisomes were removed.

Lyophilisomes that were not incubated with trypan blue showed a mean fluorescence intensity of 1,339±252. Lyophilisomes incubated in a 0.5% trypan blue solution gave a mean fluorescent intensity of 85±31, corresponding to a quenching efficacy of 94±2% (Fig. 4b). After one, two and three washings after the trypan blue incubation, the measured mean fluorescence was 161±25, 176±22, and 192±19 or 88±1%, 87±1% and 85±1% quenching efficacy, respectively. This indicates that trypan blue was not easily washed out of the lyophilisomes and fluorescence remained quenched. This is important as three washings steps were used prior to FACS analysis.

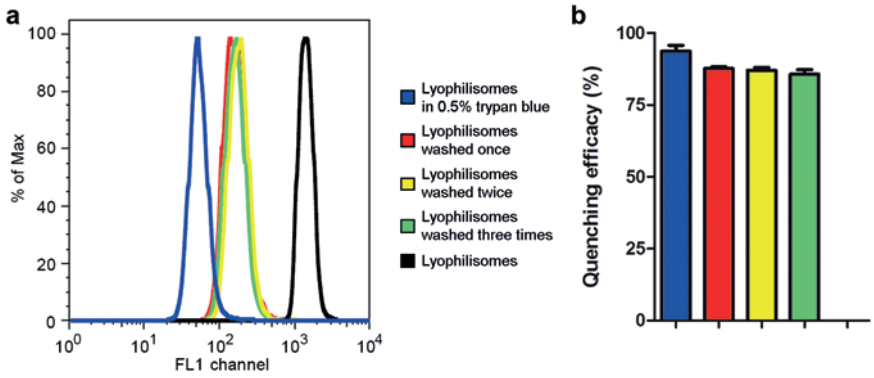

Figure 4 Quenching of FITC fluorescent lyophilisomes by trypan blue in the absence of cells. Results show decreased fluorescence (**a**) and efficient quenching (**b**) up to three washings steps of FITC fluorescent lyophilisomes by trypan blue.

To investigate whether TAT peptides can enhance internalization of sorted lyophilisomes, the trypan blue quenching assay was performed in the presence of HeLa cells (Fig. 5). Cells were incubated with 500,000 sorted lyophilisomes with and without TAT peptide. Incubation for 1 h with TAT-conjugated lyophilisomes resulted in many lyophilisome-positive cells (67±3%) and moderate cellular uptake (25%±1). In contrast, unmodified lyophilisomes showed few lyophilisome-positive cells (6±5%) and almost no internalization (1±1%). Interestingly, when lyophilisomes were incubated for 4 h, the number of lyophilisome-positive cells of TAT-conjugated lyophilisomes remained high (79±8%) and cellular uptake strongly increased (59±14%), whereas unmodified lyophilisomes still showed a moderate number of lyophilisome-positive cells (17±8%) and little internalization (7±2%).

Confocal microscopy

Internalization of TAT-conjugated lyophilisomes in HeLa cells was visualized by confocal microscopy (Fig. 6). After 4 h of incubation, TAT-conjugated lyophilisomes showed extensive uptake for both low (0.8 million / 200 µl) and high (3.5 million / 200 µl) numbers of lyophilisomes (Fig. 6c and g). Almost no internalization was observed when HeLa cells were incubated with unmodified lyophilisomes (Fig. 6a and e). The corresponding bright field images showed that lyophilisomes did not lead to detectable morphological changes of the cells (Fig. 6b, d, f and h).

Transmission electron microscopy

In order to investigate the binding and uptake of TAT-conjugated lyophilisomes in HeLa cells in detail, TEM was used (Fig. 7). When unmodified lyophilisomes were added to HeLa

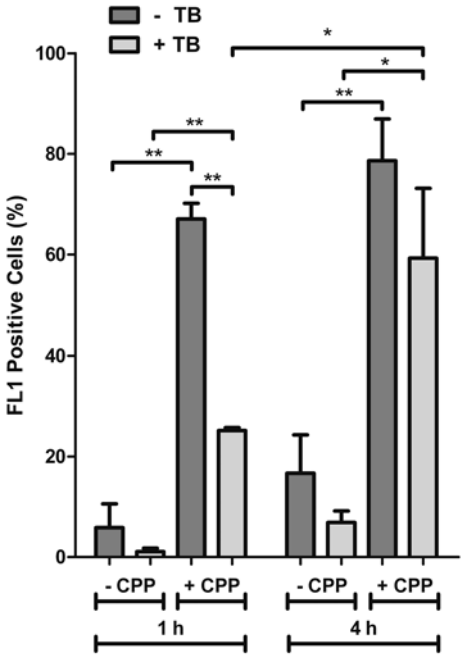

Figure 5 Internalization of lyophilisomes with and without TAT peptide into HeLa cells. FACS showed a large number of lyophilisome-positive cells for TAT-conjugated lyophilisomes after 1 h (67±3%) without trypan blue and a cellular uptake of 25±1% with trypan blue. Values for lyophilisomes without TAT peptide were low. When lyophilisomes were incubated for 4 h, TAT-conjugated lyophilisomes conserved the large number of lyophilisome-positive cells (79±8%) with an increased internalization of 59±14%, while unmodified lyophilisomes still showed few lyophilisome-positive cells and little cellular uptake. *p<0.01 **p<0.001.
CPP = cell penetrating peptide; TAT = trans-activating transcriptional activator.

cells, no binding or uptake was observed and the plasma membrane appeared largely unruffled (Fig. 7a). However, when TAT-conjugated lyophilisomes were added, multiple stages of internalization could be distinguished, including attachment and internalization (Fig. 7b and c). Initially, TAT-conjugated lyophilisomes bound to HeLa cells and initiated membrane ruffling (Fig. 7b). Subsequently, capsules were internalized (Fig. 7c). Furthermore, initial signs of degradation of lyophilisomes could be observed, as degradation products were visible (black arrows; Fig. 7d).

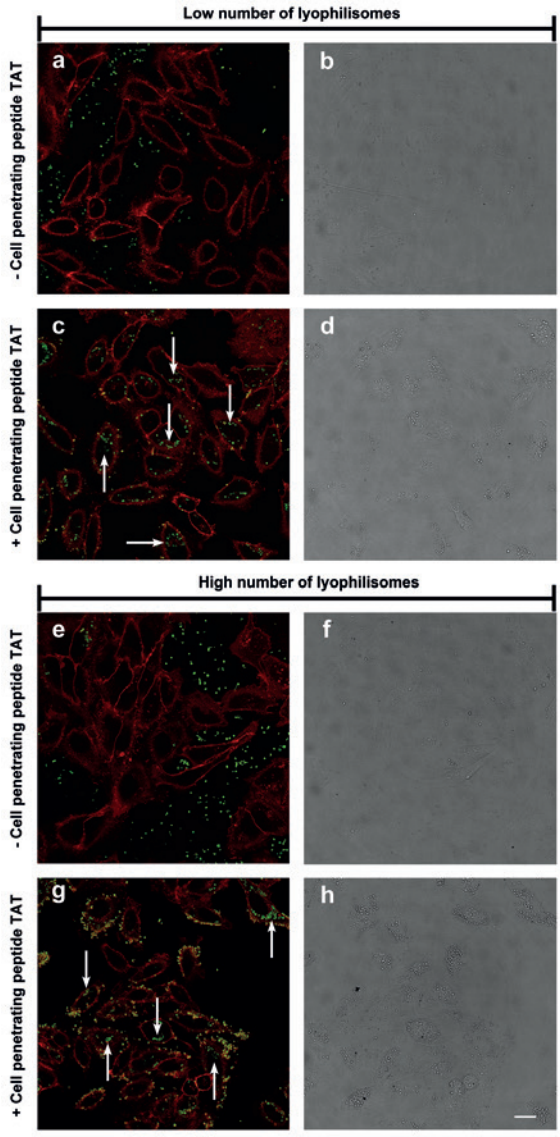

Figure 6 Internalization of lyophilisomes without and with TAT peptide by HeLa cells. Lyophilisomes without and with TAT peptide were administered to 30,000 HeLa cells using two dosages (0.8 million / 500 µl (a-d) and 3.5 million / 500 µl (**e**-**h**). Cells incubated with lyophilisomes without TAT peptide had internalized few lyophilisomes (**a** and **e**), whereas TAT-conjugated lyophilisomes showed high cellular uptake for almost all cells (**c** and **g**). Green fluorescence corresponds to lyophilisomes and red fluorescence (CellMask orange) visualizes the plasma membrane. Bright field images (**b**, **d**, **f** and **h**) show normal morphology of the cells. Scale bar represents 20 µm.
TAT = trans-activating transcriptional activator.

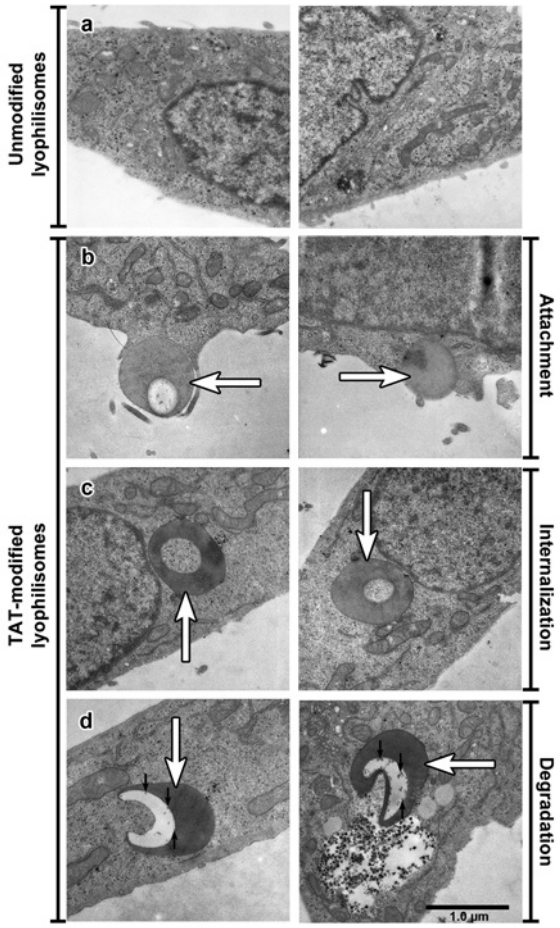

Figure 7 Cellular uptake of TAT-conjugated lyophilisomes as analyzed by transmission electron microscopy. HeLa cells were incubated with unmodified (**a**) and TAT-conjugated lyophilisomes (**b**-**d**) for 4 h. **a**) No attachment or uptake was observed using unmodified lyophilisomes. **b**-**d**) TAT-conjugated lyophilisomes (white arrows) showed various processes required for effective drug delivery systems, such as attachment (**b**) and uptake (**c**). Additionally, signs of degradation of the capsule inside the cell were visualized (black arrows, **d**). Scale bar represents 1.0 µm.
TAT = trans-activating transcriptional activator.

DISCUSSION

Our laboratory previously demonstrated that lyophilisomes show potential as a drug delivery system [11,12]. To further optimize these biocapsules, we studied the effect of TAT-functionalization on the *in vitro* internalization of lyophilisomes. Intracellular delivery

of therapeutic molecules is one of the key problems in drug delivery. Many pharmaceutical compounds have to be delivered intracellularly to exert their therapeutic action [22]. CPPs have been shown to act as a powerful transport vector for inducing the cellular uptake of a large variety of cargos [18]. At present, pharmaceutical nanocarriers are much in focus for their capacity to increase the stability of administered drugs, improve their concentration at their site-of-action and decrease undesired side effects. Various studies report increased uptake and specific delivery to intracellular organelles when conjugating CPPs to drug delivery systems, thereby increasing the efficiency of nanocarriers as drug delivery systems [35–37].

As previously reported, lyophilisomes range in size from 100 up to 3,000 nm in diameter [11]. In this study, we demonstrated that using FACS, small lyophilisomes could be sorted out of the initial population, narrowing the size distribution.

In the present study, FACS was used to investigate the total cell binding and internalization of (TAT-conjugated) lyophilisomes in HeLa, OVCAR-3, Caco-2, and SKOV-3 cells. To investigate the cellular uptake and subcellular distribution of (TAT-conjugated) lyophilisomes in HeLa cells in more detail, confocal microscopy, and TEM were utilized. FACS demonstrated a high number of lyophilisome-positive cells when incubated with TAT-conjugated lyophilisomes compared to unmodified lyophilisomes. This may be explained by interaction of the TAT peptide with negatively charged sulfated glycans at the cell surface, such as heparan sulphate [38,39]. Only SKOV-3 cells showed a high background when incubated with unmodified lyophilisomes, which has been shown for other drug carriers added to this cell line [40].

To discriminate between internalization and attachment, a trypan blue quenching assay was applied on HeLa cells incubated with lyophilisomes. This assay showed that cellular uptake was enhanced when TAT peptides were conjugated to lyophilisomes. The degree of internalization may even have been underestimated as our capsules are likely to enter the acidic lysosomes in the cell [41] and since FITC fluorescein is virtually non-fluorescent below pH 5 [42]. The trypan blue assay also demonstrated that cellular uptake of TAT-conjugated lyophilisomes increased over time. After 1 h, 25±1% of the cells internalized TAT-conjugated lyophilisomes, whereas 59±14% of cells had done so after an incubation period of 4 h. We most likely added too little lyophilisomes in the trypan blue internalization study to achieve lyophilisome internalization of all available cells. This is supported by confocal microscopy, which revealed that almost all cells internalized at least one lyophilisome when administering more lyophilisomes. TEM images showed different stages of cellular uptake (attachment and internalization) of TAT-conjugated lyophilisomes. The results strongly suggest that TAT-conjugated lyophilisomes are internalized by phagocytosis and/or macropinocytosis, as intensive plasma membrane ruffling was observed during uptake. This suggestion would be in line with the particle size of lyophilisomes [43]. However, lyophilisomes smaller than 200 nm, could still be internalized by one of the mechanisms of endocytosis.

If we compare our findings to other studies, the increased internalization efficiency compared to unmodified particles is within the range of reported values for TAT peptides conjugated to cargos such as liposomes [44,45]. However, it is difficult to compare internalization for different kinds of nanoparticles, since different cell types and different amounts and sizes of nanoparticles are used for *in vitro* experiments, *e.g.* the larger the particle the more time it takes to establish internalization [46].
The ability of CPPs to enhance cellular uptake non-specifically and receptor-independently provides the opportunity to target diverse cell types with a variety of carriers. In literature, it has been observed that next to HeLa, OVCAR-3, Caco-2 and SKOV-3 cells, the TAT peptide can enter other tumor cells, for instance bladder cancer (HTB-9, MBT2), breast cancer (SK-BR-3, MCF7), and other colon cancer (C26) cells [45,47]. However, their non-specificity presents a significant challenge in systemically administered applications for targeted delivery, as it requires precise control of CPP presentation only at the target site to prevent toxicity [48]. To overcome this problem, several approaches are being investigated to activate CPPs only at the target site. Stimulus-responsive materials may be used for this purpose, as they may provide triggered changes in material properties that allow spatially focused presentation of CPPs in response to intrinsic disease characteristics (*e.g.* abundantly present extracellular matrix proteases) or locally applied extrinsic cues (*e.g.* apply heat or light at a specific location) [49].
As demonstrated in this study, TAT peptides can enhance cellular uptake when conjugated to lyophilisomes. In previous *in vitro* studies, lyophilisomes were loaded with anti-tumor drugs, *e.g.* doxorubicin and curcumin, which could eliminate tumor cells. Antibodies were conjugated to lyophilisomes resulting in specific binding to target cells [11,12]. To probe the possibility of using lyophilisomes for the treatment of cancer, active targeting with specific antibodies and enhanced cellular uptake with CPPs can be combined with the drug delivery properties of lyophilisomes, thereby creating a potential powerful tool for drug delivery.

CONCLUSION

In the present study, albumin-based lyophilisomes were functionalized with TAT peptides to obtain a drug delivery system with enhanced cellular uptake. Lyophilisomes modified with TAT peptides efficiently bound to HeLa, OVCAR-3, Caco-2 and SKOV-3 cells. Additional cellular uptake studies were performed to verify that TAT-conjugated lyophilisomes were internalized in HeLa cells after binding. TAT-conjugated lyophilisomes may present a novel delivery system to ensure faster and higher cellular uptake of anti-tumor drugs to cancer cells.

REFERENCES

1. Davis ME, Chen ZG, Shin DM (2008) Nanoparticle therapeutics: an emerging treatment modality for cancer. Nat Rev Drug Discov 7: 771-782.
2. Haley B, Frenkel E (2008) Nanoparticles for drug delivery in cancer treatment. Urol Oncol 26: 57-64.
3. Danhier F, Ansorena E, Silva JM, Coco R, Le Breton A, et al. (2012) PLGA-based nanoparticles: an overview of biomedical applications. J Control Release 161: 505-522.
4. Torchilin V (2011) Tumor delivery of macromolecular drugs based on the EPR effect. Adv Drug Deliv Rev 63: 131-135.
5. Cho K, Wang X, Nie S, Chen ZG, Shin DM (2008) Therapeutic nanoparticles for drug delivery in cancer. Clin Cancer Res 14: 1310-1316.
6. Byrne JD, Betancourt T, Brannon-Peppas L (2008) Active targeting schemes for nanoparticle systems in cancer therapeutics. Adv Drug Deliv Rev 60: 1615-1626.
7. De Jong WH, Borm PJ (2008) Drug delivery and nanoparticles:applications and hazards. Int J Nanomedicine 3: 133-149.
8. Langer K, Balthasar S, Vogel V, Dinauer N, von Briessen H, *et al.* (2003) Optimization of the preparation process for human serum albumin (HSA) nanoparticles. Int J Pharm 257: 169-180.
9. Elzoghby AO, Samy WM, Elgindy NA (2012) Protein-based nanocarriers as promising drug and gene delivery systems. J Control Release 161: 38-49.
10. Daamen WF, Geutjes PJ, Nillesen STM, Van Moerkerk HTB, Wismans R, *et al.* (2007) Lyophilisomes: A new type of (bio)capsules. Adv Mater 19: 673-677.
11. van Bracht E, Raave R, Verdurmen WP, Wismans RG, Geutjes PJ, *et al.* (2012) Lyophilisomes as a new generation of drug delivery capsules. Int J Pharm 439: 127-135.
12. van Bracht E, Stolle S, Hafmans TG, Boerman OC, Oosterwijk E, *et al.* (2014) Specific targeting of tumor cells by lyophilisomes functionalized with antibodies. Eur J Pharm Biopharm 87: 80-89.
13. Elzoghby AO, Samy WM, Elgindy NA (2011) Albumin-based nanoparticles as potential controlled release drug delivery systems. J Control Release 157: 168-182.
14. Ibrahim NK, Desai N, Legha S, Soon-Shiong P, Theriault RL, *et al.* (2002) Phase I and pharmacokinetic study of ABI-007, a Cremophor-free, protein-stabilized, nanoparticle formulation of paclitaxel. Clin Cancer Res 8: 1038-1044.
15. Ibrahim NK, Samuels B, Page R, Doval D, Patel KM, *et al.* (2005) Multicenter phase II trial of ABI-007, an albumin-bound paclitaxel, in women with metastatic breast cancer. J Clin Oncol 23: 6019-6026.
16. Feinstein SB, Cheirif J, Ten Cate FJ, Silverman PR, Heidenreich PA, *et al.* (1990) Safety and efficacy of a new transpulmonary ultrasound contrast agent: initial multicenter clinical results. J Am Coll Cardiol 16: 316-324.
17. Geny B, Mettauer B, Muan B, Bischoff P, Epailly E, *et al.* (1993) Safety and efficacy of a new transpulmonary echo contrast agent in echocardiographic studies in patients. J Am Coll Cardiol 22: 1193-1198.
18. Koren E, Torchilin VP (2012) Cell-penetrating peptides: breaking through to the other side. Trends Mol Med 18: 385-393.
19. Wadia JS, Dowdy SF (2005) Transmembrane delivery of protein and peptide drugs by TAT-mediated transduction in the treatment of cancer. Adv Drug Deliv Rev 57: 579-596.
20. Massodi I, Bidwell GL III, Raucher D (2005) Evaluation of cell penetrating peptides fused to elastin-like polypeptide for drug delivery. J Control Release 108: 396-408.
21. striab-Fisher A, Sergueev D, Fisher M, Shaw BR, Juliano RL (2002) Conjugates of antisense oligonucleotides with the Tat and antennapedia cell-penetrating peptides: effects on cellular uptake, binding to target sequences, and biologic actions. Pharm Res 19: 744-754.
22. Torchilin VP (2008) Cell penetrating peptide-modified pharmaceutical nanocarriers for intracellular drug and gene delivery. Biopolymers 90: 604-610.
23. Qin Y, Chen H, Zhang Q, Wang X, Yuan W, *et al.* (2011) Liposome formulated with TAT-modified cholesterol for improving brain delivery and therapeutic efficacy on brain glioma in animals. Int J Pharm 420: 304-312.
24. Sawant RR, Torchilin VP (2009) Enhanced cytotoxicity of TATp-bearing paclitaxel-loaded micelles in vitro and in vivo. Int J Pharm 374: 114-118.

25. Patel LN, Zaro JL, Shen WC (2007) Cell penetrating peptides: intracellular pathways and pharmaceutical perspectives. Pharm Res 24: 1977-1992.
26. Chugh A, Eudes F, Shim YS (2010) Cell-penetrating peptides: Nanocarrier for macromolecule delivery in living cells. IUBMB Life 62: 183-193.
27. Frankel AD (1992) Activation of HIV transcription by Tat. Curr Opin Genet Dev 2: 293-298.
28. Vives E, Brodin P, Lebleu B (1997) A truncated HIV-1 Tat protein basic domain rapidly translocates through the plasma membrane and accumulates in the cell nucleus. J Biol Chem 272: 16010-16017.
29. Garza-Licudine E, Deo D, Yu S, Uz-Zaman A, Dunbar WB (2010) Portable nanoparticle quantization using a resizable nanopore instrument - the IZON qNano. Conf Proc IEEE Eng Med Biol Soc 2010: 5736-5739.
30. Tario JD Jr., Gray BD, Wallace SS, Muirhead KA, Ohlsson-Wilhelm BM, *et al.* (2007) Novel lipophilic tracking dyes for monitoring cell proliferation. Immunol Invest 36: 861-885.
31. Wallace PK, Tario JD Jr., Fisher JL, Wallace SS, Ernstoff MS, *et al.* (2008) Tracking antigen-driven responses by flow cytometry: monitoring proliferation by dye dilution. Cytometry A 73: 1019-1034.
32. Nuutila J, Lilius EM (2005) Flow cytometric quantitative determination of ingestion by phagocytes needs the distinguishing of overlapping populations of binding and ingesting cells. Cytometry A 65: 93-102.
33. Ramarao N, Meyer TF (2001) Helicobacter pylori resists phagocytosis by macrophages: quantitative assessment by confocal microscopy and fluorescence-activated cell sorting. Infect Immun 69: 2604-2611.
34. Orr G, Panther DJ, Cassens KJ, Phillips JL, Tarasevich BJ, *et al.* (2009) Syndecan-1 mediates the coupling of positively charged submicrometer amorphous silica particles with actin filaments across the alveolar epithelial cell membrane. Toxicol Appl Pharmacol 236: 210-220.
35. Oh E, Delehanty JB, Sapsford KE, Susumu K, Goswami R, *et al.* (2011) Cellular uptake and fate of PEGylated gold nanoparticles is dependent on both cell-penetration peptides and particle size. ACS Nano 5: 6434-6448.
36. Xia H, Gao X, Gu G, Liu Z, Hu Q, *et al.* (2012) Penetratin-functionalized PEG-PLA nanoparticles for brain drug delivery. Int J Pharm 436: 840-850.
37. Liu BR, Li JF, Lu SW, Leel HJ, Huang YW, *et al.* (2010) Cellular internalization of quantum dots noncovalently conjugated with arginine-rich cell-penetrating peptides. J Nanosci Nanotechnol 10: 6534-6543.
38. Tyagi M, Rusnati M, Presta M, Giacca M (2001) Internalization of HIV-1 tat requires cell surface heparan sulfate proteoglycans. J Biol Chem 276: 3254-3261.
39. Gump JM, Dowdy SF (2007) TAT transduction: the molecular mechanism and therapeutic prospects. Trends Mol Med 13: 443-448.
40. Lei T, Srinivasan S, Tang Y, Manchanda R, Nagesetti A, *et al.* (2011) Comparing cellular uptake and cytotoxicity of targeted drug carriers in cancer cell lines with different drug resistance mechanisms. Nanomedicine 7: 324-332.
41. Vieira OV, Botelho RJ, Grinstein S (2002) Phagosome maturation: aging gracefully. Biochem J 366: 689-704.
42. Geisow MJ (1984) Fluorescein conjugates as indicators of subcellular pH. A critical evaluation. Exp Cell Res 150: 29-35.
43. Brandhonneur N, Chevanne F, Vie V, Frisch B, Primault R, *et al.* (2009) Specific and non-specific phagocytosis of ligand-grafted PLGA microspheres by macrophages. Eur J Pharm Sci 36: 474-485.
44. Gupta B, Levchenko TS, Torchilin VP (2005) Intracellular delivery of large molecules and small particles by cell-penetrating proteins and peptides. Adv Drug Deliv Rev 57: 637-651.
45. Tseng YL, Liu JJ, Hong RL (2002) Translocation of liposomes into cancer cells by cell-penetrating peptides penetratin and tat: a kinetic and efficacy study. Mol Pharmacol 62: 864-872.
46. Wang J, Byrne JD, Napier ME, Desimone JM (2011) More effective nanomedicines through particle design. Small 7: 1919-1931.
47. Fretz MM, Koning GA, Mastrobattista E, Jiskoot W, Storm G (2004) OVCAR-3 cells internalize TAT-peptide modified liposomes by endocytosis. Biochim Biophys Acta 1665: 48-56.
48. Aguilera TA, Olson ES, Timmers MM, Jiang T, Tsien RY (2009) Systemic in vivo distribution of activatable cell penetrating peptides is superior to that of cell penetrating peptides. Integr Biol (Camb) 1: 371-381.
49. MacEwan SR, Chilkoti A (2013) Harnessing the power of cell-penetrating peptides: activatable carriers for targeting systemic delivery of cancer therapeutics and imaging agents. Wiley Interdiscip Rev Nanomed Nanobiotechnol 5: 31-48.

5

Biodistribution of size-selected lyophilisomes in mice

Etienne van Bracht*, René Raavé*, Igor Y. Perevyazko, Elly M. Versteeg, Theo G. Hafmans, Ulrich S. Schubert, Egbert Oosterwijk, Toin H. van Kuppevelt, Willeke F. Daamen

* These authors contributed equally to this work

European Journal of Pharmaceutics and Biopharmaceutics, 2015, In Press

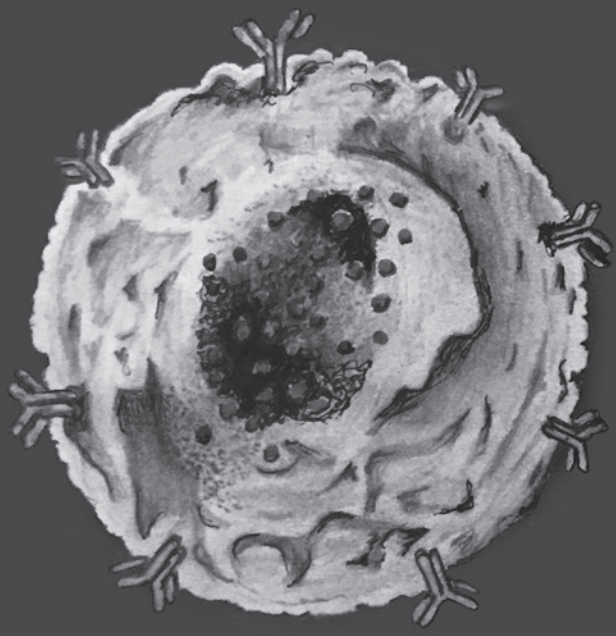

ABSTRACT

Lyophilisomes are a novel class of proteinaceous biodegradable nano/microparticle capsules developed for tumor drug delivery. The *in vivo* characteristics of lyophilisomes are unknown and, therefore, the time course of biodistribution of sized albumin-based lyophilisomes in CD1 mice after intravenous administration was studied. Lyophilisomes, prepared from Dylight680-labeled albumin, were sized using a sucrose gradient centrifugation methodology and four fractions with a mean size of approximately 200 nm, 400 nm, 550 nm, and 650 nm were pooled for *in/ex vivo* localization, (immuno) histochemistry and biochemical analysis. Lyophilisomes were rapidly taken out of the circulation by the liver and spleen. Immunohistochemistry revealed that lyophilisomes were taken up in the liver by F4/80 positive macrophages, and in the spleen by Sign-R1 positive macrophages specifically located in the marginal zones. Lyophilisomes were most likely degraded by the liver and spleen and subsequently excreted via the urine, as high levels of degraded Dylight680-labeled albumin were detected in the urine. This was corroborated by electron microscopy of the spleen, which showed intact lyophilisomes in the marginal zone 5 and 30 min after injection, but not after 120 min. In conclusion, i.v. injected lyophilisomes are rapidly entrapped by liver and splenic macrophages, biodegraded, and excreted in the urine.

INTRODUCTION

Nanoparticles and their potential application as drug delivery systems for pharmaceuticals have been extensively studied [1,2]. Research has focused on drug delivery systems assembled from a range of materials including natural or synthetic lipid liposomes, metal particles, polymeric particles, amino acid-, sugar- and nucleotide-based micelles, and protein-based particles [3]. Sizes range from a few nanometers for dendrimers and micelles [4], up to hundreds of nanometers to micrometers for liposomes, polymersomes, and (protein-based) nanospheres [5–7]. Despite the abundant research on these drug delivery systems, only a few are currently clinically applied.

For cancer therapy, an effective strategy to deliver anti-tumor drugs may be intravenous injection of drug loaded nanoparticles. This methodology exploits the enhanced permeability and retention (EPR) effect that is associated with hyperpermeability of tumor vasculature and lack of lymphatic drainage [8–10]. Through normal endothelium, nanoparticles cannot extravasate as it is prevented by tight endothelial junctions (5 to 10 nm) between endothelial cells [11]. However, the cut-off size for permeability in individual tumors is increased to 200 to 800 nm [12]. Due to this EPR effect, drug delivery particles (<800 nm) can extravasate from blood vessels to tumor tissue and accumulate, creating high local drug concentrations [13], with the potential to eliminate tumor cells more efficiently while reducing drug exposure to healthy cells.

In a quest for stable and efficient carrier systems, we have developed a drug delivery system named 'lyophilisomes' [14]. Lyophilisomes are prepared by a freezing, annealing, and lyophilization process that results in stable nano to micrometer sized capsules. As base material, a wide range of water-soluble macromolecules can be used (*e.g.* albumin, elastin, and heparin), making it an adaptable carrier system towards multiple drug delivery applications. The system is flexible, allowing the incorporation of virtually any biomolecule in the wall and/or lumen. For instance, enzymes incorporated either in the capsule wall or the lumen remain biological active, partly due to mild preparation conditions [14].

Recently, we investigated lyophilisomes prepared from bovine serum albumin. Albumin as a core material for lyophilisomes harbors a number of beneficial characteristics for drug delivery systems, as it is biocompatible, biodegradable to yield only innocuous degradation products, non-toxic and non-immunogenic. Furthermore, albumin is easy to purify and widely available, making it a suitable candidate for nanoparticle preparation [15–19]. We have shown that albumin-based lyophilisomes can be efficiently loaded with doxorubicin or curcumin and are able to efficiently eliminate tumor cells *in vitro* [20]. In order to obtain a selective drug delivery system, albumin-based lyophilisomes have also been modified with antibodies resulting in specific targeting of the cell of interest and facilitating the uptake of lyophilisomes *in vitro* [21]. Moreover, lyophilisomes conjugated with cell penetrating peptides increased cellular association and internalization in tumor cells [22]. These data indicate that albumin-based lyophilisomes may be used as a targeting system

for the delivery of therapeutic agents. Although many parameters of lyophilisomes have been investigated *in vitro*, little is known about their characteristics *in vivo*.
In this study, the biodistribution of lyophilisomes was investigated. Property sized lyophilisomes were administrated intravenously and the organ distribution and degradation characteristics were studied using bioluminescence, light/electron microscopy and biochemical assays.

MATERIALS & METHODS

Materials

Bovine serum albumin (BSA) was purchased from PAA Laboratories (Linz, Austria). Dylight680 (amine reactive) was purchased from Pierce (Rockford, IL, USE). Glutaraldehyde, formaldehyde and 4',6-diamidino-2-phenylindole (DAPI) were obtained from Merck (Darmstadt, Germany). Rat anti-mouse F4/80 monoclonal antibody (MCA497RT, clone Cl:A3-1, lot 0212) and rat-anti mouse Sign-R1 (MCA2394TI, clone Cl:ER-TR9, lot 0413) were obtained from AbD Serotec (Bio-Rad Laboratories, Hercules, CA, USA). Goat anti-rat IgG (H+L) Alexa fluor 488 conjugated antibody (A-11006, lot 52955A) and goat anti-rat IgM (µ chain) Alexa fluor 488 conjugated antibody (A-21212, lot 1252825) were purchased from Molecular Probes (Life Technologies, Grand Island, NY, USA).

Methods

Preparation of lyophilisomes

To image the lyophilisomes *in vivo*, Dylight680 (amine reactive) was conjugated to the free amine groups in albumin, applying the manufacturer's protocol, and after dialysis in 0.01 M acetic acid, labeled and non-labeled albumin were mixed in a 1:4 ratio. Albumin lyophilisomes were prepared as described [20]. Briefly, droplets of a solution of 0.25% (w/v) (labeled) BSA in 0.01 M acetic acid were frozen in liquid nitrogen (-196 °C) and then incubated at -10 to -20 °C for 3 h (annealing step), followed by lyophilization. This procedure results in hollow nano/micro spheres ("lyophilisomes"). Generally, we used 40 mL of a 0.25% BSA solution, which corresponds to 100 mg albumin (2.5 mg/mL). One batch of 40 mL was sufficient to perform the animal experiment. To stabilize lyophilisomes, they were vapor crosslinked with glutaraldehyde and formaldehyde. Subsequently, lyophilisomes were incubated in 1% (w/v) glycine (Scharlau, Barcelona, Spain) in phosphate buffered saline (PBS; pH 7.4) for 1 h under rotation to quench free aldehydes. Next, lyophilisomes were washed three times (17,000x *g*, 5 min, 4 °C) with 0.1% (v/v) Tween-20 (Sigma Aldrich, Steinheim, Germany) in phosphate buffered saline (PBS-T, pH 7.4). The final lyophilisome preparation was centrifuged three or four times at 60x *g* for 3 min to remove large lyophilisomes and sheet-like structures, until no pellet was observed. After this procedure, about 30% of the original weight of lyophilisomes remained. Lyophilisomes (1 mg/mL) were stored in PBS-T (pH 7.4).

Selecting appropriate sized lyophilisomes by density gradient centrifugation

In order to sort nanoparticles out of the lyophilisome population prepared as described above, centrifugation was used with a linear sucrose density gradient [23]. The linear sucrose density gradients were prepared in 14 mm diameter and 13.2 mL capacity ultra-centrifuge tubes (*ultra clear* tubes, Beckman, Indianapolis, IN USA) by a gradient device that is composed of two chambers connected via a channel with a stopcock. To create a border for aggregated particles, 0.5 ml 60% (w/w) sucrose solution was placed on the bottom of the tube. Subsequently, the gradient was prepared by mixing 5.6 mL 10% (w/w) and 5.6 mL 40% (w/w) sucrose solution in a mixing chamber of which the 10% sucrose solution is loaded first. The final gradient volume was 11.7 mL. The prepared gradient was stored for one h at ambient temperature and loaded with the lyophilisome suspension (0.5 mL, 1.0 mg/ml). The tubes were placed in a swinging bucket rotor (SW 41 Ti rotor, Beckman) and centrifuged at 1,543x *g* in a Beckman Optima L-XP ultracentrifuge (Beckman) for 10 min. After centrifugation, fractions were collected using a peristaltic pump and a narrow tube, inserted from top to bottom in the centrifuge tube. For each fraction, 0.5 to 1.0 mL of the solution was collected. Dynamic light scattering (DLS), qNano and analytical ultracentrifugation (AUC) were used to analyze the mean size of the fractioned lyophilisomes. The lyophilisome concentration of each fraction was determined by optical density ($\lambda = 280$ nm) to investigate recovery.

Particle characterization

Dynamic light scattering (DLS)

DLS was performed on a DynaPro Plate Reader Plus (Wyatt Technology Corporation, Santa Barbara, CA) equipped with a 60 mV linearly polarized gallium arsenide (GaAs) laser ($\lambda = 832.5$ nm), operating at an angle of 156°. DLS data were collected from lyophilisomes dispersed in PBS-T (pH 7.4). Data were analyzed using Dynamics software ver.6.10 by the method of cumulants [24].

qNano

The qNano (Izon, Science Ltd., Burnside, New Zealand) was used to measure particle size of lyophilisomes [20,25]. To ensure a continuous flow of particles, two different pore sizes were used. For unsorted lyophilisomes, a pore size of approximately 600 to 2,000 nm was used, while for sorted lyophilisomes a pore size of approximately 100 to 800 nm was used. Data were analyzed with Izon Control Suite 2.1 software.

Analytical ultracentrifugation

Sedimentation velocity experiments were performed with a ProteomeLab XLI analytical ultracentrifuge (Beckman Coulter, Brea, CA), using conventional double-sector Epon centerpieces of 12 mm optical path length and a four-hole rotor (AN-60Ti). Rotor speed was set at 3,000 – 6,000 rpm, depending on the sample. The rotor was equilibrated in

advance for approximately 1 h at 20 °C in the centrifuge. Cells were filled with 420 µL sample solution and 440 µL solvent (0.5% BSA / 0.02% sodium azide in PBS). Sedimentation (s) profiles were obtained by interference optics at similar temperature. For analysis of the sedimentation velocity data, the distributions ls-g*(s) and c(s) with a Tikhonov–Phillips regularization procedure implemented into the Sedfit program were applied. Ls-g*(s) represents a least-square boundary analysis which describes sedimentation of non-diffusing species. c(s) analysis is based on the numerical resolution of the Lamm equation assuming an equal frictional ratio value for each *s* value [26].

In vivo biodistribution

The Ethical Committee on Animal Research of the Radboud University Nijmegen Medical Centre approved this study under protocol number RUDEC 2012-202. Twenty-one female CD-1 mice (Harlan Laboratories, Horst, the Netherlands, 8 to 12 weeks old) weighing 32 to 40 g were caged in a controlled environment (23°C; 51% humidity, 12h light cycles). Food and water were available *ad libitum*. Mice were divided into seven groups of 3 mice per group. All groups received an intravenous injection of DyLight680-labeled albumin-based lyophilisomes in the tail vein at a concentration of 5.0 mg/kg body weight dissolved in PBS (1.0 mg/ml), except the control group (t=0); this group received a 5.0 mg/kg BSA in PBS injection. After 0, 5, 30 min, 2 h 5 h, 24 h and 96 h, mice were anesthetized with isoflurane/oxygen, placed on their back into a light tight chamber and imaged for 10 min with a CCD camera in an *in vivo* imaging system (Xenogen IVIS Lumina II). DyLight680-labeled lyophilisomes were excited at 640 nm and emission in the range of 695 to 770 nm. To correct for autofluorescence, DyLight680-labeled lyophilisomes were excited at 605 nm and emission was recorded in the range of 695 to 770 nm. IVIS-images were quantified using the Living Image 3.0 software (Caliper Life Sciences, Hopkinton, MA, USA).

After imaging, mice were euthanized and urine was collected. In order to visualize lyophilisomes in individual organs, liver, spleen, lung, kidney, stomach, small intestine, colon, pancreas and skin tissue were dissected. These individual organs were imaged using similar settings as for the mice. For further examination, parts of liver, spleen, lung, and kidney tissue were collected and: 1) snap frozen in optimal cutting temperature compound (Tissue Tek, Sakura, Torrance, CA) for immunohistochemistry, 2) fixed in para-formaldehyde and paraffin embedded for semi-quantification and 3) fixed in 2% (v/v) glutaraldehyde in 0.1 M phosphate buffer (pH 7.4) for transmission electron microscopy.

Semi quantitative assessment using paraffin sections

Paraffin embedded tissue sections were cut at 5 µm, deparaffinized and rehydrated using standard procedures. Nuclei were stained with 1% (w/v) DAPI in 2% (w/v) BSA in PBS containing 0.05% (v/v) Tween-20 (BSA/PBS-T) for 15 min. For each mouse, a total of six fluorescent images were quantified per organ/time point out of two sections (40x magnification; 0.405 mm^2 surface area). Sections were analyzed using a Zeiss LSM 510 laser

scanning confocal microscope (Carl Zeiss, Sliedrecht, the Netherlands). Dylight680-labeled lyophilisomes were excited at 633 nm and emission was collected between 650 and 710 nm. DAPI and Alexa fluor 488 were excited at 405 nm and 488 nm with emission collected between 420 to 480 nm and 500 to 550 nm, respectively. Dylight680-labeled lyophilisomes were quantified in tissue sections with ImageJ 1.48o (National Institutes of Health, USA) with an automated script (see Supplemental information). A conservative threshold value of 100 was used to distinguish between background pixels and lyophilisomes, so that potential positive background pixels were excluded while the number of lyophilisomes was not underestimated.

Immunohistochemistry

Frozen liver tissues were sectioned (5 µm) and air dried. Sections were fixed in ice cold methanol for 10 min. Blocking was performed with BSA/PBS-T for 10 min. Samples were subsequently incubated with primary antibody F4/80 (1:500 in BSA/PBS-T), which recognizes a Kupffer cell marker, for 1 h, washed three times with PBS-T and incubated with secondary antibody goat anti-rat IgG Alexa fluor 488 conjugated (1:200 in BSA/PBS-T) for 45 min.

Frozen spleen sections (5 µm) were air dried and blocked with 10% normal goat serum in BSA/PBS-T for 45 min and stained with primary antibody rat-anti mouse Sign-R1 (1:100), which recognizes a marker for marginal zone macrophages, in BSA/PBS-T for 1 h. Subsequently, sections were washed three times with PBS-T and blocked with 10% normal mouse serum BSA/PBS-T for 30 min. Secondary antibody Alexa fluor 488 conjugated goat anti-rat IgM (1:1,000 in BSA/PBS-T) was applied for 45 min.

All tissue sections were then washed three times with BSA/PBS-T and stained with 1% (w/v) DAPI in BSA/PBS-T for 15 min, washed three times with PBS-T and mounted with cover glasses in mowiol (Calbiochem, La Jolla, CA, USA). DAPI, Alexa fluor 488 and Dylight680 were visualized using settings as described in section '*Semi quantitative assessment using paraffin sections*' using a Zeiss LSM 510 laser scanning confocal microscope. Contrast in all fluorescent channels was increased for visibility using Fiji imaging software (saturation set to 0.35).

Analysis of urine

After bioluminescence imaging, mice were euthanized and urine was collected. To investigate the presence of Dylight680-label in urine, Dylight680 fluorescent signal contained in 20 µl urine was determined in a 96-wells plate and analyzed by the IVIS apparatus. In addition, to investigate whether Dylight680-labeled lyophilisomes were degraded, sodium dodecyl sulphate polyacrylamide gel electrophoresis was performed. Urine samples (5 µl) were diluted (2x) in sample buffer and analyzed using a 4 to 20% precise protein gel (Thermo scientific, Rockford, IL, USA). As a reference, Dylight680-labeled lyophilisomes were digested with 2.5 U papain (Sigma Aldrich) in digestion buffer

(50 mM $NaPO_4$, 2 mM cysteine, 2 mM EDTA, set at pH 6.5 with HCl) for 30 min at 65 °C. Fluorescent Dylight680 signal was detected with an Odyssey fluorescent gel scanner and analyzed using Odyssey software version 2.1 (Li-Cor Biosciences, Lincoln, Nebraska, USA). Subsequently gels were stained with 0.1% (w/v) Coomassie Brilliant Blue R-250 solution (MP Biomedicals, Santa Anna, CA) in 50% (v/v) methanol and 10% (v/v) acetic acid in water.

Transmission electron microscopy

Glutaraldehyde-fixed samples were post-fixed with 1% (w/v) osmium tetroxide, dehydrated in an ascending series of ethanol, and embedded in Epon 812. Ultrathin sections (60 nm) were cut and picked up on Formvar-coated grids, post-stained with lead citrate and uranyl acetate, and examined in a JEOL 1010 transmission electron microscope (Tokyo, Japan).

Statistical Analysis

Data are presented as mean with standard deviation. Experimental data were analyzed using a one-way ANOVA Bonferroni multiple comparison post-hoc tests. All statistical analyses were performed in Graphpad Prism 5.03 (Graphpad, San Diego, CA, USA).

RESULTS

Characterization of lyophilisomes by dynamic light scattering, qNano and analytical ultracentrifugation

Analysis by qNano gave a mean size of 1,216±95 nm for unsorted lyophilisomes (please note that standard deviation represents deviation between means of three individual measurements). To probe the possibility of using lyophilisomes for tumor targeting, lyophilisomes were sorted by ultracentrifugation using a sucrose gradient. Particle size measurements were performed on four fractions (<1,000 nm) using DLS, qNano, and AUC (Table 1). Fraction 1, 2, 3, and 4 showed a mean size of approximately 200 nm, 400 nm, 550 nm, and 650 nm, respectively (Fig. 1). The protein concentration of the fractions was determined by optical density (λ = 280 nm) to analyze recovery. The combination of the four fractions represented 16% of the total lyophilisome protein content. The number of lyophilisomes is likely higher than 16% of the initial number as small lyophilisomes contain less protein and thinner walls [14].

Biodistribution

To investigate the biodistribution of sorted lyophilisomes, Dylight680-labeled lyophilisomes were injected intravenously in mice. After multiple time intervals, the distribution of lyophilisomes was visualized and quantified using the Xenogen IVIS Lumina II imaging system. Bioluminescence imaging showed a rapid uptake of lyophilisomes in the upper abdominal area of the mice (Fig. 2). After 2 h, an additional fluorescent signal was visible in

Table 1 Lyophilisome recovery and mean size measurements of sorted lyophilisome fractions analyzed by dynamic light scattering (DLS), qNano and analytical ultracentrifugation (AUC).

	Lyophilisome protein recovery (%)	DLS (nm)	qNano (nm)	AUC (nm)
Fraction 1	3.0	260 ± 50	186 ± 19	195 ± 20
Fraction 2	3.8	445 ± 50	428 ± 40	360 ± 30
Fraction 3	4.3	610 ± 40	529 ± 57	530 ± 15
Fraction 4	5.1	690 ± 120	576 ± 75	685 ± 20

the lower abdominal area. Both fluorescent signals were considerably diminished 24 h post injection (Fig. 2). Bioluminescence images of the individual organs are presented in figure 3a. Quantitative analysis of excised individual organs indicated that the majority of the lyophilisomes accumulated in the liver (Fig. 3b). However, when taking the weight of the organs into account, the spleen showed similar uptake of lyophilisomes per gram tissue compared to the liver (Fig. 3c).

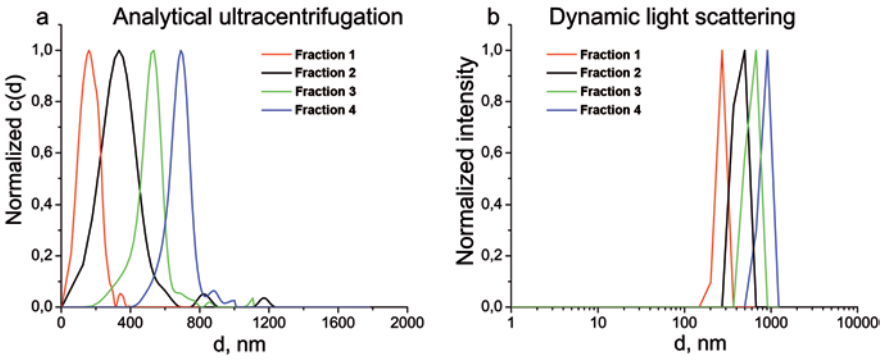

Figure 1 Size distributions of the four smallest lyophilisome fractions after a sucrose-gradient ultracentrifugation procedure as analyzed by (**a**) analytical ultracentrifugation (AUC) and (**b**) dynamic light scattering (DLS). Lyophilisomes were prepared from 2.5 mg bovine serum albumin in 0.01 M acetic acid using a freezing, annealing, and lyophilization regime. The average size distribution of the initial unfractioned lyophilisome preparation was 1,216±95 nm (qNano measurement).

The number of lyophilisomes was also analyzed in paraffin sections of liver, spleen, kidney and lung. Figure 4 indicates that the liver and spleen entrapped the majority of the lyophilisomes per surface area. An interesting observation is that this analysis showed a higher uptake in the spleen than in the liver. Although both *in vivo* imaging and quantification in paraffin sections gave similar results in general, there are minor differences between liver and spleen entrapment. This is due to the specific entrapment in the marginal zone that was present in all images used for semi-quantification, which could induce an over-estimation. Compared to the liver and spleen, the number of lyophilisomes present in the lung was very small as only a few lyophilisomes were detected. In the kidney, only very few lyophilisomes were detected. Except for the kidney, in all tissue sections a rapid uptake of lyophilisomes was found with their number decreasing over time being almost gone 24 h post injection (Fig. 4). However, some fluorescent signal was detected in the excised kidney (Fig. 3c). As a result of the presence of fluorescent signal in the organ and absence of lyophilisomes in the kidney sections, it is expected that the fluorescent signal originates from degraded lyophilisomes. This hints to degradation of lyophilisomes and excretion by the kidneys (see section '*Urine Analysis*').

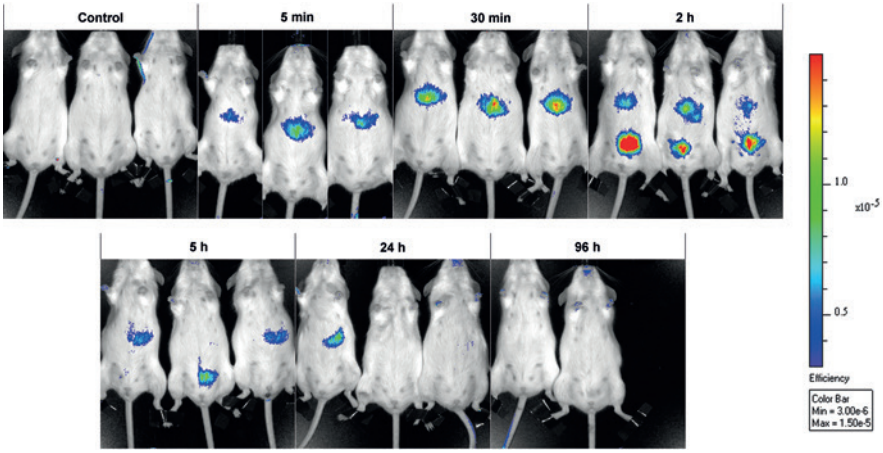

Figure 2 Biodistribution of Dylight680-labeled albumin-based lyophilisomes after intravenous injection in mice. At multiple time points, the distribution of lyophilisomes was visualized using an *in vivo* imaging system. Lyophilisomes appeared predominantly in the upper abdominal area at 5 – 30 min. In between (2 – 5 h after injection), lyophilisomes appeared also in the lower abdominal area. The signal decreased over time and is more or less absent at 24 h. Note that occasionally a fluorescent signal in the stomach was observed, due to autofluorescence of dietary chlorophyll. One mouse in the 96 h group died during the experiment of a non-experimentally related cause and was therefore not analyzed.

Immunohistochemistry

Immunohistochemistry was performed to further evaluate the distribution of the lyophilisomes and identify the cells involved in internalization. Since most lyophilisomes were found in the liver and spleen, it was hypothesized that lyophilisomes were internalized by cells of the mononuclear phagocyte system. Therefore, frozen sections of the liver and spleen were stained with mouse macrophage marker F4/80. F4/80 staining showed that the majority of lyophilisomes in the liver was internalized by F4/80 positive cells (Fig. 5). Although lyophilisomes present in the red pulp of the spleen were found in F4/80 positive cells (results not shown), most lyophilisomes were internalized by cells present in the marginal zone. Macrophages of the spleen located in the rodent marginal zone are known to lack F4/80 expression [27]. Therefore, marginal zone macrophages were stained for Sign-R1 expression, a cell surface marker specific for marginal zone macrophages. Figure 6 shows that the majority of lyophilisomes was internalized by SignR1 positive cells in the marginal zone.

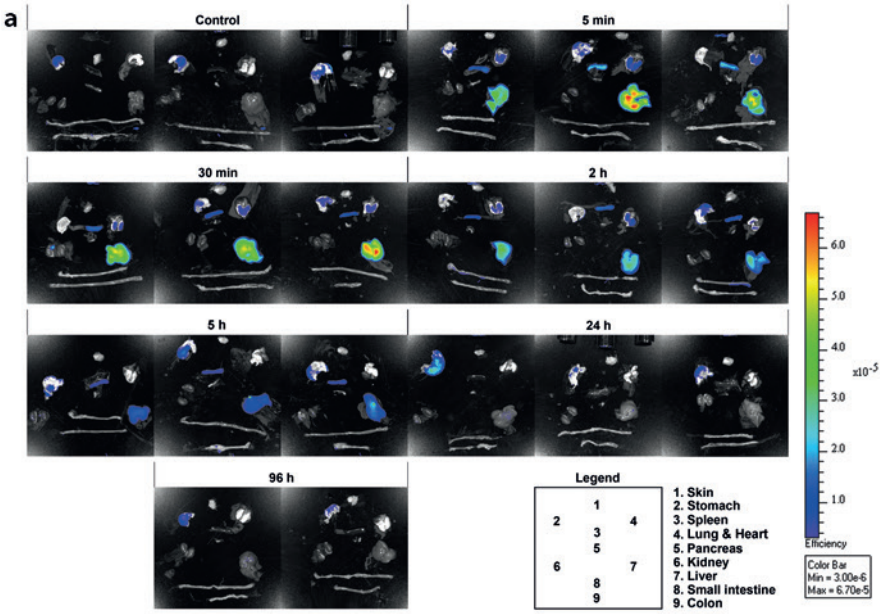

Figure 3 Bioluminescence images of excised organs (liver, spleen, lung, kidney, stomach, small intestine, colon, pancreas and skin) after intravenous injection of Dylight680-labeled albumin-based lyophilisomes in mice (**a**).

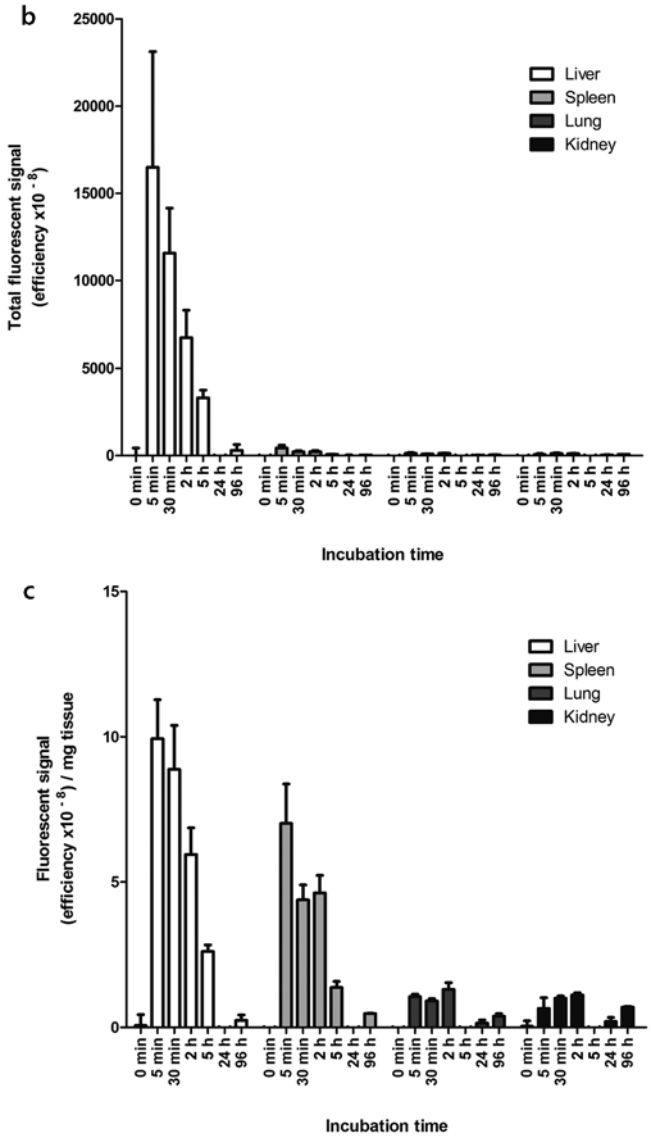

Figure 3 Continued. Quantitative analysis of fluorescent signal of lyophilisomes in liver, spleen, lung and kidney for total fluorescent signal of the organs (**b**) and fluorescent signal per mg wet weight tissue (**c**) after intravenous injection of Dylight680-labeled albumin-based lyophilisomes in mice. Absolutely, the highest uptake was observed in the liver, but per mg tissue a vast majority of lyophilisomes accumulated both in liver and spleen. In general, most fluorescence was measured after 5 – 30 min, after which the signal decreased over time. Fluorescence in stomach may be due to autofluorescence of dietary chlorophyll. Bars represent mean ± SD.

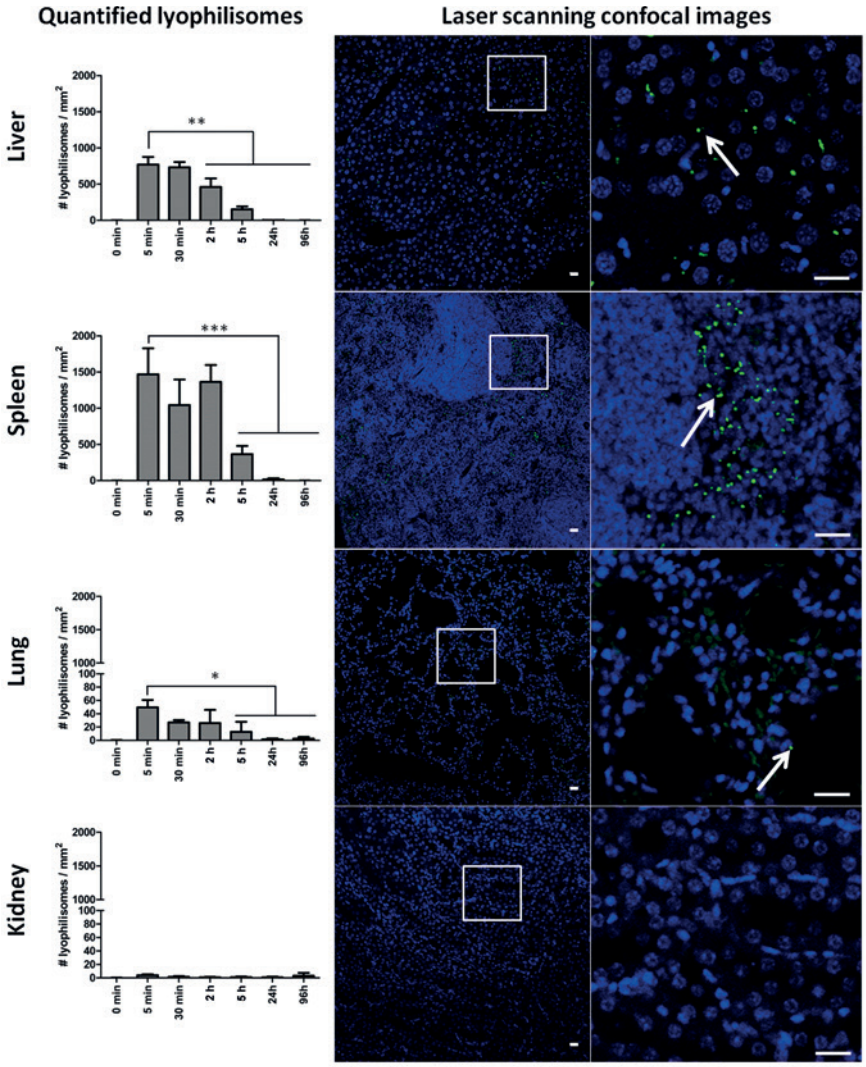

Figure 4 Quantification of lyophilisomes present in liver, spleen, lung, and kidney at distinct time points after IV injection of lyophilisomes in mice by detection of Dylight680 label in paraffin sections. Left column: the number of lyophilisomes counted in tissue sections at several time points after injection. Lyophilisomes were predominantly found in liver and spleen and to minor extent in lung. From 2 h on, there was a slow decrease over time until hardly any lyophilisomes remained after 24 h. Bars represent mean ± SD. * $p<0.05$, ** $p<0.01$ and *** $p<0.001$. Right columns: Representative images used for quantification of lyophilisomes 5 min after injection. Dylight680-albumin lyophilisomes are depicted in green and nuclei were stained with DAPI (blue). Magnifications of the white squared boxes are depicted on the far right. Arrows indicate lyophilisomes. Scale bars represent 20 µm.

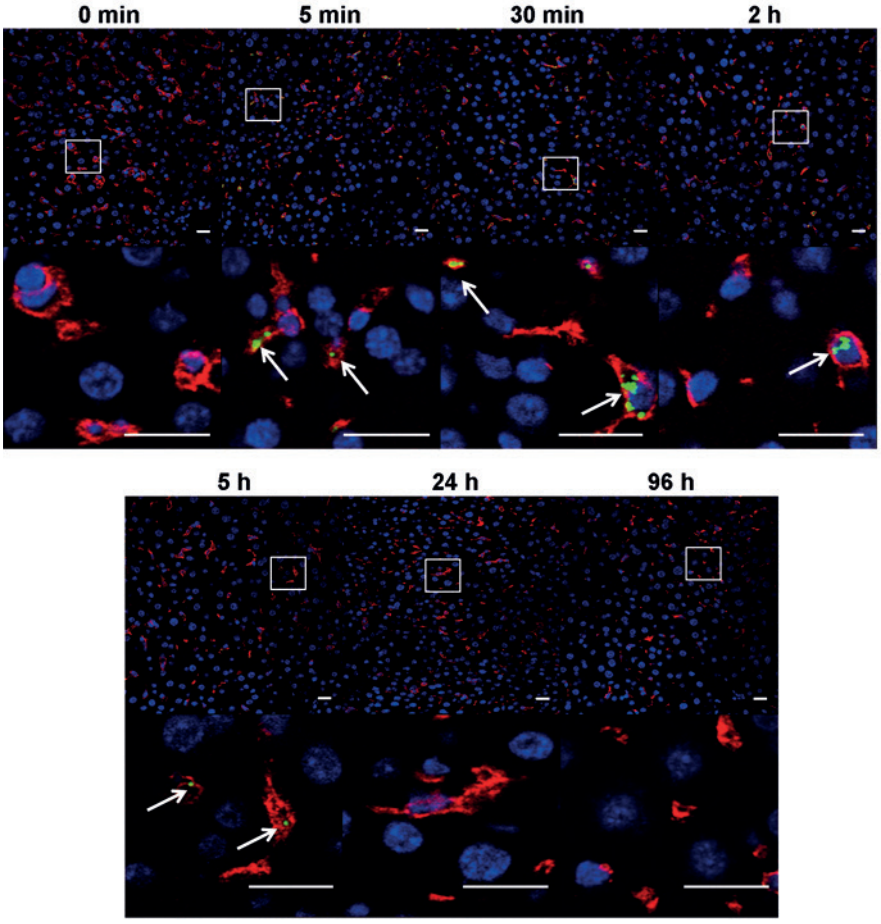

Figure 5 Uptake of Dylight680-lableded lyophilisomes by liver cells at distinct time points after intravenous injection of Dylight680-labeled albumin-based lyophilisomes in mice by detection of Dylight680 label in frozen sections. Lyophilisomes (green) were specifically internalized by F4/80 positive macrophages (red) in the liver. Nuclei were stained blue using DAPI. Magnifications of the white squared boxes are depicted in the figures below. Arrows indicate lyophilisomes. Scale bars represent 20 µm.

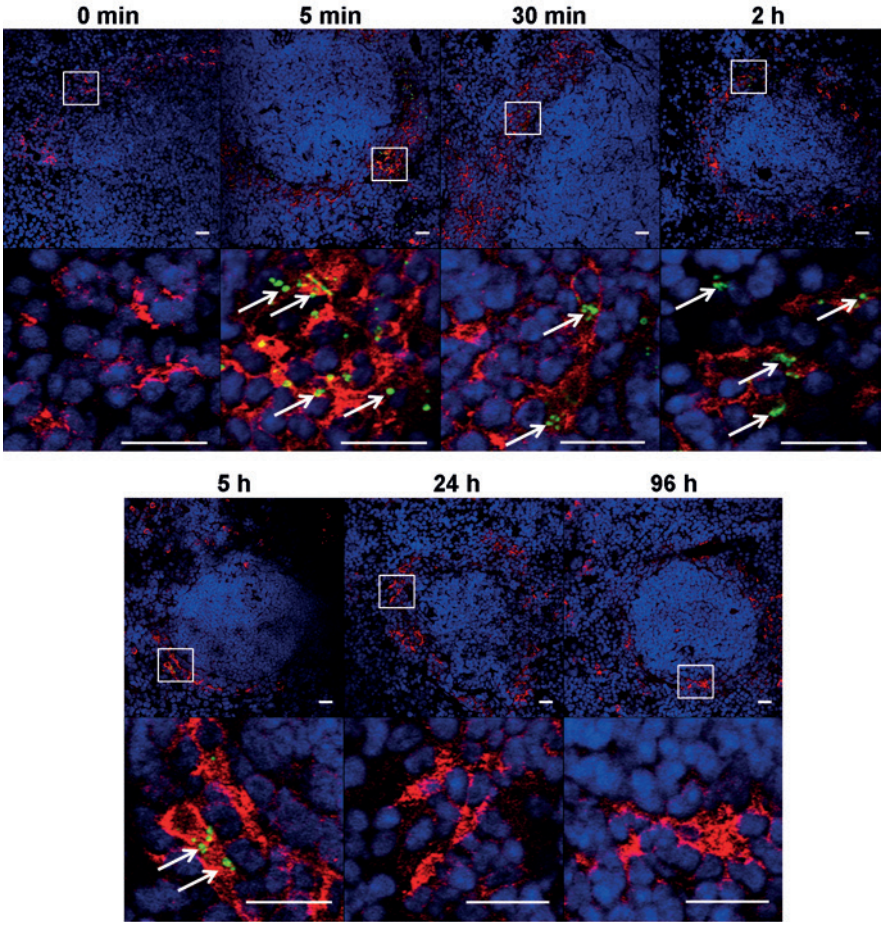

Figure 6 Uptake of Dylight680-lableded lyophilisomes by splenic cells at distinct time points after intravenous injection of Dylight680-labeled albumin-based lyophilisomes in mice by detection of Dylight680 label in frozen sections. Lyophilisomes (green) were especially taken up by Sign-R1 splenic marginal zone macrophages (red) in the spleen. Nuclei were stained blue using DAPI. Magnifications of the white squared boxes are depicted in the figures below. Arrows indicate lyophilisomes. Scale bars represent 20 µm.

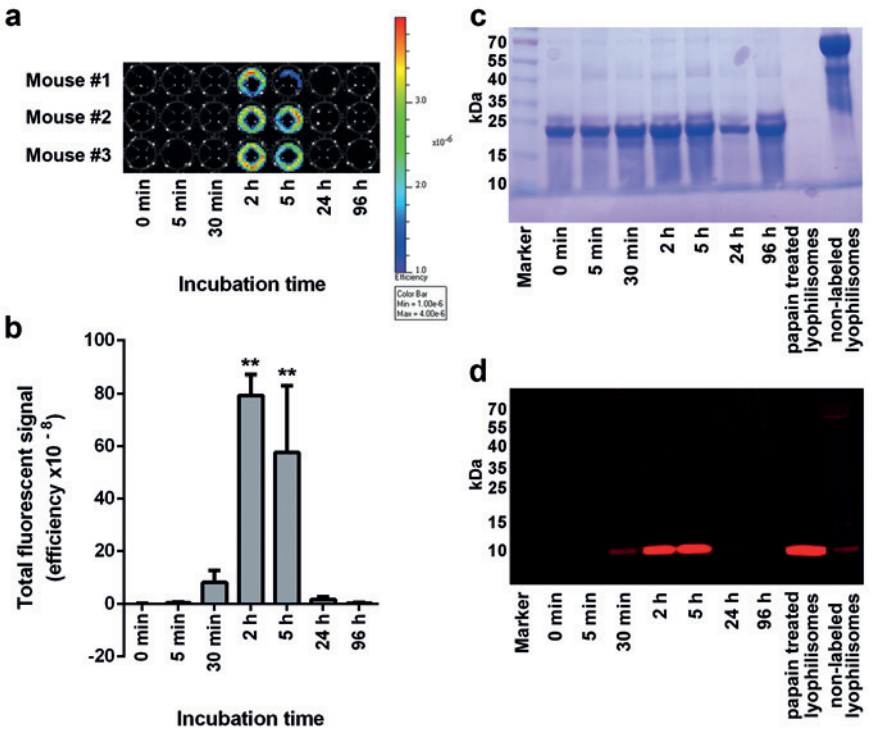

Figure 7 Excretion of degraded lyophilisomes via urine after intravenous injection of Dylight680-labeled albumin-based lyophilisomes in mice as analyzed by *in vivo* imaging (**a** and **b**) and SDS-PAGE (**c** and **d**) Dylight-680 signal in the urine was visualized (**a**) and quantified (**b**) using an *in vivo* imaging system. **c**-**d**) Gel electrophoresis analysis of urine with Coomassie brilliant blue staining (**c**) and Dylight680 detection (**d**). Normal non-digested lyophilisomes show a band around 70 kDa indicating albumin. Papain digested Dylight680 lyophilisomes do not show this band but do show fluorescence in the dye front of the gel, indicating degradation. In urine, major urinary proteins (±19 kDa) but no albumin/lyophilisomes (±70 kDa) were present. Presence of Dylight680 signal in dye front in urine samples taken 2 – 5 h after injection suggests lyophilisome degradation and excretion through urine. Bars represent mean ± SD. **2 and 5 h are significantly different from other time points ($p<0.01$).

Urine analysis

To investigate the fluorescent signal in the lower abdominal area, urine was collected after euthanizing the mice, and analyzed for the presence of Dylight680-label. Using the Xenogen IVIS Lumina II, a high fluorescent value was detected in urine 2 and 5 h post injection (Fig. 7a and b). To evaluate whether lyophilisomes were degraded and excreted in the urine, urine samples were analyzed on a protein gel in combination with fluorescence imaging (Fig. 7c and d). All urine samples, including controls, showed large bands around

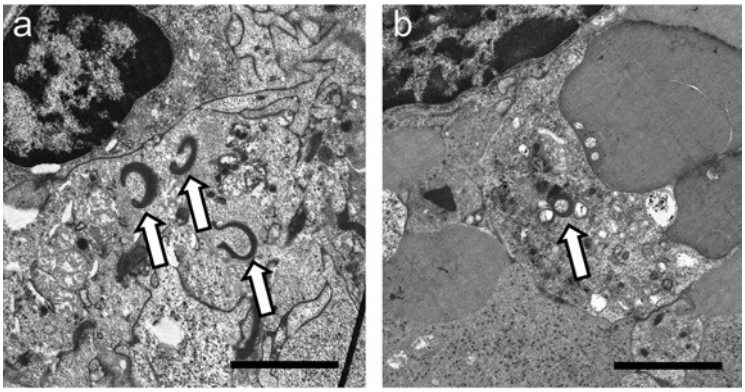

Figure 8 Transmission electron microscopical images of lyophilisomal structures in the spleen 5 min (**a**) and 30 min (**b**) after intravenous injection of Dylight680-labeled albumin-based lyophilisomes in mice. Lyophilisomal structures were found in the marginal zone area in the spleen. Scale bar represents 2 µm.

19 kDa corresponding to major urinary proteins [28,29]. Lyophilisomes (unlabeled) display a major band at about 70 kDa, representing albumin. After proteolytic digestion of lyophilisomes (Dylight680-labeled) using papain, no clear protein band was visible indicating major degradation (Fig. 7c). In this case, the fluorescent label was found in the dye front of the gel (Fig. 7d). A similar pattern was found in urine from mice 2 and 5 h after injection: no clear protein band visible at about 70 kDa but a clear fluorescent label in the gel's dye front. This indicates that lyophilisomes are degraded and excreted in urine within 300 min after injection.

Transmission electron microscopy

In order to visualize lyophilisomes within cells, transmission electron microscopy (TEM) was performed, focusing on the marginal zone areas in the spleen. Lyophilisomes that were largely intact could be identified primarily at time points 5 and 30 min after injection (Fig. 8). At 2 h, no lyophilisomes or lyophilisome-like structures could be detected, which suggests degradation (results not shown). Control samples also did not show any lyophilisomes-like structures (results not shown).

DISCUSSION

Drug delivery systems require several properties to successfully deliver their cargo at the target site. Ideally, they are biocompatible, biodegradable, non-immunogenic and able to specifically deliver their cargo to target cells. Lyophilisomes are considered as new candidates for drug delivery. Recently, it has been shown that lyophilisomes can be loaded with anti-tumor drugs [20] and can specifically target MUC1 expressing tumor cells [21]. To ensure an effective treatment *in vivo*, long circulation times are preferred, whereas accumulation in non-targeted organs and premature degradation should be avoided. Particle size is considered as an important factor for circulation time since removal from circulation increases if the diameter of particles increases [30–32]. Previously, we sorted lyophilisomes using fluorescent activated cell sorting [21]. In this study, a straightforward sucrose-gradient centrifugation methodology was used to size lyophilisomes into fractions with mean diameters of about 200 nm, 400 nm, 550 nm and 650 nm. These four fractions were pooled to have sufficient lyophilisomes for the *in vivo* study. Since human albumin has a circulation time up to 19 days under physiological conditions [16,17], and is used to coat nanoparticles to improve circulation time [33], it was expected that our bovine albumin-based lyophilisomes would also exhibit a long circulation time. However, *in vivo* fluorescence imaging revealed that the majority of intravenously injected albumin-based lyophilisomes were rapidly removed from circulation by the liver and spleen from 5 min after injection. Semi-quantitative histology of paraffin tissue sections confirmed these findings.

Rapid removal from the circulation is a common problem for drug delivery systems. The specific removal from circulation into liver and spleen can most likely be assigned to members of the mononuclear phagocyte system (MPS), also known as the reticulo-endothelial system [16,34]. As the MPS is responsible for clearance of particles from the circulation, it was hypothesized that organs of this system clear lyophilisomes as well. Indeed, results indicate rapid removal from circulation by MPS members. Staining for F4/80 expression, a cell surface marker for macrophages cells [35], and Sign-R1, a cell surface marker specific for marginal zone macrophages, confirmed MPS based removal [35,36].

Our results are consistent with the kinetics and biodistribution of other non-modified drug delivery systems. Rapid removal of unmodified (nano)particles from circulation into liver and spleen has been observed for drug delivery systems prepared from various materials such as poly(lactic-*co*-glycolic) acid [37], poly D,L-lactide (PLA) [33], and egg phosphatidylcholine combined with cholesterol [38]. Albumin-based particles that were prepared by other methods than used in lyophilisome preparation were also scavenged by the liver and spleen. For instance, almost 60% of drug loaded BSA particles (mean diameter 600 nm) injected in rats were entrapped in the liver after 1 h [39]. In another drug loaded BSA particle system (mean size 826 nm), approximately 70% of the injected drug

from particles ended up in the liver of mice after 24 h, indicating phagocytic uptake [40]. Moreover, a biodistribution study in rats with three different sized HSA particles (180, 430 and 1,800 nm) showed uptake in the liver of the 180 and 430 nm particles within 5 min, and uptake of larger particles mainly in the lung [41]. These studies are in contrast with the kinetics of smaller particles. Particles in the sub-100 nm range show prolonged circulation times and increased tumor accumulation [42], while smaller particles are directly excreted in the urine through the kidney's fenestrae [43]. As larger particles are removed more rapidly from the circulation [30–32], the rapid removal of lyophilisomes and other albumin particles may be explained by their size. To verify this, lyophilisomes should be sized to a sub-100 nm size range to investigate whether size does indeed matter for this specific drug delivery system.

Depending on the biodegradability of the applied material, nanoparticles will either be degraded in MPS organs or accumulate and potentially induce toxic effects [44]. Lyophilisomes show superior degradation characteristics compared to less or non-degradable particles such as gold [45,46], titaniumoxide [47], silver [48] and silica nanoparticles [49], which accumulate in tissue organs for longer periods of time, specifically in liver in which they induced inflammation [45], apoptosis [45] and hepatic necrosis [49]. The remarkably rapid observed degradation and urinary excretion suggest that lyophilisomes most probably will not cause side-effects in these organs. Several lines of evidence indicate that lyophilisomes are degraded and do not accumulate in the body. We observed a significant decrease of lyophilisome signal after 5 h compared to 5 min after injection in combination with almost no signal after 24 h observed by full body *in vivo* imaging, substantiated by histological quantitative analysis and urine analysis. Polyak *et al.* observed a similar urine excretion with HSA particles [41]. Our TEM results indicate that lyophilisomes could be identified in the spleen up to 30 min, while lyophilisomes or lyophilisome-like fragments could not be found at the next time point (2 h), again suggesting rapid degradation and excretion. As a great part of the injected lyophilisomes was removed from the circulation by the liver, excretion through the hepato-biliarily route may be expected. However, in the current experimental set-up it was not possible to evaluate fluorescence in the hepato-biliary route due to autofluorescence of dietary chlorophyll.

When lyophilisomes are to be used as a drug delivery system, longer circulation times are required. Various methods have been developed to enable prolonged circulation times, such as PEGlyation [37,44], mimicking "self" by conjugating small peptide markers of self CD47 to the particle wall [50] or the use of smaller capsules [30]. Albumin Dylight680-lyophilisomes as prepared in this study are rapidly removed from circulation and efficiently degraded. To increase circulation times, lyophilisomes could also be modified by either PEGlyating or a more biological method by using self peptides. To investigate the importance of lyophilisomal size and its effect on biodistribution, a study investigating the biodistribution of only the smallest sized fraction (with a mean size of about 200 nm in diameter) should be performed.

Lyophilisomes may also be used in other settings that do not rely on long circulation times, but do take into account the biodegradability of albumin lyophilisomes. One example is the application of lyophilisomes in intraperitoneal chemotherapy [51,52] of malignant ascites, caused by ovarian, colorectal, pancreatic, or uterine cancers [53]. There is evidence that after intraperitoneal administration small particles (50 to 720 nm) are removed more rapidly than large particles (>4 μm) due to lymphatic drainage [54]. Originally developed lyophilisomes with sizes ranging from 200 nm to 10 μm [14] would very well fit this application. In addition, a previous study indicated that non-sized antibody-modified lyophilisomes were able to specifically target ovarian cancer cells under dynamic conditions making them suitable for this application [21]. This suggests that for future clinical IP administration, sizing of lyophilisomes and/or modification to prevent rapid removal from circulation may not even be necessary.

Acknowledgements

Bianca Lemmers, Henk Arnts (both Central Animal Facility), and Arie Oosterhof (Dept. of Biochemistry) are kindly acknowledged for their technical assistance during the animal experiment.

SUPPLEMENTAL INFORMATION

Automated script to count Dylight680 albumin labeled lyophilisomes in tissue sections using ImageJ 1.48o (National Institutes of Health, USA) with a conservative threshold value of 100.

```
// Get data set root folder from user
        sourcePath = getDirectory("Choose a Directory");
//create a goal path
goalPath = createGoalPath(sourcePath);
File.makeDirectory(goalPath);
//list the files
fileList = getFileList(sourcePath);
for (i=0; i<fileList.length; i++) {
if (endsWith(fileList[i], "/")) {
imageList = getFileList(sourcePath + fileList[i]);
for (j = 0; j < imageList.length; j++) {
if (endsWith(imageList[j], ".lsm")) {
imagePath = sourcePath + fileList[i] + imageList[j];
fileName = fileList[i] + imageList[j];
id = openImage(imagePath);
cOneFileName = fileName + " - C=1";
cTwoFileName = fileName + " - C=3";
cThreeFileName = fileName + " - C=0";
selectWindow(fileName + " - C=1");
setAutoThreshold("Default dark");
//run("Threshold...");
setThreshold(100, 255);
run("Convert to Mask");
run("Make Binary");
run("Watershed");
run("Analyze Particles...", "size=1-Infinity pixel circularity=0.00-1.00 show=Outlines clear summarize");
// close the image
closeImage(id);
closeImage(id);
closeImage(id);
closeImage(id);
                                                    } // end if
                                                } // end for
                                            } // end if
                                        } // end for
//create goal path
function createGoalPath(sourcePath) {
firstCharacter = 0;
finalCharacter = lengthOf(sourcePath) - 1;
cleanSourcePath = substring(sourcePath, firstCharacter, finalCharacter);
```

```
goalPath = cleanSourcePath + "_enhanced";
File.makeDirectory(goalPath)
return "" + goalPath + "/";
}
// Open an image
	function openImage(path) {
		run("Bio-Formats Importer", "open=[path] autoscale color_mode=Default split_channels view=Hyperstack stack_
order=XYCZT");
                                                return getImageID();
	}
	// Close an image
	function closeImage(id) {
		close();
	}
```

REFERENCES

1. Svenson S (2014) What nanomedicine in the clinic right now really forms nanoparticles? Wiley Interdiscip Rev Nanomed Nanobiotechnol 6: 125-135.
2. Alexis F, Pridgen EM, Langer R, Farokhzad OC (2010) Nanoparticle technologies for cancer therapy. Handb Exp Pharmacol 55-86.
3. Wang AZ, Langer RS, Farokhzad OC (2012) Nanoparticle Delivery of Cancer Drugs. Annu Rev Med 63: 185-198.
4. Alexis F, Pridgen E, Molnar LK, Farokhzad OC (2008) Factors affecting the clearance and biodistribution of polymeric nanoparticles. Mol Pharm 5: 505-515.
5. Torchilin VP (2005) Recent advances with liposomes as pharmaceutical carriers. Nat Rev Drug Discov 4: 145-160.
6. Rao JP, Geckeler EG (2011) Polymer nanoparticles: Preparation techniques and size-control parameters. Prog Polym Sci 36: 887-913.
7. Elzoghby AO, Samy WM, Elgindy NA (2012) Protein-based nanocarriers as promising drug and gene delivery systems. J Control Release 161: 38-49.
8. Torchilin V (2011) Tumor delivery of macromolecular drugs based on the EPR effect. Adv Drug Deliv Rev 63: 131-135.
9. Matsumura Y, Maeda H (1986) A new concept for macromolecular therapeutics in cancer chemotherapy: mechanism of tumoritropic accumulation of proteins and the antitumor agent smancs. Cancer Res 46: 6387-6392.
10. Maeda H, Wu J, Sawa T, Matsumura Y, Hori K (2000) Tumor vascular permeability and the EPR effect in macromolecular therapeutics: a review. J Control Release 65: 271-284.
11. Hofheinz RD, Gnad-Vogt SU, Beyer U, Hochhaus A (2005) Liposomal encapsulated anti-cancer drugs. Anticancer Drugs 16: 691-707.
12. Gaumet M, Vargas A, Gurny R, Delie F (2008) Nanoparticles for drug delivery: the need for precision in reporting particle size parameters. Eur J Pharm Biopharm 69: 1-9.
13. Torchilin VP (2010) Passive and active drug targeting: drug delivery to tumors as an example. Handb Exp Pharmacol 3-53.
14. Daamen WF, Geutjes PJ, Nillesen STM, Van Moerkerk HThB, Wismans R, *et al.* (2007) Lyophilisomes: A new type of (bio)capsules. Adv Mater 19: 673-677.
15. Elzoghby AO, Samy WM, Elgindy NA (2011) Albumin-based nanoparticles as potential controlled release drug delivery systems. J Control Release 157: 168-182.
16. Cavadas M, Gonzalez-Fernandez A, Franco R (2011) Pathogen-mimetic stealth nanocarriers for drug delivery: a future possibility. Nanomedicine 7: 730-743.
17. Kratz F (2008) Albumin as a drug carrier: design of prodrugs, drug conjugates and nanoparticles. J Control Release 132: 171-183.
18. Vogel V, Lochmann D, Weyermann J, Mayer G, Tziatzios C, *et al.* (2005) Oligonucleotide-protamine-albumin nanoparticles: preparation, physical properties, and intracellular distribution. J Control Release 103: 99-111.
19. Mayer G, Vogel V, Weyermann J, Lochmann D, van den Broek JA, *et al.* (2005) Oligonucleotide-protamine-albumin nanoparticles: Protamine sulfate causes drastic size reduction. J Control Release 106: 181-187.
20. van Bracht E, Raave R, Verdurmen WP, Wismans RG, Geutjes PJ, *et al.* (2012) Lyophilisomes as a new generation of drug delivery capsules. Int J Pharm 439: 127-135.
21. van Bracht E, Stolle S, Hafmans TG, Boerman OC, Oosterwijk E, *et al.* (2014) Specific targeting of tumor cells by lyophilisomes functionalized with antibodies. Eur J Pharm Biopharm 87: 80-89.
22. van Bracht E, Versteegden LRM, Stolle S, Verdurmen WP, Woestenenk R, *et al.* (2014) Enhanced cellular uptake of albumin-based lyophilisomes when functionalized with cell-penetrating peptide TAT in HeLa cells. PLoS One 9: e110813.
23. Vollrath A, Pretzel D, Pietsch C, Perevyazko I, Schubert S, *et al.* (2012) Preparation, cellular internalization, and biocompatibility of highly fluorescent PMMA nanoparticles. Macromol Rapid Commun 33: 1791-1797.
24. Koppel DE (1972) Analysis of Macromolecular Polydispersity in Intensity Correlation Spectroscopy: The Method of Cumulants. J Chem Phys 57: 4814-4820.
25. Garza-Licudine E, Deo D, Yu S, Uz-Zaman A, Dunbar WB (2010) Portable nanoparticle quantization using a resizable nanopore instrument - the IZON qNano. Conf Proc IEEE Eng Med Biol Soc 2010: 5736-5739.
26. Schuck P (2000) Size-distribution analysis of macromolecules by sedimentation velocity ultracentrifugation and lamm equation modeling. Biophys J 78: 1606-1619.

27. Taylor PR, Martinez-Pomares L, Stacey M, Lin HH, Brown GD, *et al.* (2005) Macrophage receptors and immune recognition. Annu Rev Immunol 23: 901-944.
28. Cheetham SA, Smith AL, Armstrong SD, Beynon RJ, Hurst JL (2009) Limited variation in the major urinary proteins of laboratory mice. Physiol Behav 96: 253-261.
29. Kwak J, Grigsby CC, Rizki MM, Preti G, Koksal M, *et al.* (2012) Differential binding between volatile ligands and major urinary proteins due to genetic variation in mice. Physiol Behav 107: 112-120.
30. Decuzzi P, Godin B, Tanaka T, Lee SY, Chiappini C, *et al.* (2010) Size and shape effects in the biodistribution of intravascularly injected particles. J Control Release 141: 320-327.
31. Mitragotri S, Lahann J (2009) Physical approaches to biomaterial design. Nat Mater 8: 15-23.
32. Champion JA, Walker A, Mitragotri S (2008) Role of particle size in phagocytosis of polymeric microspheres. Pharm Res 25: 1815-1821.
33. Bazile DV, Ropert C, Huve P, Verrecchia T, Marlard M, *et al.* (1992) Body distribution of fully biodegradable [14C]-poly(lactic acid) nanoparticles coated with albumin after parenteral administration to rats. Biomaterials 13: 1093-1102.
34. Hume DA (2006) The mononuclear phagocyte system. Curr Opin Immunol 18: 49-53.
35. Hume DA (2008) Differentiation and heterogeneity in the mononuclear phagocyte system. Mucosal Immunol 1: 432-441.
36. van Furth R, Cohn ZA, Hirsch JG, Humphrey JH, Spector WG, *et al.* (1972) The mononuclear phagocyte system: a new classification of macrophages, monocytes, and their precursor cells. Bull World Health Organ 46: 845-852.
37. Panagi Z, Beletsi A, Evangelatos G, Livaniou E, Ithakissios DS, *et al.* (2001) Effect of dose on the biodistribution and pharmacokinetics of PLGA and PLGA-mPEG nanoparticles. Int J Pharm 221: 143-152.
38. Allen TM, Hansen C (1991) Pharmacokinetics of stealth versus conventional liposomes: effect of dose. Biochim Biophys Acta 1068: 133-141.
39. Yang L, Cui F, Cun D, Tao A, Shi K, *et al.* (2007) Preparation, characterization and biodistribution of the lactone form of 10-hydroxycamptothecin (HCPT)-loaded bovine serum albumin (BSA) nanoparticles. Int J Pharm 340: 163-172.
40. Santhi K, Dhanaraj SA, Koshy M, Ponnusankar S, Suresh B (2000) Study of biodistribution of methotrexate-loaded bovine serum albumin nanospheres in mice. Drug Dev Ind Pharm 26: 1293-1296.
41. Polyak A, Palade EA, Balogh L, Postenyi Z, Haasz V, *et al.* (2011) In vitro and biodistribution examinations of Tc-99m-labelled doxorubicin-loaded nanoparticles. Nucl Med Rev Cent East Eur 14: 55-62.
42. Perrault SD, Walkey C, Jennings T, Fischer HC, Chan WC (2009) Mediating tumor targeting efficiency of nanoparticles through design. Nano Lett 9: 1909-1915.
43. Choi HS, Liu W, Misra P, Tanaka E, Zimmer JP, *et al.* (2007) Renal clearance of quantum dots. Nat Biotechnol 25: 1165-1170.
44. Owens DE III, Peppas NA (2006) Opsonization, biodistribution, and pharmacokinetics of polymeric nanoparticles. Int J Pharm 307: 93-102.
45. Cho WS, Cho M, Jeong J, Choi M, Cho HY, *et al.* (2009) Acute toxicity and pharmacokinetics of 13 nm-sized PEG-coated gold nanoparticles. Toxicol Appl Pharmacol 236: 16-24.
46. Balasubramanian SK, Jittiwat J, Manikandan J, Ong CN, Yu LE, *et al.* (2010) Biodistribution of gold nanoparticles and gene expression changes in the liver and spleen after intravenous administration in rats. Biomaterials 31: 2034-2042.
47. Fabian E, Landsiedel R, Ma-Hock L, Wiench K, Wohlleben W, *et al.* (2008) Tissue distribution and toxicity of intravenously administered titanium dioxide nanoparticles in rats. Arch Toxicol 82: 151-157.
48. Lankveld DP, Oomen AG, Krystek P, Neigh A, Troost-de JA, *et al.* (2010) The kinetics of the tissue distribution of silver nanoparticles of different sizes. Biomaterials 31: 8350-8361.
49. Xie G, Sun J, Zhong G, Shi L, Zhang D (2010) Biodistribution and toxicity of intravenously administered silica nanoparticles in mice. Arch Toxicol 84: 183-190.
50. Rodriguez PL, Harada T, Christian DA, Pantano DA, Tsai RK, *et al.* (2013) Minimal "Self" peptides that inhibit phagocytic clearance and enhance delivery of nanoparticles. Science 339: 971-975.
51. Elias D, Gilly F, Boutitie F, Quenet F, Bereder JM, *et al.* (2010) Peritoneal colorectal carcinomatosis treated with surgery and perioperative intraperitoneal chemotherapy: retrospective analysis of 523 patients from a multicentric French study. J Clin Oncol 28: 63-68.

52. Armstrong DK, Bundy B, Wenzel L, Huang HQ, Baergen R, *et al.* (2006) Intraperitoneal cisplatin and paclitaxel in ovarian cancer. N Engl J Med 354: 34-43.
53. Sangisetty SL, Miner TJ (2012) Malignant ascites: A review of prognostic factors, pathophysiology and therapeutic measures. World J Gastrointest Surg 4: 87-95.
54. Bajaj G, Yeo Y (2010) Drug delivery systems for intraperitoneal therapy. Pharm Res 27: 735-738.

6

Summary
Samenvatting in het Nederlands

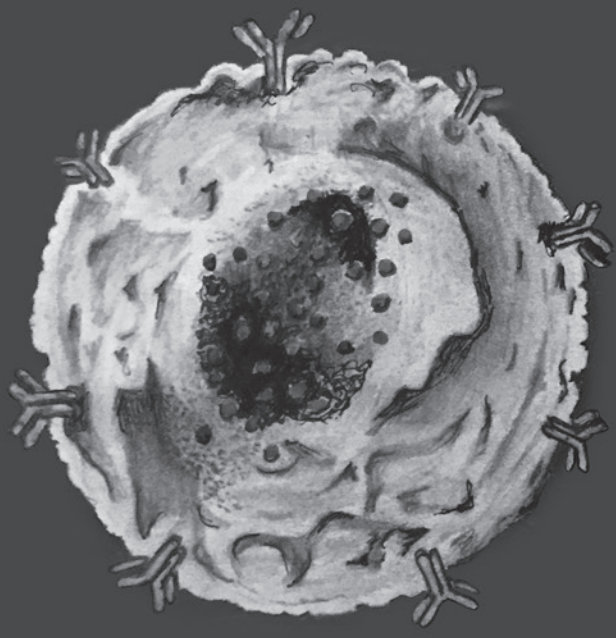

SUMMARY

Cancer is a leading cause of death and the global burden of cancer continues to increase rapidly because of aging and growth of the world population. For effective cancer therapy, it is necessary to improve our knowledge of cancer physiopathology, discover new anti-cancer drugs and develop novel biomedical technologies. Nanoparticulate drug delivery systems are currently explored to overcome critical challenges associated with classical administration forms. An overview concerning the use of nanoparticulate drug delivery systems to treat cancer and the most commonly used systems currently available are described in **Chapter 1**.

The aim of this thesis was to modify lyophilisomes, a novel class of proteinaceous biodegradable nano/micro drug delivery capsules, in order to obtain albumin-based nanoparticles that can act as a drug delivery system to eliminate ovarian tumor cells.

Chapter 2 describes protein-based lyophilisomes loaded with anti-tumor drugs. Among the available drug carrier systems, protein-based nanoparticles are particularly interesting as they hold certain advantages such as increased stability during storage, non-toxicity, biocompatibility, and biodegradability *in vivo*. Albumin-based lyophilisomes were prepared by freezing, annealing and lyophilization. To probe the possibility to use lyophilisomes for tumor targeting, lyophilisomes were loaded with a high concentration of doxorubicin or curcumin. When tumor cells were exposed to doxorubicin or curcumin loaded albumin-based lyophilisomes, cell proliferation and viability of multiple tumor cell lines was strongly reduced. This work provided the basis that lyophilisomes may be suitable as a drug delivery system *in vitro* and further development is justified.

As a further development of lyophilisomes as a drug delivery system, **chapter 3** describes the specific targeting of antibody-conjugated lyophilisomes to tumor cells. Lyophilisomes modified with hKC4-antibodies against mucin-1 (MUC1) were shown to specifically target ovarian tumor cells overexpressing the MUC1 antigen. To establish the specificity of hKC4-modified lyophilisomes, MUC1 positive and negative tumor cells were cultured in one culture flask. This experiment showed that hKC4-antibody conjugated lyophilisomes specifically targeted to MUC1 overexpressing ovarian tumor cells. In continuation of chapter 3 to further modify lyophilisomes, **chapter 4** describes the effect of cell penetrating peptides (CPPs) conjugated to lyophilisomes. CPPs including the TAT peptide can be used for intracellular delivery of a broad variety of cargos including nanoparticulate pharmaceutical carriers. Lyophilisomes modified with a TAT-peptide demonstrated that intracellular uptake was facilitated in a time-dependent manner. In addition, when using lyophilisomes for tumor targeting, lyophilisomal size is also an important parameter. Chapter 4 also focused on fractionation of the lyophilisome preparation (size up to 2.8 µm) to obtain nanosized lyophilisomes with a more monodisperse capsule population. Using FACS, lyophilisomes could be sorted with a particle diameter smaller than 1 µm.

Chapter 5 describes the biodistribution of nano-sized lyophilisomes. Using a sucrose gradient centrifugation, lyophilisomes could be size-selected more precisely (to the nm range) and resulted in a higher yield compared to FACS as described in chapter 4. The biodistribution in mice demonstrated that lyophilisomes did not induce acute toxic effects and were released through the urine after degradation. An effective drug delivery system should circulate in the blood stream long enough to reach the tumor site. Lyophilisomes were rapidly removed from the circulation by the mononuclear phagocyte system (predominantly liver and spleen), postulating that lyophilisomes should be modified in size or outer surface to prevent early removal from the circulation.

In conclusion, this thesis describes the potential of albumin-based lyophilisomes as a drug delivery system for anti-tumor drugs. In order to use lyophilisomes *in vivo*, more research is needed including modifications to increase circulation times.

SAMENVATTING

Kanker is inmiddels wereldwijd de belangrijkste doodsoorzaak en zal in de toekomst alleen maar toenemen als gevolg van de veroudering en groei van de wereldbevolking. Voor het ontwikkelen van effectieve kankertherapieën is het noodzakelijk om onze kennis van de fysiopathologie van tumorweefel te verbeteren, nieuwe cytostatica te ontdekken en innovatieve biomedische technologieën te ontwikkelen. Tegenwoordig wordt er veel onderzoek verricht naar nanodeeltjes die als drug delivery systeem (medicijnafgifte-systeem) kunnen dienen om de beperkingen die gepaard gaan met de klassieke kanker-therapie te overwinnen. **Hoofdstuk 1** geeft een overzicht hoe nanodeeltjes functioneren als drug delivery systeem om kanker te behandelen en beschrijft de meest gebruikte nanodeeltjes die kunnen fungeren als drug delivery systemen.
Het doel van dit proefschrift was het modificeren van lyophilisomen, een nieuwe categorie op eiwit gebaseerde biologisch afbreekbare nano/micro drug delivery capsules, om nanocapsules van albumine te verkrijgen die kunnen dienen als een drug delivery systeem om ovariumtumorcellen te elimineren.
Hoofdstuk 2 beschrijft lyophilisomen gemaakt van albumine en opgeladen met anti-tumor medicijnen. Nanodeeltjes gemaakt van eiwitten zijn bijzonder interessant in vergelijking met de huidige beschikbare carriersystemen, omdat deze deeltjes meerdere voordelen hebben zoals verbeterde stabiliteit tijdens opslag. Daarnaast zijn ze niet toxisch, biocompatibel en *in vivo* biologisch afbreekbaar. Lyophilisomen worden gemaakt door middel van drie verschillende processen: invriezen, opwarmen tot -10 °C en vriesdrogen. Om te onderzoeken of lyophilisomen gebruikt kunnen worden als kankertherapie, zijn de capsules opgeladen met een hoge concentratie doxorubicine en curcumine. Tumorcellen die werden blootgesteld aan albumine-lyophilisomen opgeladen met doxorubicine of curcumine, lieten een sterke daling in celproliferatie en viabiliteit zien bij verschillende tumorcellijnen. Bovenstaand werk vormt de basis voor de toepassing van lyophilisomen als drug delivery systeem *in vitro* en rechtvaardigt verdere ontwikkeling van dit systeem. Om lyophilisomen verder te ontwikkelen als drug delivery systeem, beschrijft **hoofdstuk 3** lyophilisomen waaraan antilichamen zijn geconjugeerd om specifiek tumorcellen te targeten. Lyophilisomen gemodificeerd met hKC4 antilichamen gericht tegen mucin1 (MUC1) binden specifiek aan tumorcellen die het MUC1 antigen tot overexpressie brengen. Om de specificiteit van hKC4 gemodificeerde lyophilisomen vast te stellen is een experiment ontwikkeld waarbij twee celtypen -een MUC1 positieve en negatieve cellijn- werden gecombineerd in één celkweek. Dit experiment toonde aan dat hKC4-geconjugeerde lyophilisomen specifiek binden aan de tumorcellen die MUC1 tot overexpressie brengen. Als vervolg op hoofdstuk 3, om de lyophilisomen verder te modificeren, beschrijft **hoofdstuk 4** het effect van cel-penetrerende peptiden (CPPs) geconjugeerd aan lyophilisomen. CPPs, waaronder het TAT peptide, kunnen worden gebruikt voor de intracellulaire afgifte van verschillende ladingen inclusief nanodeeltjes. Lyophilisomen

gemodificeerd met het TAT peptide werden sneller opgenomen door de tumorcel in vergelijking tot lyophilisomen zonder TAT peptide in een tijdsafhankelijk proces. Naast de opname van een nanodeeltje is ook de grootte van het deeltje belangrijk. Dit hoofdstuk benadrukt daarom ook het fractioneren van lyophilisomen (diameter tot 2.8 µm) en leidt tot een populatie lyophilisomen met minder variatie in diameter. Met behulp van FACS konden lyophilisomen worden gesorteerd tot een diameter kleiner dan 1 µm.

Hoofdstuk 5 beschrijft de biodistributie van gesorteerde nano-lyophilisomen. Met behulp van sucrosegradiënt-centrifugatie kunnen lyophilisomen nauwkeuriger worden gesorteerd (in de nanometer range). Daarnaast resulteerde deze methode ook in een hogere opbrengst in vergelijking met FACS zoals beschreven in hoofdstuk 4. De biodistributie in muizen toonde aan dat lyophilisomen geen acute toxische effecten induceerden en werden na afbraak uitgescheiden via de urine. Effectieve drug delivery systemen moeten lang genoeg in de bloedstroom circuleren om via "lekke bloedvaten" de tumor te bereiken. Lyophilisomen worden snel uit de circulatie verwijderd door het mononucleaire fagocytensysteem (voornamelijk lever en milt). Met de vergaarde kennis is duidelijk geworden dat lyophilisomen voor toekomstig onderzoek verder moeten worden gesorteerd (kleinere diameter) of aan het oppervlak moeten worden aangepast om vroegtijdige verwijdering uit de circulatie te voorkomen.

Concluderend beschrijft dit proefschrift de potentie van albumine-lyophilisomen als een drug delivery systeem voor anti-tumor medicijnen. Om lyophilisomen in de toekomst *in vivo* te kunnen gebruiken is verder onderzoek nodig waaronder aanpassingen om de circulatietijd van lyophilisomen te verlengen.

7

Future directions
Toekomstvisie in het Nederlands

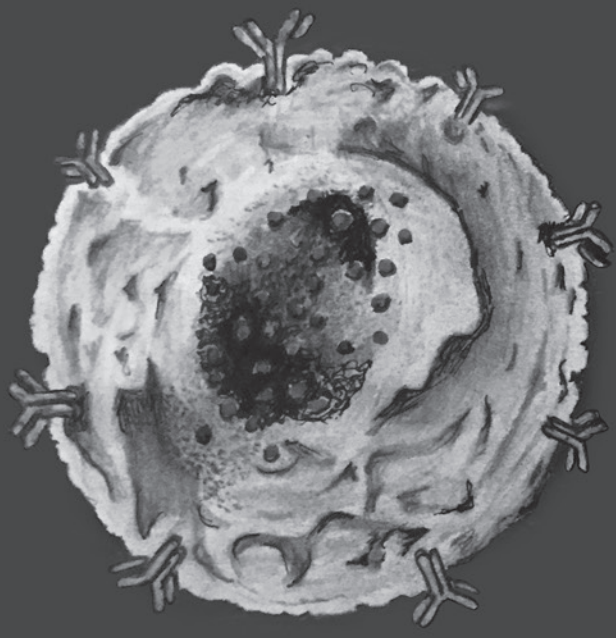

FUTURE DIRECTIONS

Design and synthesis of efficient drug delivery systems are of vital importance for medicine and healthcare. Materials innovation and nanotechnology continues to be an expanding field, and in this thesis we showed the potential of albumin-based lyophilisomes for drug delivery. We developed albumin-based lyophilisomes that can be loaded with anti-tumor drugs and functionalized with antibodies and cell penetrating peptides (CPPs) in order to be used as a comprehensive drug delivery system.

The ideal nanoparticulate drug delivery systems should consist of nanoparticles that can specifically deliver a high quantity of anti-tumor drug into the tumor cell in order to eliminate the cancer. It has already been demonstrated that multiple drug delivery systems can be loaded with various anti-cancer drugs [1]. However, when drug delivery systems are administered intravenously, they need to be able to reach the tumor site. This generally occurs due to the enhanced permeability effect. Theoretically, one would prefer to only eliminate the tumor cells and preserve healthy tissue. Antibodies may improve the specificity substantially, as demonstrated in Chapter 3. They may specifically target the nanoparticle to the tumor cells when extravasated out of the circulation. In addition, CPPs are a powerful tool that allow penetration of the cellular membrane and, when coupled to nanocapsules, facilitate their cellular uptake (Chapter 4). For future research, a key investigation would be to combine CPPs with tumor-specific antibodies [2,3]. Due to their larger size, antibodies may cover the CPPs preventing intracellular uptake of the capsules by healthy tissue and allowing CPPs to only function at the tumor site after binding. In combination with cytotoxic agents, antibodies will provide specificity, while CPPs will ensure rapid internalization of the lyophilisome, as not all antibodies trigger internalization, thereby reducing the negative side effects of cytostatic agents on healthy cells, and potentially even resulting in accelerated tumor degradation. Harnessing the power of CPPs for tumor targeted delivery has been pursued by a variety of mechanisms. Stimulus-responsive materials may be applied for this purpose, as they may provide triggered changes in material properties that allow spatially focused presentation of CPPs in response to intrinsic disease characteristics (*e.g.* abundantly present extracellular matrix proteases) or locally applied extrinsic cues (*e.g.* application of heat or light at a specific location) [4,5]. In *in vitro* experiments, it has been shown that lyophilisomes modified with antibodies and CPPs, result in specific targeting and enhanced cellular uptake. In addition, lyophilisomes could be loaded with anti-tumor drugs resulting in strongly reduced cell viability *in vitro*. Further studies on the combination of these modifications are needed to provide evidence-based data to support this approach to fight cancer.

Besides *in vitro* research, more *in vivo* investigation is required. Before drug delivery systems reach the target site, they need to travel through the vascular bed. Particle size has a fundamental effect on the biodistribution [6]. In this thesis, lyophilisomes were sized-selected using Fluorescent Activated Cell Sorting (FACS) and sucrose-gradient centrifugation.

Although these methodologies resulted in a more monodisperse particle population within the nanometer range, more research is needed to develop a method to increase the amount of nano-sized lyophilisomes (±200 nm). These size-selected lyophilisomes are more suitable to employ the enhanced permeability effect in tumors. In addition, a better understanding of the behavior of lyophilisomes *in vivo* may lead to the identification of important parameters that can be adjusted to increase circulating times. Various methods have been developed to enable prolonged circulation times, such as PEGlyation [7,8], albumin coating [9], the use of smaller capsules [6]. Recently Rodriguez *et al.* demonstrated a minimal "self" peptide that inhibited phagocytic clearance and enhanced delivery of nanoparticles [10]. Lyophilisomes could be modified to achieve longer circulation times by one of these methodologies. However, besides intravenous administration to target tumor tissue, cancers such as ovarian, colorectal, pancreatic, or uterine cancer can also profit from intraperitoneal (IP) administration of chemotherapeutics [11]. IP chemotherapeutics allow higher dosages and more frequent administration of drugs, and it appears to be more effective in eliminating cancer cells in the peritoneal cavity [12,13]. However, IP chemotherapy has also led to significantly higher toxic side effects, since both tumor cells and healthy cells in the peritoneal cavity are exposed to high concentrations of the chemotherapeutic [14,15]. Nano/microparticulate drug delivery systems can potentially improve current IP treatment of ovarian cancer, especially when delivering chemotherapeutics with targeting moieties through cancer cell surface markers [16,17]. There is evidence that intraperitoneally, small particles (50 to 720 nm) are removed more rapidly compared to larger (>4 μm) particles due to lymphatic drainage [18]. As the originally developed unsized lyophilisomes showed a size ranging from 200 nm to 10 μm [19], they may be suitable for IP applications. As demonstrated in this thesis, antibody-modified lyophilisomes, which were not sized, were able to specifically target cancer cells under dynamic conditions, making them suitable for this application. Future research into IP applications/therapies should therefore be pursued. For clinical IP applications, sizing of lyophilisomes and modification to prevent rapid removal from circulation may not even be necessary.

For biomedical applications, it would be advantageous if capsules could be prepared from a wide repertoire of natural (proteinaceous) macromolecules. As Daamen *et al.* demonstrated, lyophilisomes could be prepared from a variety of macromolecules, including serum albumin (67 kDa), type I collagen (280 kDa), and heparin (15 kDa), a highly negatively charged polysaccharide [19]. This indicates the versatility of lyophilisomes and the ability to address the variety of medical demands. One may think of lyophilisomes that are prepared from specific macromolecules that will be degraded at the site of action, were it subsequently releases the drug. Therefore, future research should also focus on the feasibility to prepare lyophilisomes from a variety of macromolecules and obtain more knowledge of those carriers with respect to drug delivery.

When these issues can be addressed, lyophilisomes may result in an innovative (albumin)-based drug delivery system that will have a significant contribution to treat multiple cancer types.

TOEKOMSTVISIE

Het ontwerp en de ontwikkeling van efficiënte drug delivery systemen (medicijnafgiftesystemen) is van vitaal belang voor de geneeskunde en de gezondheidszorg. Het onderzoeksgebied waar materiaalinnovatie en nanotechnologie elkaar raken, ontwikkelt zich nog steeds. Dit proefschrift laat de potentie van albumine-lyophilisomen zien in relatie tot gerichte drug delivery. De ontwikkelde albumine-lyophilisomen kunnen worden opgeladen met geneesmiddelen tegen kanker en worden gefunctionaliseerd met antilichamen en cel-penetrerende peptiden (CPPs), wat resulteert in een uitgebreid drug delivery systeem.

Het optimale drug delivery systeem moet bestaan uit nanodeeltjes die specifiek een grote hoeveelheid aan anti-tumor geneesmiddel in een tumorcel kunnen afleveren om de kanker te elimeneren. In eerder onderzoek is aangetoond dat meerdere drug delivery systemen kunnen worden opgeladen met verschillende anti-tumor medicijnen (1). Wanneer drug delivery systemen intraveneus worden toegediend, moeten ze in staat zijn het tumorweefsel te bereiken. Dit gebeurt doorgaans door middel van het verhoogde permeabiliteitseffect. Theoretisch zou men graag alleen de tumorcellen elimineren en het gezonde weefsel behouden. Antilichamen kunnen de specificiteit van geneesmiddelen tegen tumoren aanzienlijk verbeteren, zoals wordt aangetoond in Hoofdstuk 3. Antilichamen kunnen het nanodeeltje specifiek naar de tumorcellen leiden na extravasatie uit het bloed. Daarnaast is er een actieve interesse in CPPs die gemakkelijk celmembranen kunnen passeren zonder de hulp van celmembraanreceptoren. Als CPPs aan nanocapsules worden gekoppeld, zorgt dit voor een versnelde opname van de capsule (Hoofdstuk 4). Een belangrijk experiment voor toekomstig onderzoek is het combineren van CPPs met tumor-specifieke antilichamen (2, 3). Antilichamen zijn door hun grootte mogelijk in staat om CPPs te beschermen waardoor de capsules niet worden opgenomen door gezond weefsel en CPPs pas functioneel worden na binding op de plek van de tumor. In dit geval zorgen de antilichamen voor specificiteit en de CPPs voor versnelde opname aangezien niet alle antilichamen aanzetten tot internalisatie. Gecombineerd met cytostatica zullen de negatieve bijwerkingen op gezond weefsel afnemen, wat potentieel zelfs kan resulteren in een versnelde tumorafbraak.

Om CPPs te gebruiken voor tumorspecifieke drug delivery en slechts te activeren op de plaats van bestemming zijn verscheidene mechanismen nagestreefd, gebaseerd op stimulus-reagerende materialen. Deze materialen kunnen specifieke triggers initiëren waardoor de eigenschap van het materiaal verandert en de presentatie van CPPs mogelijk maakt. Bijvoorbeeld in reactie op intrinsieke kenmerken van de ziekte zoals de aanwezigheid van een overvloed aan extracellulaire matrixeiwitten of lokaal toegepaste extrinsieke signalen zoals het toepassen van warmte of licht op een bepaalde locatie (4, 5). *In vitro* experimenten toonden aan dat gemodificeerde lyophilisomen met antilichamen en CPPs zorgen voor specifieke targeting en versnelde opname. Bovendien kunnen lyophilisomen worden

opgeladen met anti-tumor geneesmiddelen wat leidt tot een sterk verminderde celviabiliteit *in vitro*. Verder onderzoek naar de combinatie van antilichamen en CPPs is essentieel om deze strategie te ondersteunen met meer data.

Naast *in vitro* onderzoek is ook meer *in vivo* onderzoek noodzakelijk. Voordat drug delivery systemen hun doel (tumorcellen) *in vivo* bereiken circuleren ze door het bloedvatenstelsel. De diameter van het drug delivery systeem heeft een fundamentele invloed op de biodistributie (6). In dit proefschrift zijn lyophilisomen geselecteerd op basis van grootte door middel van Fluorescent Activated Cell Sorting (FACS) en sucrose-gradiënt centrifugatie. Deze methodes hebben geleid tot een populatie lyophilisomen met minder variatie in diameter (nanometer range). Echter, meer onderzoek is nodig om een methode te ontwikkelen waarbij grotere hoeveelheden lyophilisomen van ±200 nm kunnen worden verkregen, omdat nanodeeltjes van deze grootte beter geschikt zijn om gebruik te maken van het verhoogde permeabiliteitseffect in tumoren. Bovendien zal meer *in vivo* kennis van lyophilisomen leiden tot een beter inzicht in het gedrag van lyophilisomen in bloed, waaruit vervolgens belangrijke parameters kunnen worden geïdentificeerd om de circulatietijden te vergroten. Verschillende methodes zijn ontwikkeld om nanodeeltjes langdurig in de bloedbaan te laten circuleren, zoals PEGylatie (7, 8), albumine coating (9), en het gebruik van kleinere capsules (6). Recentelijk is door Rodriguez *et al*. een "eigen" peptide aangetoond die de fagocyterende klaring remt en anderzijds zorgt voor een verhoogd aantal nanodeeltjes die de tumor bereikt (10). Lyophilisomen kunnen door bovenstaande methodes worden gemodificeerd om een langere circulatietijd te bereiken. Echter, naast intraveneuze toediening om tumors te bereiken kunnen andere soorten kanker zoals ovarium-, darm-, alvleesklier-, of baarmoederkanker ook baat hebben bij intreperitoneale (IP) toediening van anti-tumor medicijnen (11).

IP anti-tumor medicijnen kunnen in hogere doseringen en frequenter worden toegediend en lijken effectiever in het elimineren van tumorcellen in de buikholte (12, 13). Echter, IP chemotherapie heeft ook geleid tot significant meer toxische bijwerkingen doordat zowel tumorcellen als gezonde cellen in de buikholte worden blootgesteld aan hoge concentraties van de anti-tumor medicijnen (14, 15). Drug delivery systemen in de nano/micrometer range kunnen mogelijk de huidige IP behandeling van ovarium kanker verbeteren door anti-tumor medicijnen specifiek te richten tegen markers op het oppervlak van de tumorcel (16, 17). Literatuur bewijst dat kleine deeltjes (50 tot 720 nm) sneller worden verwijderd in de buikholte door lymfatische drainage in vergelijking met grotere (>4 µm) deeltjes (18). De oorspronkelijk ontwikkelde (niet gesorteerde) lyophilisomen hebben een diameter variërend van 200 nm tot 10 µm (19). Dit proefschrift toonde aan dat antilichaam-gemodificeerde lyophilisomen (niet gesorteerd) in staat zijn om tumorcellen specifiek te targeten onder dynamische condities. Dit maakt lyophilisomen eventueel geschikt voor IP-toepassingen. Daarom moet toekomstig onderzoek naar IP toepassingen/therapieën worden voortgezet. Voor klinische IP toepassingen is het mogelijk niet eens nodig om lyophilisomen te sorteren en te modificeren om snelle verwijdering uit de circulatie te voorkomen.

Voor biomedische toepassingen zou het een voordeel zijn als capsules geproduceerd kunnen worden uit een brede selectie van natuurlijke (eiwithoudende) macromoleculen. Zoals aangetoond door Daamen *et al.* kunnen lyophilisomen gemaakt worden van verschillende macromoleculen, zoals serum albumine (67 kDa), type 1 collageen (280 kDa) en heparine (15 kDa), een sterk negatief geladen polysaccharide (19). Dit geeft de veelzijdigheid aan van lyophilisomen en het vermogen om aan de vraag naar verschillende medische toepassingen te voldoen. Lyophilisomen kunnen bijvoorbeeld gemaakt worden van specifieke macromoleculen, die worden gedegradeerd op de plaats van bestemming waar vervolgens het medicijn vrij komt. Daarom zal toekomstig onderzoek zich ook moeten richten op de productie van lyophilisomen van verschillende macromoleculen om meer kennis te verkrijgen van deze carriers in relatie tot drug delivery.
Als deze problemen worden aangepakt kunnen lyophilisomen tot een innovatief drug delivery systeem leiden dat een significante bijdrage kan leveren aan de behandeling van meerdere soorten kanker.

REFERENCES

1. Zhang Y, Chan HF, Leong KW (2013) Advanced materials and processing for drug delivery: the past and the future. Adv Drug Deliv Rev 65: 104-120.
2. Zhu Y, Cheng L, Cheng L, Huang F, Hu Q, *et al.* (2014) Folate and TAT Peptide Co-Modified Liposomes Exhibit Receptor-Dependent Highly Efficient Intracellular Transport of Payload In Vitro and In Vivo. Pharm Res 31: 3289-3303.
3. Takara K, Hatakeyama H, Ohga N, Hida K, Harashima H (2010) Design of a dual-ligand system using a specific ligand and cell penetrating peptide, resulting in a synergistic effect on selectivity and cellular uptake. Int J Pharm 396: 143-148.
4. MacEwan SR, Chilkoti A (2013) Harnessing the power of cell-penetrating peptides: activatable carriers for targeting systemic delivery of cancer therapeutics and imaging agents. Wiley Interdiscip Rev Nanomed Nanobiotechnol 5: 31-48.
5. Felice B, Prabhakaran MP, Rodriguez AP, Ramakrishna S (2014) Drug delivery vehicles on a nano-engineering perspective. Mater Sci Eng C Mater Biol Appl 41C: 178-195.
6. Decuzzi P, Godin B, Tanaka T, Lee SY, Chiappini C, *et al.* (2010) Size and shape effects in the biodistribution of intravascularly injected particles. J Control Release 141: 320-327.
7. Panagi Z, Beletsi A, Evangelatos G, Livaniou E, Ithakissios DS, *et al.* (2001) Effect of dose on the biodistribution and pharmacokinetics of PLGA and PLGA-mPEG nanoparticles. Int J Pharm 221: 143-152.
8. Owens DE III, Peppas NA (2006) Opsonization, biodistribution, and pharmacokinetics of polymeric nanoparticles. Int J Pharm 307: 93-102.
9. Bazile DV, Ropert C, Huve P, Verrecchia T, Marlard M, *et al.* (1992) Body distribution of fully biodegradable [14C]-poly(lactic acid) nanoparticles coated with albumin after parenteral administration to rats. Biomaterials 13: 1093-1102.
10. Rodriguez PL, Harada T, Christian DA, Pantano DA, Tsai RK, *et al.* (2013) Minimal "Self" peptides that inhibit phagocytic clearance and enhance delivery of nanoparticles. Science 339: 971-975.
11. Sangisetty SL, Miner TJ (2012) Malignant ascites: A review of prognostic factors, pathophysiology and therapeutic measures. World J Gastrointest Surg 4: 87-95.
12. Kwa M, Muggia F (2013) Ovarian Cancer: A Brief Historical Overview of Intraperitoneal Trials. Ann Surg Oncol 21: 1429-1434.
13. Schmid BC, Oehler MK (2014) New perspectives in ovarian cancer treatment. Maturitas 77: 128-136.
14. Armstrong DK, Bundy B, Wenzel L, Huang HQ, Baergen R, *et al.* (2006) Intraperitoneal cisplatin and paclitaxel in ovarian cancer. N Engl J Med 354: 34-43.
15. Gould N, Sill MW, Mannel RS, Thaker PH, Disilvestro PA, *et al.* (2012) A phase I study with an expanded cohort to assess feasibility of intravenous docetaxel, intraperitoneal carboplatin and intraperitoneal paclitaxel in patients with previously untreated ovarian, fallopian tube or primary peritoneal carcinoma: A Gynecologic Oncology Group study. Gynecol Oncol 133: 433-438.
16. Wang AZ, Gu F, Zhang L, Chan JM, Radovic-Moreno A, *et al.* (2008) Biofunctionalized targeted nanoparticles for therapeutic applications. Expert Opin Biol Ther 8: 1063-1070.
17. Werner ME, Karve S, Sukumar R, Cummings ND, Copp JA, *et al.* (2011) Folate-targeted nanoparticle delivery of chemo- and radiotherapeutics for the treatment of ovarian cancer peritoneal metastasis. Biomaterials 32: 8548-8554.
18. Bajaj G, Yeo Y (2010) Drug delivery systems for intraperitoneal therapy. Pharm Res 27: 735-738.
19. Daamen WF, Geutjes PJ, Nillesen STM, Van Moerkerk HTB, Wismans R, *et al.* (2007) Lyophilisomes: A new type of (bio)capsules. Adv Mater 19: 673-677.

8

Curriculum Vitae
List of publications
Dankwoord

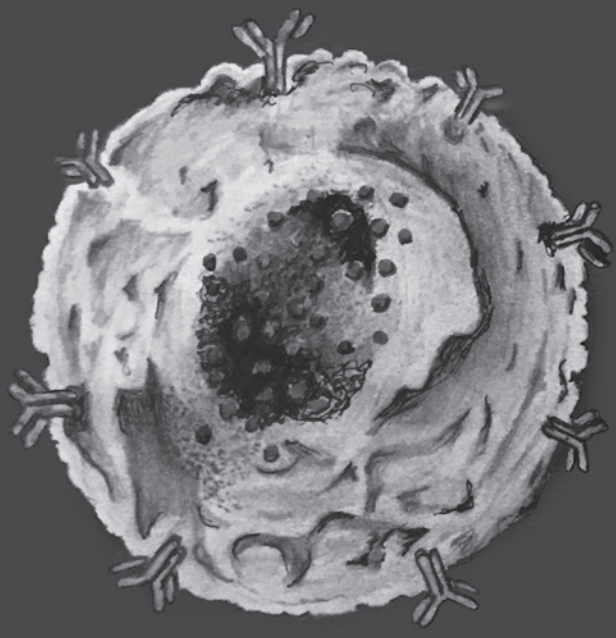

CURRICULUM VITAE (ENGLISH)

Etienne van Bracht was born November 11th, 1984 in Nijmegen, the Netherlands. In 2003 he obtained his VWO diploma at the Stedelijke Scholen Gemeenschap Nijmegen (SSGN). The same year he started his studies Biomedical Sciences at the Radboud University Nijmegen, with majors in Toxicology and Pathobiology. Part of his education were internships at the department of Nuclear Medicine and (Matrix) Biochemistry at the Radboud University Nijmegen and an internship at the department Toxicology at the Karalinska Institutet, Stockholm, Sweden.

In December 2008 he graduated and started his Ph.D. research at the Radboud University, Nijmegen Centre for Molecular Life Sciences (NCMLS) under supervision of Toin van Kuppevelt and Willeke Daamen. The results obtained during his Ph.D. are described in this thesis. During this period of time, he was involved in several educational responsibilities and had multiple students under his supervision. He presented his results on various international congresses, including ESF-UB conference in Biomedicine; Nanomedicine: reality now and soon (Sant Feliu de Guixols, Spain, 2010) en de Nanotech conference & expo (Santa Clara, CA, USA, 2012).

From October 2013, he is working as Trainee at Janssen Biologics, part of Pharmaceutical Companies of Johnson & Johnson. During this two-year training program, he will focus on a variety of areas of expertise within the pharmaceutical industry.

CURRICULUM VITAE (NEDERLANDS)

Etienne van Bracht werd op 11 November 1984 geboren te Nijmegen. In 2003 haalde hij zijn VWO diploma aan de Stedelijke Scholen Gemeenschap Nijmegen (SSGN). In datzelfde jaar begon hij zijn studie Biomedische Wetenschappen aan de Radboud Universiteit Nijmegen. Binnen deze opleiding werd gekozen voor de hoofdvakken Phatobiology en Toxicologie. Onderdeel van de studie vormde een stage op de afdeling Nucleaire Geneeskunde en (Matrix) Biochemie aan de Radboud Universiteit Nijmegen en een stage op de afdeling toxicologie aan het Karalinska Institutet te Zweden.
In December 2008 ontving hij zijn doctoraal diploma. Vanaf december 2008 was hij werkzaam als onderzoeker in opleiding op de afdeling Biochemie aan de Radboud Universiteit Nijmegen, Nijmegen Centre for Molecular Life Sciences (NCMLS) onder begeleiding van Toin van Kuppevelt en Willeke Daamen. De resultaten van het promotie-onderzoek staan beschreven in dit proefschrift. Tijdens zijn promotie is hij betrokken geweest bij diverse onderwijs taken en heeft hij meerdere studenten begeleid. Tevens heeft hij zijn resultaten op verschillende internationale congressen gepresenteerd, waaronder ESF-UB conference in Biomedicine; Nanomedicine: reality now and soon (Sant Feliu de Guixols, Spanje, 2010) en de Nanotech conference & expo (Santa Clara, CA, USA, 2012).
Sinds Oktober 2013 is hij werkzaam als Trainee bij Janssen Biologics, onderdeel van Pharmaceutical Companies of Johnson & Johnson. Gedurende dit tweejarige opleidings-traject zal hij zich focussen op verschillende aspacten binnen de farmaceutische industrie.

LIST OF PUBLICATIONS

van Bracht E*, Raavé R*, Brock RE, Oosterwijk E, van Kuppevelt TH, Daamen WF. Biodistribution of sized lyophilisomes in mice. *Eur J Pharm Biopharm*. 2015 (In Press)

van Bracht E, Versteegden LRM, Stolle S, Verdurmen WP, Woestenenk R, Hafmans TG, Oosterwijk E, Brock R, van Kuppevelt TH, Daamen WF. Enhanced cellular uptake of albumin-based lyophilisomes when functionalized with cell-penetrating peptide TAT in HeLa cells. *PLoS ONE*. 2014 Nov;9(11):e110813.

van Bracht E, Stolle S, Hafmans TG, Boerman OC, Oosterwijk E, van Kuppevelt TH, Daamen WF. Specific targeting of tumor cells by lyophilisomes functionalized with antibodies. *Eur J Pharm Biopharm*. 2014 May;87(1):127-135.

van Bracht E, Raavé R, Verdurmen WP, Wismans RG, Geutjes PJ, Brock RE, Oosterwijk E, van Kuppevelt TH, Daamen WF. Lyophilisomes as a new generation of drug delivery capsules. *Int J Pharm*. 2012 Dec 15;439(1-2):127-135.

van Bracht E, Geutjes PJ, Woestenenk R, Wismans RG, Oosterwijk E, van Kuppevelt TH, Daamen WF. Lyophilisomes: potential carriers for tumor targeting. *J Control Release*. 2010 Nov 20;148(1):e7-8.

* These authors contributed equally to this work

DANKWOORD

Eindelijk, het is zover. De promotie zit erop. Het boekje is af! Een promotie afronden is iets speciaals. Dit kan niet tot stand komen zonder de hulp en morele ondersteuning van collega's, vrienden en familie, waarvoor ik mijn dank uitspreek.

Roland, ik wil je graag bedanken voor je rol als promotor. Ondanks dat wij als onderzoeksgroep (Matrix Biochemie) twee verdiepingen lager zitten, heb jij altijd willen meedenken over de manuscripten en waar mogelijk kennis en netwerk gedeeld voor het opzetten van nieuwe experimenten/samenwerkingsverbanden. Ik heb dit altijd zeer op prijs gesteld.
Toin & Willeke, jullie wil ik bedanken voor het vertrouwen en het feit dat ik mijn promotieonderzoek bij jullie op de afdeling heb kunnen uitvoeren. Willeke, ik ben officieel de eerste promovendus onder jouw hoede. In het begin zijn we beide zoekende geweest naar het juiste plan van aanpak. Momenteel, tijdens het schrijven van mijn dankwoord kan ik alleen maar zeggen dat er veel positieve veranderingen hebben plaatsgevonden en ik onze samenwerking als prettig ervaar. Een mailtje, appje, telefoontje, het maakt niet uit, altijd bereikbaar voor haar promovendi. Ontzettend bedankt hiervoor. Ik wens je al het goede in je carrière. Toin, jouw deur stond altijd open. Bij jou binnen wandelen om even één vraag te stellen of je mening te vragen kon al snel uitlopen tot een half uur. Je eindeloze ideeën hebben mij veel energie en wetenschappelijke inspiratie gegeven en zijn een lust om naar te luisteren. Daar wil ik je hartelijk voor bedanken.

Paul, samen met Willeke de grondleggers van de lyophilisomen. Ondanks je aanstelling bij Urologie heb je altijd interesse getoond en ben je betrokken geweest bij mijn onderzoek. Studenten bij urologie liet je zelfs aan de lyophilisomen werken. Je enthousiasmse is enorm aanstekelijk en tesamen met je kritische blik ben je een heel fijn persoon om mee samen te werken, dank je wel.
Egbert, ik wil je graag bedanken voor de samenwerking, en je altijd kritische blik op mijn manuscripten heb ik zeer gewaardeerd.

(Matrix) Biochemie, de afdeling waar ik 4 jaar aan mijn proefschrift heb gewerkt en veel leuke collega's heb leren kennen. Natuurlijk wil ik iedereen bedankten voor de hulp en gezelligheid. René, begonnen als bachelorstudent aan mijn zijde en nu promoveren op het onderwerp waar het allemaal mee begonnen is. Jij hebt veel werk verzet voor mijn promotie als student en als promovendus in mijn afrondende fase. Ontzettend bedankt voor je inzet en fijne samenwerking. Ik wens je veel succes met het afronden van je promotie en fijn dat je mijn paranimf wilt zijn. Marianne, U-genoot en eigenlijk een vreemde eend in de bijt (afd. Longziekten), maar een gezellige collega. Altijd even opstarten met een praatje, soms 5 minuten en af en toe iets langer…….. Elly en Arie, de dragende kracht van het lab en altijd bereid om te helpen of vragen te beantwoorden.

Bedankt voor jullie hulp en gezelligheid, het gaat jullie goed en Arie, nikmati masa depan Anda di Bali. Ronnie, bedankt voor de EM plaatjes en coupes die je voor me hebt gesneden. Theo, schroefdraad, prikkeldraad etc., hele normale woorden die naar een paar biertjes behoorlijk van betekenis kunnen veranderen. Bedankt voor je EM werk, gezelligheid en sfeer die je zowel binnen als buiten de afdeling bracht. Els, Gerdy, Herman en Keauis, jullie morgen niet ontbreken op het lijstje, Bedankt voor alle support en gezelligheid.
Allemaal hetzelfde doel: promoveren. Dit schept een band en brengt mensen dichter bij elkaar. Alle medepromovendi, Martin, Gerwen, Peter, Katrien, Xander, Henk, Myrtille, Michiel, Corien, Luuk, Sophieke en René bedankt voor de leuke tijd en luisterend oor op zijn tijd. De donderdagavonden, dagjes uit, paaslunch, AIO-retraites etc. gaven de benodigde ontspanning en waren altijd een succes. Dit heeft mij een geweldige tijd bezorgd.
Tijdens mijn onderzoek heb ik een flink aantal studenten mogen begeleiden, zowel binnen als buiten de afdeling. Wouter, Marie, Ruud, Farnaz, Aslihan en Elahe, jullie bijdrage is zeer waardevol geweest als basis voor mijn promotie en ik wens jullie veel succes voor de toekomst. Speciale dank gaat uit naar René, Luuk, en Sarah. Drie talentvolle studenten die ik voor een langere periode wegwijs heb kunnen maken in de onderzoekswereld. Hartelijk dank voor jullie enorme bijdrage en nogmaals gefeliciteerd met de co-auteurschappen. Veel succes met jullie verdere carrière.

Ook wil ik de mensen bedanken waar ik mee heb samengewerkt voor de diverse hoofdstukken in dit proefschrift. Rob, een echte teamspeler met een brede interesse in onderzoek. Je positieve energie, doorzettingsvermogen en oneindige kennis van de flowcytometer hebben mij altijd doen geloven in een goede afloop. Hartelijk dank voor de vele sorteringen die je voor mij hebt gedaan met je collega's. Wouter, bedankt voor de prettige samenwerking en hulp met de CPP experimenten. Otto, ontzettend bedankt voor het meedenken over ons onderzoek en het delen van je netwerk. De samenwerking met Immunomedics heeft uiteindelijk geresulteerd in een mooie publicatie! Bianca en Henk, hartelijk bedankt voor alle hulp rondom het CDL. Dear Igor, to complete the last chapter of my thesis you provided me "smaller lyophilisomes". Despite we never met in person, I would like to thank you for your extensive knowledge to sort nanoparticles, positive attitude and easygoing correspondence.

Sip, Rick en Lotte ontzettend bedankt voor jullie vriendschap, de goede gesprekken en alle leuke momenten die we hebben meegemaakt. Job, Lex, Rob, Jasper, hartstikke bedankt voor jullie vriendschap, biertjes en de nodige ontspanning op zijn tijd. En niet te vergeten de harde kern van T.C. de Linden, bedankt mannen!

Familie Groenen, Cools, Smeekens en Pigmans bedankt voor de Brabantse gezelligheid :-).
Ad en Brigitte, ontzettend bedankt voor de schitterende tekening!

Lieve Tess, Roel en Raf, ontzettend bedankt voor jullie belangstelling, advies, humor en een plek waar we altijd welkom zijn. Tegen de tijd van mijn verdediging hoop ik opnieuw een trotse oom te zijn. Lieve Tess, Ik vind het heel speciaal dat je mijn paranimf bent.

Lieve pap en mam, jullie onvoorwaardelijke steun en geloof in mij is voor jullie de normaalste zaak van de wereld. Het heeft mij een sterke basis gegeven om te staan waar ik nu sta. Nu mijn promotie bijna is afgerond kunnen we zeggen dat de vele kaarsjes uiteindelijk toch geholpen hebben. Ondanks de moeilijke tijd van afgelopen jaren staan we altijd voor elkaar klaar. Daar zal nooit iets of iemand afbreuk aan kunnen doen!

Lieve Cin, jij begrijpt wat een promotie met zich meebrengt. Met jouw steun, motivatie, vertrouwen en liefde heb ik dit alles tot een goed eind kunnen brengen. Daar kan ik je niet genoeg voor bedanken. Ik prijs me ontzettend gelukkig met jou naast me en ik kijk met veel plezier uit naar onze toekomst samen. Love You!